ABSTRACT

Title of Dissertation: **GENETIC MANIPULATION OF ANOPHELES STEPHENSI IMMUNITY TO INCREASE PLASMODIUM FALCIPARUM SALIVARY GLAND SPOROZOITE INFECTION LEVELS**

Kasim I. George,
Doctor of Philosophy, 2016

Dissertation directed by: Professor David A. O'Brochta,
Institute for Bioscience &
Biotechnology Research
Department of Entomology

Human malaria is responsible for over 700,000 deaths a year. To stay abreast of the threat posed by the parasite, a constant stream of new drugs and vector control methods are required. This study focuses on a vaccine that has the potential to protect against parasite infection, but has been hindered by developmental challenges. In malaria prevention, live, attenuated, aseptic, *Plasmodium falciparum* sporozoites (PfSPZ) can be administered as a highly protective vaccine. PfSPZ are produced using adult female *Anopheles stephensi* mosquitoes as bioreactors. Production volume and cost of a PfSPZ

vaccine for malaria are expected to be directly correlated with *Plasmodium falciparum* infection intensity in the salivary glands. The sporogonic development of *Plasmodium falciparum* in *A. stephensi* to fully infected salivary gland stage sporozoites is dictated by the activities of several known components of the mosquito's innate immune system. Here I report on the use of genetic technologies that have been rarely, if ever, used in *Anopheles stephensi* Sda500 to increase the yield of sporozoites per mosquito and enhance vaccine production. By combining the Gal4/UAS bipartite system with *in vivo* expression of shRNA gene silencing, activity of the IMD signaling pathway downstream effector *LRIM1*, an antagonist to *Plasmodium* development, was reduced in the midgut, fat body, and salivary glands of *A. stephensi*. In infection studies using *P. berghei* and *P. falciparum* these transgenic mosquitoes consistently produced significantly more salivary gland stage sporozoites than wildtype controls, with increases in *P. falciparum* ranging from 2.5 to 10 fold. Using *Plasmodium* infection assays and qRT-PCR, two novel findings were identified. First, it was shown that 14 days post *Plasmodium* infection, transcript abundance of the IMD immune effector genes *LRIM1*, *TEP1* and *APL1c* are elevated, in the salivary glands of *A. stephensi*, suggesting the salivary glands may play a role in post midgut defense against the parasite. Second, a non-pathogenic IMD signaling pathway response was observed which could suggest an alternative pathway for IMD activation. The information gained from these studies has significantly increased our knowledge of *Plasmodium* defense in *A. stephensi* and moreover could significantly improve vaccine production.

GENETIC MANIPULATION OF ANOPHELES STEPHENSI IMMUNITY TO INCREASE PLASMODIUM FALCIPARUM SALIVARY GLAND SPOROZOITE INFECTION LEVELS

by

Kasim I. George

Dissertation submitted to the Faculty of the Graduate School of the
University of Maryland, College Park, in partial fulfillment
of the requirements for the degree of
Doctor of Philosophy
2016

Advisory Committee:
Dr. David A. O'Brochta, Chair
Dr. Utpal Pal
Dr. Raymond J. St. Leger
Dr. Louisa P. Wu
Dr Najib M. El Sayed, Dean's Representative

Dedication

I would like to dedicate this dissertation to my wonderful parents, Lionel and Joycelyn, and to my siblings Darren and Kim, for their unconditional love, support and encouragement.

Acknowledgements

I would like to express my profound gratitude to my mentor Dr. David *A.* O'Brochta for his guidance, teachings, and encouraging advice. Your mentorship and support have been crucial to the advancement of my research throughout my time at The University of Maryland and for that, I will be forever grateful.

I would also like to thank all of my committee members: Dr. Louisa Wu, Dr. Utpal Pal, Dr. Najib El-Sayed, and Dr. Raymond St. Leger, for their support and valuable advice. I appreciate their time and efforts in reviewing and discussing my dissertation.

In addition, I would like to extend my gratitude to all past and present members of the O'Brochta laboratory: Kristina Pilitt, Robert Alford, Hanfu Xu, Noble Surendran Sinnathamby, William Reid, Frank Criscione and Valerie Saffer. Thank you all for the, support, help, and discussions throughout my graduate career, it is greatly appreciated.

I am also grateful to the University of Maryland Insect Transformation Facility: Robert Harrell, Channa Aluvihare, and Yonas Gebremicale for their expertise and assistance generating transgenic mosquitoes, and to our collaborator, Sanaria Inc. for their help with infection studies.

Special thanks go to my family, especially my parents, Lionel and Joycelyn, siblings Darren and Kim, and my aunt, Rose and uncle, Lenny. You have always been there for me and made this possible.

To every person who has offered their support, I am profoundly grateful.

Table of Contents

List of Tables

List of Figures

Abbreviations

AFB	Artificial feeding buffer
AMA1	apical membrane antigen-1
ANOVA	Analysis of Variance
AP-1	Activator Protein 1
APL1C	Anti-plasmodium response leucine rich repeat 1
APN1	Aminopeptidase
C3	Complement component 3
CDC	Center for Disease Control
CFU	Colony forming unit
ChAds	Chimpanzee adenoviruses
CSP	Circumsporozoite protein
DALYs	Disability adjusted ife years
DNA	Deoxy-ribonucleic acid
dsAgLRIM1	double stranded *Anopheles gambiae* LRIM1
dsAsLRIM1	double stranded *Anopheles stephensi* LRIM1
dsEGFP	double stranded enhanced green fluorescent protein
dsRNA	double stranded ribonucleic acid
IMD	Immune deficiency
JAK	Janus Kinase
JNK	c-Jun N-terminal Kinase

kb	kilobases
LB	Luria-Bertani
LRIM1	Leucine rich immune molecule 1
LRR	Leucine rich repeat
MSP1	Merozoite surface protein-1
MVA	Modified vaccinia virus Ankara
NK-kB	nuclear factor kappa-light-chain-enhancer of activated B cells
NOD	Nucleotide-binding oligomerization domain receptors proteins
PAMP	Pathogen associated molecular patterns
PBF	Post blood feed
PCR	Polymerase chain reaction
PGRP-SA	Peptidoglycan recognition protein SA
PGRP-SD	Peptidoglycan recognition protein SD
PM	Peritrophic matrix
PRR	Pathogen Recognition Receptors
qRT-PCR	Quantitative real-time PCR
RA PfSPZ	Radiation attenuated *Plasmodium falciparum* sporozoites vaccine
RAS	Radiation attenuated sporozoites
Rel2-S	Reslish 2 shortened
RNA	Ribonucleic acid
RNAi	Ribonucleic acid interference
RT	Room temperature
RT-PCR	Reverse Transcriptase Polymerase Chain reaction

shRNA	Short hairpin RNA
SOCS	Suppressor of cytokine signaling
STAT	Signal Transducer and Activator of Transcription
TEP1	Thioester containing protein 1
TNF	Tumor necrosis factor
TRAP	Thrombospondin-related adhesion protein
UAS	Upstream activation sequences
UNWTO	United Nations World Tourism Organization
Upd	Unpaired
WHO	World Health Organization

Chapter 1: Introduction & Literature Review

1.1 Statement of Purpose

Human malaria is responsible for over 700,000 deaths a year (WHO 2014). To stay abreast of the threat posed by the parasite, a constant stream of new drugs and vector control methods are required (WHO 2014). Vector control is one of the most effective strategies used for the suppression of mosquito-borne diseases (Rani et al. 2009). In areas where malaria is endemic, insecticide spraying and insecticide-treated bed nets have proven effective in reducing transmission (Christophides 2005). Advancements in mosquito molecular genetics have enabled researchers to target the mosquito immune system to deplete or incapacitate the disease transmitting population (Christophides 2005). Presently, one of the most promising methods of disease control, proposes the use of vaccines developed from live radiation attenuated sporozoites (RAS) (Hill 2011). In clinical studies, a live RAS vaccine developed by Sanaria Inc, a biotechnology company in Rockville Maryland conferred protection against the development of blood stage infection to 100 percent of the volunteers (Seder et al. 2013). However, vaccine production is limited in part by the number, also referred to as intensity, of sporozoites in the mosquito salivary glands. The effective immune system of the mosquito in particular the immune deficiency pathway (IMD), is able to kill the parasite, reducing the number of sporozoites reaching the salivary glands. We hypothesize that mosquitoes with modified innate immune systems can enhance the susceptibility to *Plasmodium falciparum* thereby increasing sporozoite intensity and subsequently improving vaccine production. Leucine-rich repeat (LRR) proteins play

a key role in anti-*Plasmodium* resistance in mosquitoes (Fraiture et al. 2009). Recent studies have shown that *leucine-rich repeat immune molecule 1* (*LRIM1*), an effector gene in the IMD pathway, functions in a complement-like mechanism leading to the targeting and destruction of *Plasmodium* parasites (Fraiture et al. 2009; Baxter et al. 2010; Povelones et al. 2011; Garver et al. 2012). In this study we will examine the current models of *LRIM1* anti-*Plasmodium* response and expression in *Anopheles stephensi (A. stephensi)*, by employing techniques novel to the field of vector biology. We hope our findings will give us a better understanding of the biology of *LRIM1* in *A. stephensi* and ultimately lead to our ability to increase sporozoite infection intensity leading to increased vaccine production.

1.2 The Global Impact of Human Malaria

Human malaria, is a persistent global public health threat and the leading cause of death in many developing countries (WHO 2014). More than 3 billion individuals live in 106 malaria endemic countries (Figure 1.1), with 1.2 billion in areas where the chance of getting human malaria is greater than 1:1000 (WHO, 2014). In 2013 there were an estimated 283 million clinical cases and 755,000 deaths attributed to human malaria worldwide. Ninety percent of those deaths occurred in the African region, with an estimated 76% being children under the age of five (WHO 2014). The severity of the disease in the African region is a result of several factors. 1) A very efficient vector, *Anopheles gambiae;* 2) The parasite species predominantly found in the region, *Plasmodium falciparum*, is most likely to cause severe illness and death; 3) The climate is conducive to year round transmission and 4) economic instability in the region (WHO 2014).

Human malaria has a substantial economic impact, costing more than US$ 12 billion per year with even more significant indirect costs. Infected individuals incur treatment related costs in addition to reduced income resulting from lost work days (WHO). Globally, human malaria infection is the 8th leading cause of Disability Adjusted Life Years (DALYs) and is the 2nd leading cause of DALYs in Africa (Snow et al., 2003). Governments also incur significant costs to purchase drugs, maintain health facilities and carry out public health interventions such as insecticide spraying and distribution of insecticide-treated bed nets (WHO 2014).

The United Nations World Tourism Organization (UNWTO) estimates that by 2020, 800 million travelers will visit a country at risk for human malaria transmission every year. Infected travelers or migrants who travel to countries that have eradicated malaria or have very low transmission can expose a very susceptible population to the disease. Even though malaria has been eliminated in the United States and some parts of Europe, there is still the possibility of outbreaks (WHO 2014). Since 1950, there have been 63 outbreaks in the U.S.A, (CDC) and malaria vectors, *A. quadrimaculatus*, *A. freeborni*, and *A. albimanus* are still widely prevalent in North America, making reemergence of the disease possible (Filler et al. 2006).

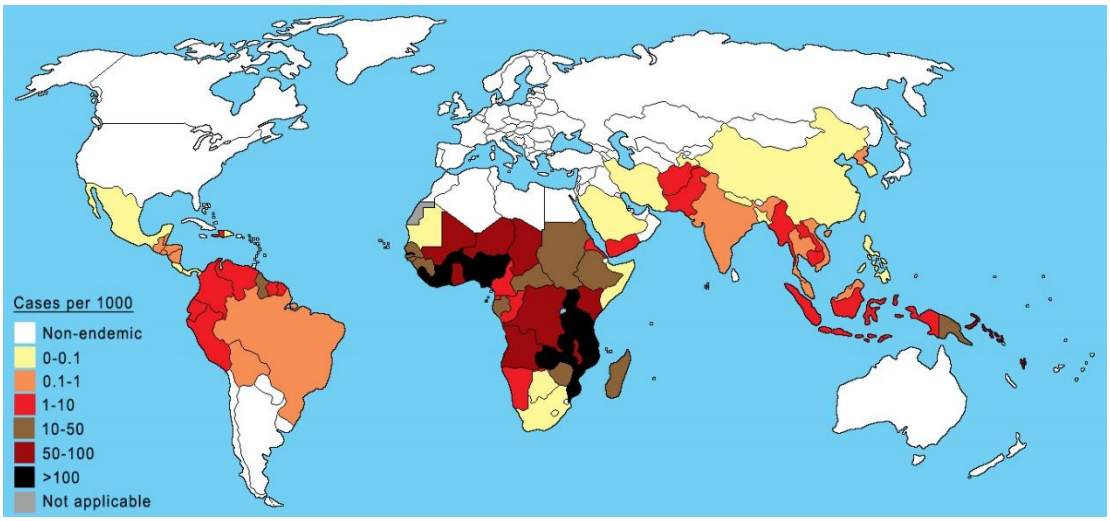

Figure 1.1- Global cases of human malaria in 2013. Human malaria is one of the world's most severe public health problems. An estimated 3.3 billion individuals live in 106 human malaria endemic areas. 1.2 billion individuals live in areas where the chance of getting human malaria is greater than 1:1000. Ninety percent of all malaria deaths worldwide occur in the African region. (Adapted from National malaria control reports)

1.3 Malaria Parasitology & Prevention

The malaria parasite is a single cell protozoan of the genus *Plasmodium* with a complex life cycle that involves the *Anopheles* vector and a vertebrate host. There are five *Plasmodium* species that infect humans (*P. falciparum, P. vivax, P. ovale, P. malariae* and *P. knowlesi*) (White 2008) and all five exhibit a similar life cycle (Wiser 2009)

An individual develops malaria after being bitten by a female *Anopheles* mosquito infected with the *Plasmodium* parasite. When the female mosquito bites an individual, sporozoites in the mosquito saliva are injected into the human host during feeding (Hill 2011) (Figure 1.2). Sporozoites enter the blood stream from the avascular tissue and are carried by the circulatory system to the liver and invade hepatocytes (Vanderberg and Frevert 2004; Vaughan et al. 2008). The intracellular sporozoites undergo asexual reproduction known as exoerythrocytic schizogony that culminates in the production of merozoites that are later released from ruptured hepatocytes into the blood stream (Vaughan et al. 2008). Circulating merozoites invade erythrocytes and enter a trophic period where the parasite enlarges forming a ring structure (Bannister et al. 2000). The trophozoite enlargement is accompanied by active metabolism within the blood cell that involves ingestion of the host cytoplasm and proteolysis of hemoglobin into amino acids (Soulard et al. 2015). At the end of the trophic period there are rounds of nuclear division, without cytokinesis that results in a schizont. Merozoites bud from these mature schizonts and are released after rupture of the erythrocyte (Huff and Coulston 1944; Soulard et al. 2015). The invasion of the erythrocytes and subsequent release of merozoites trigger another round of the blood

stage replicative cycle (Rosenmund 1991; Cox 1991). Blood stage infection is responsible for the pathology associated with human malaria. (Suhrbier 1991; Rosenmund 1991; Cox 1991). Malaria patients suffer from intermittent fever paroxysm caused by the synchronous rupture of infected erythrocytes. Symptoms can last 48 to 72 hours depending on the *Plasmodium* species. In the case of *Plasmodium falciparum* fevers are persistent and result in higher morbidity and mortality (Rosenmund 1991). The increased virulence of *P. falciparum* is also due in part to the higher level of paracetemia. Also the sequestration of trophozoites and schizont-infected erythrocytes in deep tissue results in more complications (Suhrbier 1991; Cox 1991; Rosenmund 1991)

The parasite can develop into two sexual forms called microgametocytes and macrogametocytes. Gametocytes are large parasites that contain only one nucleus and fill up the erythrocytes (Ott 1967; Soulard et al. 2015). During a blood meal from a vertebrate host, the female *Anopheles* ingests gametocyte infected erythrocytes. The drop in temperature from the host to the mosquito, an increase in carbon dioxide and other mosquito metabolites induces gametogenesis and escape of microgametes and macrogametes from the erythrocytes (Soulard et al. 2015). Marcogametes are fertilized by microgametes to form a zygote. The zygote develops into a mobile okinete which is able to traverse the midgut epithelium and form a robust oocyst that undergoes multiple rounds of replication to produce sporozoites (Shahabuddin 1998). Rupture of the oocysts releases the sporozoites into the hemocoel of the mosquito. The sporozoites migrate to and invade the salivary glands to complete the cycle (Aly et al. 2009).

Historically, human malaria control has involved a combination of vector-based interventions and antimalarial drugs (WHO 2008). Traditional interventions included the use of insecticides, physical barriers such as bed nets and destruction of mosquito breeding sites (Walker 2002). Past eradication initiatives have been successful in parts of Europe and North America due in principle to control of the mosquito vector populations and access to effective medical treatment (Walker 2002). However new human malaria cases continue to arise in part due to insecticide-resistant vectors and drug-resistant parasites among other challenges (WHO 2008). These failures have stipulated the need for integrative malaria interventions that utilize innovative scientific research to interrupt transmission at all stages of the parasite life cycle (WHO 2008). Vaccines have the potential to interrupt the human malaria parasite at different stages in the life cycle, however low efficacy and coverage in vaccine trials, coupled with other developmental challenges has hindered progress (WHO 2006; WHO 2008).

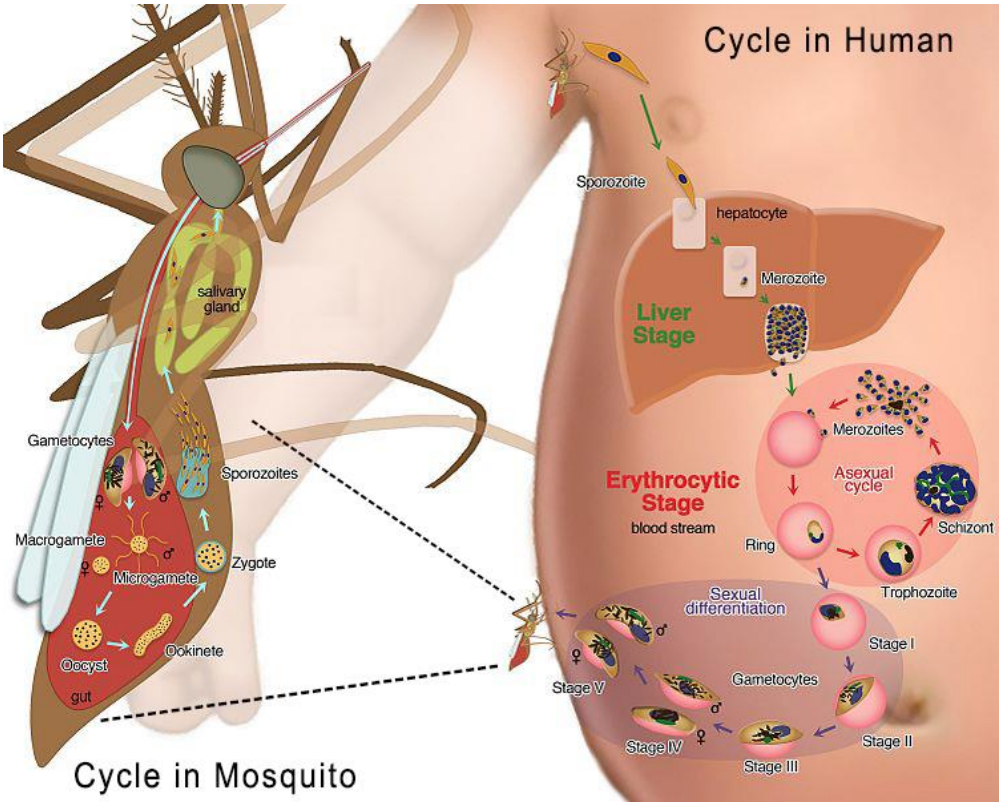

Figure 1.2- Life cycle of the malaria parasite. Diagram depicts the mosquito vector stage of the life cycle on the left and the vertebrate host stage on the right. Generally, the life cycle for all *Plasmodium* species is the same. (Adapted from "Creative Commons Falciparum life cycle" by Le Roche Lab UC Riverside, used under CC BY 3.0 *http://ucrtoday.ucr.edu/19520*)

1.4 Developing Vaccines against Malaria

The challenge of developing a highly effective malaria vaccine has led to the design and assessment of a wide range of new approaches (Hill 2011). Early infection studies using radiated sporozoites in mice (Nussenzweig et al. 1967) and later in humans (Clyde et al. 1975), coupled with the analysis of the mechanism of immunity (Doolan and Hoffman 1997) have formed the basis for modern malaria vaccine development. The aforementioned studies by Clyde and colleagues demonstrated that a high level of protection to subsequent malaria infections could be induced in humans after being bitten by irradiated infectious mosquitoes.

Pre-erythrocytic Vaccines

Vaccines that aim to protect against development of the parasite in the hepatocytes are termed pre-erythrocytic vaccines (Chia et al. 2014). These vaccines stimulate an immune response to prevent infection of hepatocytes or attack already infected cells (Hill 2011). The Malaria Vaccine Institute categorizes these vaccines as such:

- Live, attenuated vaccines that contain of a weakened form of the whole parasite (the sporozoite) as the vaccine's main component.
- Vectored/Recombinant or genetically engineered antigens from the surface of the parasite or from the infected liver cell.
- DNA vaccines that contain the genetic information for antigen production in the vaccine recipient.

Whole Parasite Vaccines

The development of a whole parasite vaccine for human malaria had been considered clinically impractical (Hoffman et al. 2010). Studies with humans Clyde, Mccarthy, et al. (1973); Clyde, Most, et al. (1973) and Clyde et al. (1975; Hoffman et al. 2002) demonstrated that for high-level efficacy, individuals required approximately 1000 bites from infected mosquitoes, an impractical method for public administration of a vaccine. High efficacy also required the parasites be alive when administered, meaning the vaccine would have to be injectable. In addition, the vaccine would need to be stable, cryopreservable, aseptic and scalable for large quantity manufacturing. (Hoffman et al. 2010; Hill 2011). Despite the challenges facing this approach, a major effort has been made by a US biotech company, Sanaria, to develop a pre-erythrocytic vaccine comprising whole sporozoites (Hoffman et al. 2010). The catalyst behind this approach is the knowledge that irradiated sporozoites delivered by mosquito bites have induced very high levels of protective efficacy. In 2013, Sanaria reported the results of clinical trials which showed that a live radiation attenuated *Plasmodium falciparum* sporozoites vaccine (RA PfSPZ) conferred protection against the development of blood stage infections. Twelve of fifteen volunteers immunized using the live RA PfSPZ vaccine were protected against blood stage malaria including 100% protection for 6 volunteers who received higher doses (Seder et al. 2013). Live attenuated irradiated sporozoites are able to invade liver cells but develop into defective schizonts that cannot rupture the hepatocytes to release merozoites that would normally invade red blood cells resulting in blood stage malaria. These defective schizonts express antigens that can induce a protective immune response. In animal models, protection via the

whole parasite approach was likely achieved through the activity of induced CD8 T cells that clear infected human liver cells, but this remains to be demonstrated (Hill 2011). Even though high-level efficacy can be achieved using this approach, the challenge of manufacturing cost remains (Chia et al. 2014).

Efforts have also been made to eliminate the need for irradiating sporozoites. Genetically attenuated sporozoites that are incapable of developing beyond the liver-stage of the disease are being developed (Vaughan et al. 2010). Parasites engineered to progress to a later stage of development within the hepatocytes than irradiated parasites could present more antigens and possibly be more efficacious (Vaughan et al. 2010). With no radiation however, there are concerns about the safety and the possibility of break-through infections even if multiple mutations are introduced (Hill 2011).

In an extension to the whole parasite vaccines approach, researchers have investigated the possibility of using blood stage whole parasites to induce immunity (Hill 2011; Butler et al. 2012). In clinical trials it was demonstrated that very low, repeated doses of blood stage whole parasite could induce immunity to subsequent challenges in both animals and humans in the absence of induced antibodies. (McCarthy and Good 2010). However a major challenge to this approach is an acceptable method for growth of large enough numbers of parasites in blood or blood substitute (McCarthy and Good 2010).

Vectored/Recombinant Vaccines

These pre-erythrocytic vaccines are aimed mainly at inducing cellular immunity against the liver-stage of the parasite (Chia et al. 2014). These vaccines

mimic the mechanism of the immune response to irradiated sporozoites observed in animal models which is due to chiefly to CD8 T cells and appears to target multiple antigens (Doolan and Hoffman 1997). Several generations of vectored vaccines have been assessed clinically in attempts to induce comparable efficacy (Hill 2011). However, generating high-level efficacy with vectors encoding single antigens has proven to be difficult, in part because the levels of T cells required are exceptionally high (Reyes-sandoval et al. 2010) and also because of the large number of protein antigens (>5,000) expressed by the eukaryotic parasite and the complexity of the organism (Gardner et al. 2002; Butler et al. 2012). Eukaryotic parasites have complex multi-stage life cycles and at each stage there can be an enormous variation in the proteins expressed (>5,000) (Gardner et al. 2002; Butler et al. 2012). To increase T cell levels a "prime boost" approach (Ewer et al. 2013) has been developed that uses chimpanzee adenoviruses (ChAds) encoding a pre-erythrocytic antigen, thrombospondin-related adhesion protein (TRAP) and another viral vector, modified vaccinia virus Ankara (MVA) that encodes another copy of TRAP to prime an immune response (Hill et al. 2010; Reyes-sandoval et al. 2010). Other priming methods using a DNA priming vector and a human adenovirus Ad5 have also been developed (Chuang et al. 2013). To date further antigens including circumsporozoite protein (CSP) and the blood-stage antigens apical membrane antigen-1 (AMA1) and merozoite surface protein-1 (MSP1) have been assessed (Chia et al. 2014; Foquet et al. 2014).

Blood-stage Vaccines

Blood-stage vaccines target the most destructive stage of the parasite life cycle; rapid replication in the erythrocytes (Goodman and Draper 2010) . Unlike pre-

erythrocytic vaccines, blood stage vaccines do not aim to block all infections but decrease the number of parasites in the blood, and in so doing, reduce the severity of disease (Goodman and Draper 2010). Evidence suggests that people who have survived regular exposure to malaria develop natural immunity over time. The goal of a vaccine that contains antigens or proteins from the surface of the blood-stage parasite (the merozoite) would be to allow the body to develop that natural immunity with less risk of getting ill (Osier et al. 2014).

Development of blood-stage vaccines has generally been slower compared to pre-erythrocytic vaccines (Goodman and Draper 2010). Blood stage vaccines that have progressed to clinical studies have not yet achieved good evidence of protective efficacy against clinical malaria. Many of these vaccine candidates are based on just a few antigens, MSP1 and AMA1 in particular, although there are hundreds or perhaps thousands of antigens expressed by blood-stage parasites that might be used in vaccine development (Chia et al. 2014; Osier et al. 2014). Majority of these candidate vaccines have been a protein-adjuvant combination designed to induce protective antibodies that impair parasite growth (Ellis et al. 2009; Druilhe et al. 2005). Three particular challenges for the development of blood-stage vaccines are 1) Large-scale production of conformationally correct large antigens, 2) weak antibody response (Ellis et al. 2009) and 3) the extensive polymorphism of many leading candidate blood-stage antigens (Takala et al. 2009).

Transmission-Blocking Vaccine (VIMTs)

Transmission-blocking vaccines work by inducing antibodies that interrupt development of the parasite in the mosquito after it takes a blood meal from a vaccinated person (Coutinho-Abreu and Ramalho-Ortigao 2010; Arévalo-Herrera et al. 2011; Nunes et al. 2014). Transmission-blocking vaccines would not prevent a person from getting malaria, nor lessen the symptoms of the disease but would limit the spread of infection by preventing mosquitoes that fed on an infected person from spreading malaria to new hosts (Hill 2011). Antigens from the gametocyte or sexual stage of the malaria parasite are used to immunize individuals (Rhoel R. Dinglasan and Marcelo Jacobs-Lorena 2008). The principle that immunization with gametocyte or ookinete antigens could reduce or ablate oocyst development in the mosquito was first reported by (Carter & Chen 1976). However, concern that utilization of such a transmission-blocking vaccine would be impractical because of the mass vaccination needed initially limited development. However, new findings such as the possible ookinete receptor, aminopeptidase (APN1), along with the potential cross species activity of transmission blocking vaccines, has rekindled interest (Dinglasan et al. 2007).

Sanaria's Malaria Vaccine: RA-PfSPZ

Sanaria is a biotechnology company located in Rockville Maryland with a mission to develop and commercialize a whole-sporozoite vaccine that confers high-level, long-lasting protection against the malaria parasite *Plasmodium falciparum*. (Sanaria Inc.). Results of a small human experiment reported in 2013 demonstrated 100% protection against blood stage infection for volunteers who received a high dose of Sanaria's RAPfSPZ vaccine. Sanaria estimates that a successful malaria vaccine has

the potential to be the largest revenue producing vaccine in the world, generating $1-$3 billion annually with many potential markets that include military personnel, government officials, and tourists who travel to malaria endemic countries.

Manufacturing of the RAPfSPZ vaccine is an expensive and labor intensive process that involves manual dissection of the salivary glands of infected female *A. stephensi* Sda 500 mosquitoes followed by purification of sporozoites away from the mosquito tissue and cells (Hoffman et al. 2010). Sanaria calculates that the cost of their RAPfSPZ vaccine is directly related to the number of sporozoites that develop in each infected salivary gland. Therefore, any increase in manufacturing efficiency will have a direct impact on reducing the cost of production. To improve manufacturing efficiency Sanaria plans to adapt genetically modified *A. stephensi* Sda500 that regular yield more sporozoites than the wildtype mosquito to their manufacturing platform.

1.5 The *Anopheles* Mosquito: The Malaria Vector

The *Anopheles* genus of mosquitoes is comprised of almost 500 species of which only 8-10% are vectors of the human malaria parasite (Collins and Paskewitz 1995). *A. gambiae,* the primary vector in the African region is the most studied species. Other species, such as *A. stephensi*, and *A. darlingi* are important vectors in Southeast Asia and South America, respectively (Sinka et al. 2012). See Figure 1.3 for a map of global malaria vectors. Various *Anopheles* sub-species and reproductively isolated genetic forms also contribute to the complexity of the genus (Lee et al. 2013; Lefèvre et al. 2009). For instance, *A. gambiae* is a species complex comprised of many geographically overlapping cryptic sub-species yet remaining genetically distinct. It is

hypothesized that genetic adaptations to varying environments among other factors drive speciation within the *Anopheles* genus (Caputo et al. 2014). *Anopheles stephensi* Sda500 used in the vaccine manufacturing platform of Sanaria , is a laboratory strain that was obtained through genetic selection of female mosquitos of the Sind strain that were exposed to highly infective in-vitro reared *P. falciparum* gametocytes (Feldmann and Ponnudurai, 1989). Feldman and Ponnudurai observed that Sda500 yielded twice as many oocyst in the midgut than the unselected Sind strain.

Regardless of environmental adaptive differences, *Anopheles* mosquitoes undergo a similar life cycle. Anautogenous adult females require a blood meal to produce eggs. Gravid females will oviposit approximately 50-200 eggs approximately 48-72hrs post blood-meal in a suitable, aqueous environment. Under optimal conditions most of the eggs will hatch within 3 days of oviposition, however temperature variability can result in hatch times 2-30 days or longer. Larvae cycle through 4 developmental stages (L1, L2, L3, L4) that can range from 5-14 days (Bray & Garnham 1982) . After the L4 stage, larvae pupate and undergo metamorphosis into adults (Charlesworth 2014). After mating males typically die off whereas females go in search of a blood meal. *Anopheles* mosquitoes are anautogenous and the female mosquito requires a blood meal to produce eggs to continue the life cycle (Hillyer 2010). Females may take more than one blood meal during their life span, and these additional blood meals are responsible for transmission of malaria parasites (Elliott 1972).

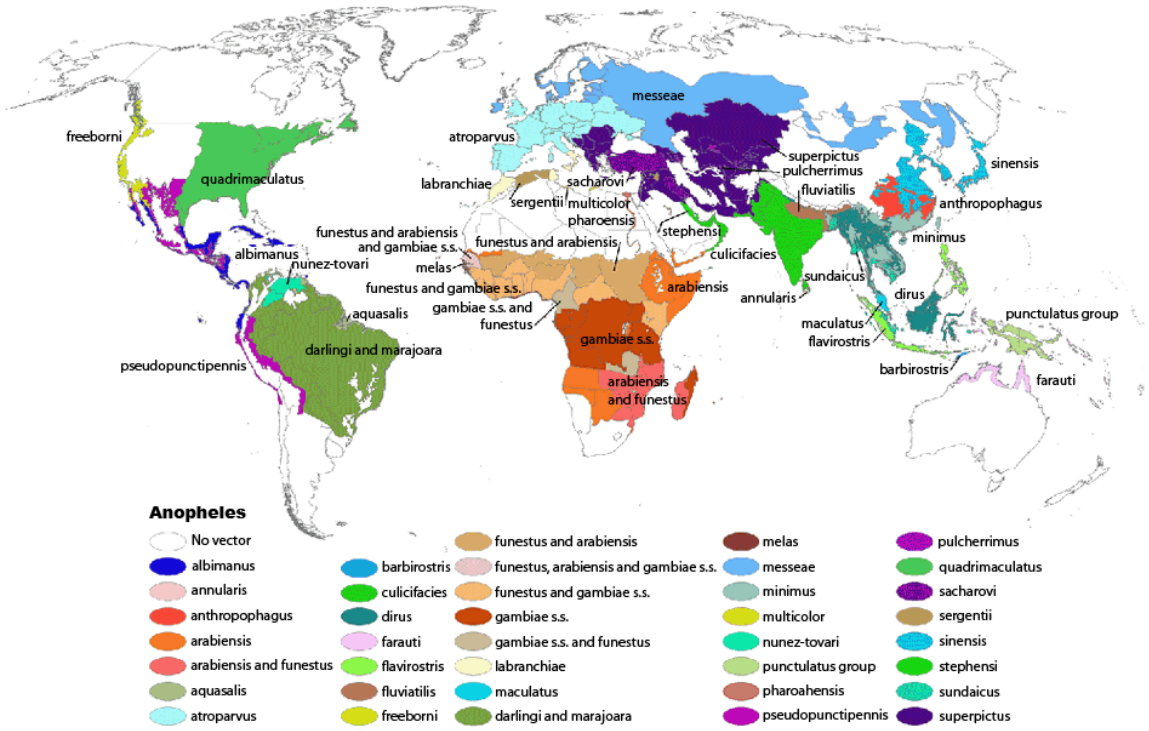

Figure 1.3- Geographic location of malaria vectors. Distribution of mosquitoes of the *Anopheles* genus that are vectors of the malaria parasite. (From Kiszewski et al. 2004)

1.6 Unravelling the Mosquito Immune System for Malaria Control

The *Anopheles* genome contains many uncharacterized genes that are regulated by *Plasmodium* infection (Dong et al. 2006). Genome re-sequencing, high throughput transcriptomics analysis of malaria vectors, coupled with the advances in mosquito molecular genetics, have enabled researchers to identify genes potentially involved in insecticide resistance, host and mate seeking behaviors and refractoriness to *Plasmodium* (Lynd and Lycett 2012). Recent proposals aimed at preventing parasite transmission include creating *Plasmodium* resistant mosquitoes and introduction of transgenic mosquitoes into native mosquito habitats that will convert later generations of mosquitoes into non-vectors (Marshall and Taylor 2009).

Anopheles gene function has been primarily characterized through the use of transient RNA interference (RNAi) (Shin, V.A. Kokoza, et al. 2003). Although functional characterization of genes using transient RNAi is possible in adult mosquitoes (Catteruccia and Levashina 2009) this method is limited not least by the non-systemic nature of gene silencing in mosquitoes (Lycett et al. 2006). The Gal4/UAS bi-partite system (Figure 1.4) is a powerful functional genomics tool that has been routinely used with great success in *Drosophila* and has been more recently adapted for use in *Anopheles* (Lynd & Lycett 2012; O'Brochta et al. 2012). The system can be used in a wide variety of applications such as generating phenotypes through transgene mis- or over-expression, enhancer detection and stable gene knockdown through RNAi and refined mosaic analyses (Duffy 2002).

The bi-partite system uses a transgenic “driver” line with the yeast transactivator, Gal4, under the transcriptional control of a specific regulatory region; and a transgenic ‘‘responder’’ line that contains a candidate gene under the transcriptional control of an upstream activation sequences (UAS) containing multiple Gal4 binding sites (Fischer et al. 1988; Ornitz et al. 1991; Brand and Perrimon 1993). Since most species, do not contain Gal4 equivalents, the candidate gene is only expressed in the progeny of crosses between driver and responder lines, when Gal4 and UAS transgenes are brought together in the same genome (Lynd and Lycett 2012). The expression of the candidate gene is dictated by the temporal and spatial pattern of the promoter or enhancer driving Gal4 expression (Lynd and Lycett 2012). Analysis of genes whose expression may exert a high fitness cost or dominant lethal or sterile phenotypes is also possible, since activation only occurs after crossing. Thus the effects of mis-expression can be studied even if they are somewhat deleterious (Brand and Perrimon 1994).

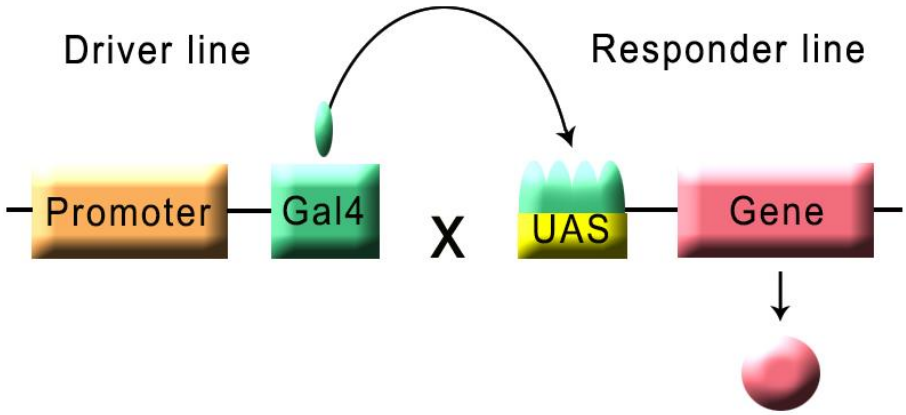

Figure 1.4- Gal4/UAS bi-partite system. The Gal4/UAS system utilizes a transgenic "driver" line with the yeast transactivator, Gal4, under the transcriptional control of a specific regulatory region; and a transgenic ‘‘responder’’ line that contains a candidate gene under the transcriptional control of the upstream activation sequences (UAS) also known as Gal4 binding sites. The system can be used to control the spatial and temporal pattern of a candidate gene expression and to analyze gene that may have a high fitness cost or lethal phenotype. (Adapted from Lynd & Lycett 2012)

1.7 Mosquito Innate Immunity

Mosquitoes like other organisms are exposed to the constant threat of infection and are specifically susceptible to infection by blood-borne pathogens such as *Plasmodium* during a blood meal (Hillyer 2010). Invertebrates including mosquitoes lack an adaptive immune system but utilize a highly effective innate immune system for their defense (Osta, Christophides, Vlachou, et al. 2004), (Dimopoulos 1997) During *Plasmodium* infection the innate immune system in combination with physical barriers such as the peritrophic matrix (PM) can reduce parasitemia 10^7 fold (Alavi et al. 2003; Hillyer 2010). Three major immune signaling pathways that have been demonstrated to protect the mosquito from pathogens are; the Toll pathway, the Jak/Stat pathway and the IMD pathway (figure1. 5) (Dimopoulos 1997; Christophides, Zdobnov, Barillas-Mury, Birney, Blandin, Blass, Brey, Collins, Danielli, Dimopoulos, Hetru, Hoa, J. a Hoffmann, et al. 2002; Shin, V. Kokoza, et al. 2003; Osta, Christophides, Vlachou, et al. 2004; Cirimotich et al. 2010; Yassine and M. a Osta 2010; Hillyer 2010; Pike et al. 2014)

Toll Pathway

The Toll pathway is activated during invasion by gram positive bacteria or fungi (Cirimotich et al. 2010). It has also been implicated in defense against viruses in mosquitoes (Xi et al. 2008) and fruit flies (Zambon et al. 2005). In the *Anopheles* malaria vector the Toll pathway has been demonstrated to respond to rodent malaria, *Plasmodium berghei* infection (Frolet et al. 2006). Pathogen associated molecular patterns (PAMP) are recognized by pathogen recognition receptors (PRR) such as PGRP-SA and -SD that trigger proteolytic cleavage of the cytokine Späetzle, that binds

to and activates the Toll receptor. This triggers signaling through the adaptor proteins MyD88, Tube, and Pelle, resulting in the phosphorylation and degradation of the Toll pathway negative regulator Cactus (Ip et al. 1993; Barillas-Mury et al. 1996; Han and Ip 1999; Manfruelli et al. 1999; Meng et al. 1999; Christophides, Zdobnov, Barillas-Mury, Birney, Blandin, Blass, Brey, Collins, Danielli, Dimopoulos, Hetru, Hoa, J.A. Hoffmann, et al. 2002). Degradation by Cactus enables the NF-kappa-B like Rel1 transcription factor to translocate to the nucleus and initiate transcription of Toll pathway immune factors (Belvin et al. 1995; Barillas-Mury et al. 1996; Wu and Anderson 1998).

JAK-STAT Pathway

The JAK-STAT pathway named for the Jak kinase and STAT transcription factor has been demonstrated to play a role in the immune response against pathogenic bacterial infections in the gut of *Drosophila* (Buchon et al. 2009; Cronin et al. 2009) and against viral activity in *Drosophila* (Dostert et al. 2005) and *Aedes aegypti* (Souza-Neto et al. 2009). Gupta et al. 2009 demonstrated that the JAK-STAT pathway plays a role in *P. falciparum* and *P. berghei* infections post midgut stage infection however the mechanism by which this is done is less understood (Cirimotich et al. 2010). Activation of the JAK-STAT pathway is triggered by Unpaired (Upd) binding to the receptor Dome, activating the receptor-associated Hop Janus kinases, which phosphorylate each other and recruit and phosphorylate STAT. STAT undergoes dimerization and translocates to the nucleus to activate transcription of target genes (Agaisse and Perrimon 2004). Two transcription factors STAT A and STAT B have been identified in *A. gambiae*. Depletion of STAT A has been demonstrated to increase oocysts levels

of *P. berghei* while depletion of the JAK/STAT negative regulator, SOCS, decreased infection (Gupta et al. 2009).

Immune Deficiency (IMD) Pathway

The IMD pathway in *Anopheles*, has been shown to play a major role in the mosquito refractory response to bacteria (Meister et al. 2005) and *Plasmodium* (Richman et al. 1997; Osta, Christophides & Kafatos 2004; Meister et al. 2005; Garver et al. 2009; Garver et al. 2012; Meister et al. 2009; Pike et al. 2014; Cirimotich et al. 2010; Yassine & M. a Osta 2010). The IMD pathway, can be compared to the tumor necrosis factor (TNF) signaling pathway in mammals (Kaneko and Silverman 2005; Aggarwal and Silverman 2008). Pathogens detected by peptidoglycan recognition proteins (PGRPs) initiate intracellular signaling through the adaptor IMD protein and various caspase-like proteins and kinases, leading to a functional split in the pathway (Rutschmann et al. 2000; Georgel et al. 2001; Choe et al. 2002; Leulier et al. 2002; Leulier et al. 2003; Choe et al. 2005; Kleino et al. 2005; Tanji and Ip 2005). One branch is similar to the c-Jun N-terminal Kinase (JNK) pathway of mammals and uses JNK to activate the transcription factor AP-1, while the other branch, an NF-kappaB activating branch, culminates in the processing of the transcription factor Rel2 (Tanji & Ip 2005b; Gupta et al. 2009; Meister et al. 2005; Stoven et al. 2003; Hedengren et al. 1999; Dushay et al. 1996; Kallio et al. 2005; Silverman et al. 2000; Stoven et al. 2000; Sluss et al. 1996; Hoa & Zheng 2007). The REl2 transcription factor exists as two splice variants (Meister et al. 2005; Luna et al. 2006). The constitutively active form Rel2-S is a shortened form that lacks the ankyrin inhibitory domain and is responsible for basal immune response whereas Rel2-F, the full length form of the transcription factor

remains inactive until there is immune signaling (Meister et al. 2005; Luna et al. 2006). Activation of the IMD pathway leads to cleavage of the carboxyl terminal end of Rel2-F and exposes the nuclear localization signal (Meister et al. 2005; Luna et al. 2006). Cleaved Rel2-F translocates to the nucleus to initiate transcription of immune factors such as leucine rich immune molecule 1 (LRIM1), *Anopheles Plasmodium* responsive leucine rich repeat 1 (APL1) and thioester containing protein 1 (TEP1) (Cirimotich et al. 2010).

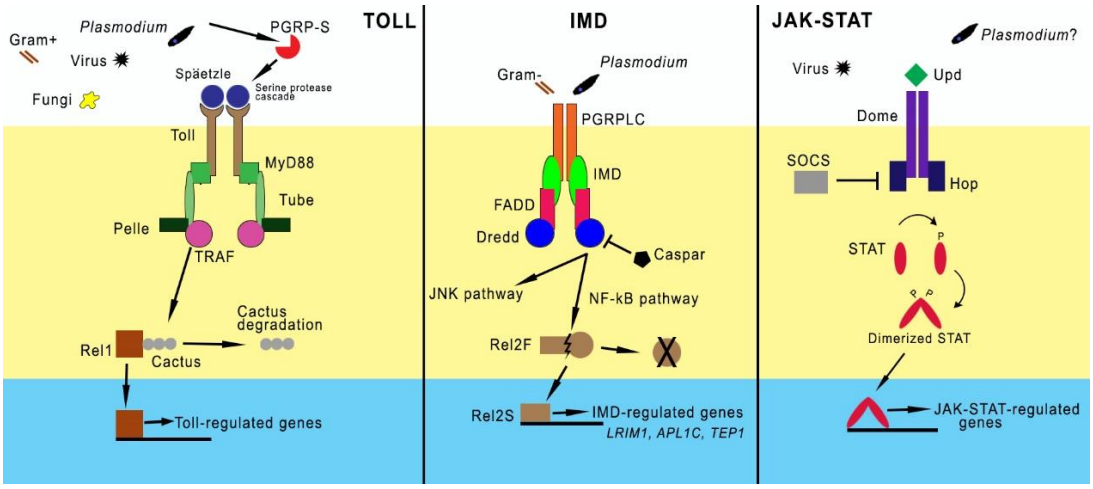

Figure 1.5- Mosquito humoral immune signaling pathways. In Toll pathway signaling, detection of pathogen-derived ligands by PRRs results in Rel1 translocation to the nucleus and activate transcription of Toll-pathway regulated genes. The IMD pathway is activated by ligand binding to PGRP-LCs and -LEs. This triggers signaling through IMD and various caspases and kinases, leading to a functional split in the pathway. One branch triggers JNK signaling to activate the transcription factor AP1, while the other results in the phosphorylation of transcription factor Rel2. Activated Rel2 translocates to the nucleus to activate IMD-regulated transcription. The JAK-STAT pathway is triggered by Unpaired (Upd) binding to the receptor Dome, activating the receptor-associated Hop Janus kinases, which phosphorylate each other and subsequently recruit and phosphorylate the STAT transcription factor. Phosphorylated STATs dimerize and translocate to the nucleus to activate JAK-STAT-regulated transcription (Adapted from Sim et al. 2014)

1.8 Mosquito Immune Effectors

Analysis of the transcriptional profile of mosquitoes at different stages of the *Plasmodium* infection, especially in the midgut during ookinete invasion has identified anti-*Plasmodium* effector molecules. These effector molecules have mainly been characterized through RNAi-based transcript depletion that results in increased levels of *Plasmodium* infection. Further characterization has associated some of these effector molecules with specific immune pathways and processes (Cirimotich et al. 2010). Although there are a number of anti-*Plasmodium* effector molecules, only the most pertinent ones are covered here.

Thioester-containing protein 1

Thioester-containing protein 1 (TEP1) is an anti-*Plasmodium* effector molecule and one of the most well studied. TEP1 is involved in range of immune responses including phagocytosis, parasite lysis, and melanization (Blandin et al. 2004; Yassine & M. *A.* Osta 2010; Garver et al. 2012; Yassine et al. 2012). Studies have shown that it controls both *P. berghei* and *P. falicparum* infection in the mosquito midgut (Garver et al. 2013; Garver et al. 2009). Blandin et al., 2004 identified TEP1 as the mosquito orthologue of complement component 3 (C3) in the human complement system. Recent studies have established the role of TEP1 in a highly regulated complement-like process in the mosquito, in which TEP1 is deposited on the surface of pathogens (Yassine et al. 2014). *TEP1* expression is strongly regulated by the IMD pathway (Garver et al. 2009). Although there are other Tep molecules in the mosquito, their role in anti-*Plasmodium* defense is not yet known.

Leucine-Rich Immune Molecule 1

Another important anti-*Plasmodium* effector molecule is leucine-rich immune molecule 1 (LRIM1) that has been shown to control *P. berghei* (Meister et al. 2005) and *P. falciparum* infections (Garver et al. 2012). Research has shown that TEP1 forms complexes with leucine-rich proteins on the surface of parasites, indicating these molecules may be involved in the complement-like process (Fraiture et al. 2009; Povelones and Waterhouse 2009; Baxter et al. 2010; Povelones et al. 2011). However, the principal mechanism behind this finding is not well understood and there are possibly many more interacting partners of leucine-rich proteins.

Leucine-rich repeat (LRR) containing proteins are found in various organisms and have been shown to have multiple functions (Povelones and Waterhouse 2009). Insects and mammals contain Toll-like receptors involved in initiating an innate immune response to pathogens (Vasselon and Detmers 2002). Nucleotide-binding oligomerization domain receptors proteins (NOD) in mammals and plants contain LRR structures and are involved in immunity and host-defense responses (Loimaranta et al. 2009). The LRR superfamily is composed of LRR proteins with various domain architectures such as Toll receptors with intracellular Toll-interleukin receptor domains (Waterhouse et al. 2010). Proteomic analysis of the *Anopheles* mosquito has identified over 180 LRR superfamily members, 24 belonging to the LRIM family which has only been identified in mosquitoes (Waterhouse et al. 2010). LRIM family members are composed of an N-terminal signal peptide, repeated LRRs that form a horseshoe-like structure, a pattern of cysteine residues and a coiled coil domain (Waterhouse et al.

2010) (Figure 1.6). LRIM family members that contain all these sequence patterns are grouped into the Long LRIM subfamily (Waterhouse et al. 2010). Further LRIM subfamilies identified by Waterhouse and colleagues include a short LRIM subfamily that contain 6-7 repeated LRR, and Transmembrane LRIM subfamily which have predicted C-terminal transmembrane domains. Leucine rich immune molecule 1 is a LRR protein found in mosquitoes. LRIM 1 is a member of the long LRIM subfamily in mosquitoes. It has been shown to be an effector molecule in the IMD pathway of *Anopheles* mosquitoes and a strong suppressor of parasite development, during low to medium infection intensities (Garver et al. 2012) playing a role in both melanization (Warr et al. 2006), and lysis (Jaramillo-Gutierrez et al. 2009), (Habtewold et al. 2008) of the parasite. *LRIM1* expression in *A. gambiae* has been demonstrated to be regulated by *Plasmodium* infection with maximum expression coinciding with the movement of *Plasmodium* ookinetes across the basal gut epithelium (Han et al. 2000; Osta, Christophides & Kafatos 2004; Marinotti et al. 2005). RNAi studies have demonstrated that silencing of *LRIM1*expression with dsRNA increased the intensity of *Plasmodium berghei* oocysts infection 3 - 4.5 fold in *A. gambiae* (Osta, Christophides, and Kafatos 2004). In similar studies, (O'Brochta et al. unpublished) demonstrated that silencing *LRIM1* expression in *A. stephensi* using dsRNA transcribed *in vitro* using *A. gambiae LRIM1* as a template increased the number of sporozoites in the salivary glands 2.5 fold

The present model suggests that LRIM1 functions in a complement-like pathway leading to the activation of a C3-like protein, TEP1, that localize to the surface of the pathogen, targeting it for destruction (Fraiture et al. 2009), (Povelones and Waterhouse 2009), (Baxter et al. 2010). LRIM1 covalently binds intracellularly to

APL1 forming a heterodimer (Figure 1.7) that is secreted into the hemolymph. The LRIM1/APL1 complex then binds to a mature cleaved TEP1 molecule stabilizing it and promoting binding to the pathogen surface (Fraiture et al. 2009; Waterhouse et al. 2010; Baxter et al. 2010; Povelones et al. 2011).

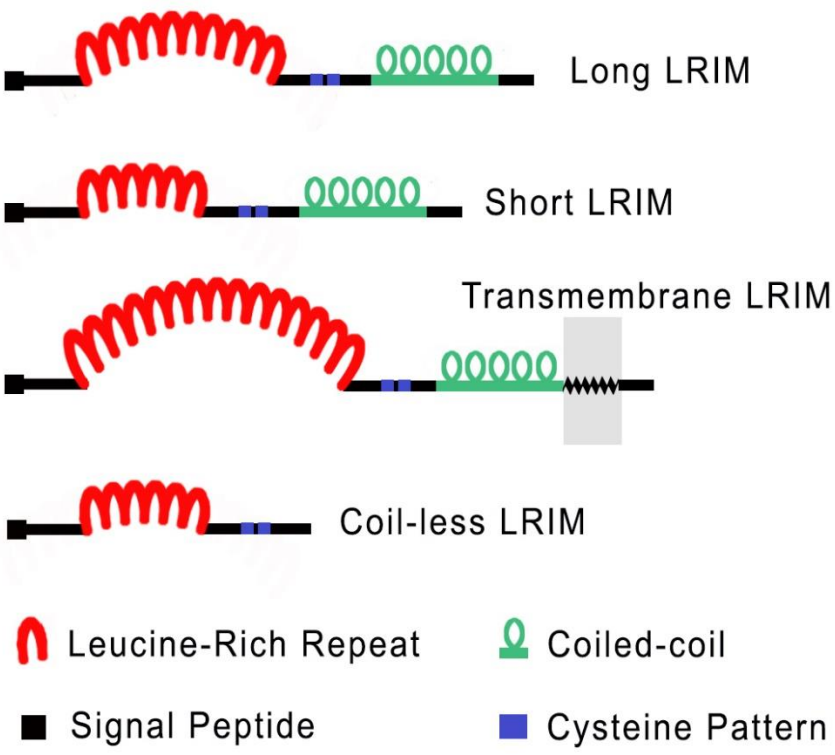

Figure 1.6- Structure of LRIM family members. Members of the LRIM family are characterized by four structural patterns. An N-terminal signal peptide; repeated LRR which form a horseshoe like structure; a pattern of cysteine residues, and a coiled coil domain region. Further sub-families includes Transmembrane LRIMs which have predicted C-terminal transmembrane domains and Coil-less LRIMs with all the characteristic structures except the coiled coil domain. (Adapted from Waterhouse et al. 2010)

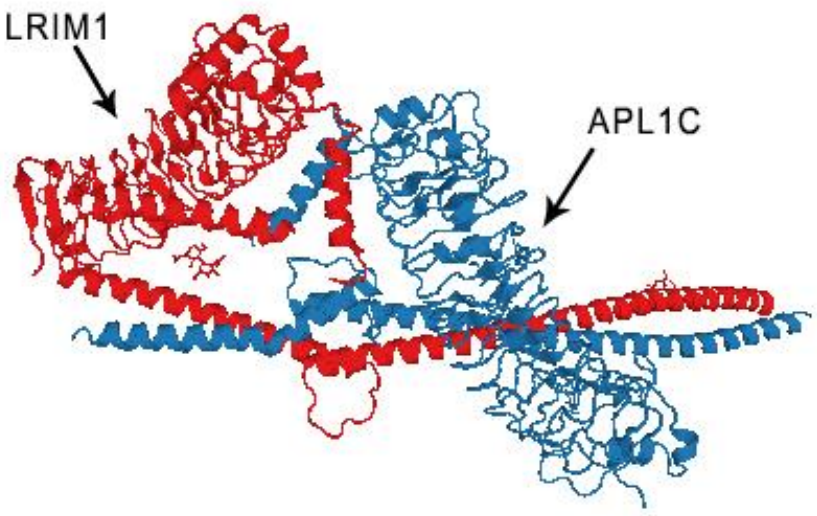

Figure 1.7- Crystal structure of the LRIM1/APL1C heterodimer. The LRIM1/APL1C heterodimer is secreted into the hemolymph where it bind to a cleaved TEP1 molecule stabilizing it. The TEP1/LRIM1/APL1C complex bind to the surface of foreign bodies or pathogens targeting them for destruction by the immune system. (Adapted from PDB ID: 30JA, Baxter et al. 2010)

1.9 Summary and rationale of dissertation research

In the first part of this work I investigate the immune response of *Plasmodium* susceptible *Anopheles stephensi* Sda500 to infection by *Plasmodium falciparum* NF54. The mosquito immune response to *Plasmodium* has been demonstrated to be dominated by IMD pathway effector molecules in *Plasmodium* refractory strains of *A. gambiae* and *A. stephensi*. Sanaria's vaccine manufacturing platform utilizes the laboratory derived strain of *A. stephensi* which was selected for its susceptibility to *Plasmodium* infection. Since the aim of the project is to attenuate the immune response to increase sporozoite infection in the salivary glands, the immune response and specifically the IMD pathway response in *A. stephensi* Sda500 is assessed during *Plasmodium* and bacterial infection. After identifying homologs of IMD effector genes in *A. stephensi* I used real-time quantitative PCR to assess gene expression during infection. The unique findings demonstrate an IMD immune response to *Plasmodium* infection and may indicate the regulation of IMD effector genes by different pathways.

In the second part of this work I explore the use of the Gal4/UAS bi-partite system for stable gene knockdown using shRNA. Due to strict manufacturing protocols, injecting mosquitoes with dsRNA is not feasible, therefore a stable transgenic mosquito line with regulated silencing cassettes is developed. The Gal4/UAS system is commonly used in *Drosophila* and has been recently adapted for use in mosquito. However work to date has not used the system for gene knockdown in mosquitoes. I designed a plasmid containing an inverted repeat of a region of *LRIM1* under the regulatory control of UAS and inserted it into the genome of *A. stephensi* Sda500 using transposon-based gene vectors. The unique findings demonstrate the

adaptation of the Gal4/UAS system for spatial and temporal gene silencing in mosquitoes. Infection studies of transgenic mosquitoes demonstrated that silencing of *LRIM1* can increase sporozoite infection in the salivary glands and therefore these transgenic mosquitoes are excellent candidates for being incorporated into the sporozoite and vaccine production process at Sanaria Inc.

In the third part of this work I identify and clone the *LRIM1* promoter region to identify the tissues where *LRIM1* is expressed. This could allow for targeted knockdown of *LRIM1* expression to increase sporozoite infection in the salivary glands. The current model of *LRIM1* function proposes that *LRIM1* is expressed in the fat body, midgut and hemocytes of *A. gambiae*. However, microarray experiments of *A. gambiae* have shown evidence of *LRIM1* expression in the head, salivary glands, ovaries and malpighian tubules of adult females. It is therefore unclear exactly where and when *LRIM1* is expressed and how this relates to its purported function. Here, I attempt to determine the spatial and temporal pattern of *LRIM1* expression by creating transgenic mosquitoes that will make use of the bi-partite Gal4::UAS system to control the expression of a fluorescent gene.

Chapter 2: Validation of *Anopheles stephensi LRIM1* as a viable target for immune system modification in Sda500

2.1 Introduction

Development of a live-attenutated *Plasmodium falciparum* sporozoites vaccine for malaria was thought to be clinically impractical for three primary reasons: (1) Sporozoites would need to be delivered alive to be effective; (2) the vaccine would need to be stable, aeseptic and cryopreservable, and (3) the difficulty of efficiently generating sufficient sporozoites for vaccine manufacturing (Hoffman et al. 2010). Presently, Sanaria Inc. has addressed the challenge of vaccine delivery by developing a clinically accepted intravenous route for vaccine administration, and they have also developed a proprietary method for rearing aseptic mosquitoes to produce stable, aseptic sporozoites that are cryopreservable. However vaccine production still remains an expensive, labor intensive process and is expected to directly impact vaccine cost (Sanaria Inc.). To produce the vaccine, sporozoites are taken directly from the salivary glands of infected female mosquitoes, therefore directly linking vaccine production to salivary gland infection intensity and prevalence (Sanaria Inc.). The mosquito's immune system plays a major role in limiting the parasite's development and the infection intensity of sporozoites. (Cirimotich et al. 2010; Hillyer 2010). Therefore, we hypothesized that modifying the immune system of the mosquito to increase salivary gland infection intensity would increase vaccine production and lower its cost.

The Immune Deficiency (IMD) pathway in *Anopheles*, has been shown to play a major role in the mosquito's immune response to *Plasmodium falciparum* (Cirimotich et al. 2010; Hillyer 2010). Female *Anopheles* are exposed to *Plasmodium* during a

blood meal. During development in the mosquito, the number of parasites can be reduced by as much as 10^7 fold by the innate immune system (Alavi et al. 2003; Hillyer 2010).

LRIM 1 is an effector molecule in the IMD pathway of *Anopheles* mosquitoes and has been shown to be a strong antagonist of parasite development during low to medium infection intensity (Garver et al. 2012) and plays a role in both melanization (Warr et al. 2006), and lysis (Jaramillo-Gutierrez et al. 2009; Habtewold et al. 2008) of the parasite. RNA interference (RNAi) studies have demonstrated that silencing *LRIM1* expression with dsRNA increased the intensity of *Plasmodium berghei* infection 3 - 4.5-fold in *A. gambiae* as reflected in the number of oocysts (Osta, Christophides, and Kafatos 2004). In similar studies, O'Brochta et al. (unpublished) demonstrated that silencing *LRIM1* expression in *A. stephensi* using dsRNA transcribed *in vitro* using *A. gambiae LRIM1* increased the number of sporozoites in the salivary glands 2.5-fold.

The laboratory strain *Anopheles stephensi* Sda500 is the mosquito used as Sanaria Inc's manufacturing platform due to its high susceptibility to *Plasmodium* infection, consistently having 2-fold higher infection intensity, compared to *Sind* strains (Feldmann et al. 1990). The mechanism for its increased susceptibility is presently unknown, but could be a result of mis-regulation of the IMD pathway which could make the IMD pathway a poor target for genetic modification in this strain. Furthermore, previous studies looking at the effects of *LRIM1* on parasite survival have concentrated on *Anopheles gambiae* and other *Plasmodium falciparum* resistant

Anopheles species. Therefore it is unclear whether *LRIM1* would be good target for increasing the susceptibility of *A. stephensi* to *Plasmodium falciparum*.

The aim of this project was to test the validity of *A. stephensi LRIM1* as a viable candidate for immune modification by identification and cloning of *A. stephensi LRIM1* and examining the expression pattern of *A. stephensi LRIM1* under challenge with *Plasmodium falciparum* and *E. coli*.

2.2 Materials and Methods

Materials and Methods can be found on page 111

2.3 Results

Cloning of *Anopheles stephensi* Sda500 *Leucine Rich Immune Molecule 1*

Anopheles stephensi Sda500 cDNA was generated by *in vitro* reverse transcription of *A. stephensi* Sda500 RNA was used as the template in a polymerase chain reaction (PCR) using primers AsLRIM1fw (5' - CCC GCC GGT ATA GCT TAT CAG – 3') and AsLRIM1rv (5'- CAA ATA GTG CTC GTC TGC GC - 3') that were designed based on a known *A. gambiae LRIM1* sequence aligned to an assembled draft genome sequence of *A. stephensi* created by Dr. Zhijian Tu at Virginia Polytechnic Institute and State University, Blacksburg VA 24061. Polymerase chain reaction generated a 1.8 kilobase fragment. Nucleotide pairwise sequence alignment to the known *A. gambiae LRIM1* sequence showed 58 percent sequence identity. Amino acid pairwise alignment (Clustal Omega) showed 60 percent amino acid identity of *A. stephensi LRIM1* to *A. gambiae LRIM1*. Further sequence analysis using LRR finder (Bej et al. 2014) identified 9 Leucine-rich repeat domains consisting of 19 to 41 amino

acid residues(Figure 2.1). Marcoil analysis (Delorenzi and Speed 2002) with a 99% threshold identified two coiled coil domains in the region of amino acid residues 318 to 366 and 424 to 459 (Figure 2.1). SignalP-4.0 (Petersen et al. 2011) identified a signal peptide region from residue 1 to 19 (Figure 2.1). Further analysis using the most current *A. stephensi* genome release, VB-2015-10, AsteS1 (Jiang et al. 2014) identified our predicted *LRIM1* gene as long leucine rich immune protein LRIM1 (ASTE000814).

MVSLRVCTVLLAFVCVATAIHQVKHQGSKYKIEKVMDITLKHALESIRPSAWNVK
ELDLSGNLLSKISADDLAPFTNLEVLNVSSNVVYESLDVRSLSKLQTIDLNNNFVT
EVLVGPAIQTLHAANNNISSVICYGERQGWGSKRLYLANNKIGSCRSRVEYLDL
KLNEIDMLDFGDLAASSETLKHLNLEYNFIFDVKNQRNVVFSQLEMLDLSSNKLA
HLGPEFAAVSQGRSINLSNNKLVLLSEVKFSPAVTSFDLRGNGLQCATLKKFFK
KNKQLESVSIATVRDATGRDKEACTDTDKYEGPYCCENLVAPYAERLIDLKRKE
YALFSRVGSEKERAECEKENKDRLRKVDMIKKQYSTTIDEETRRNQMKIQLTQT
KTALERKLPALQNAYNELAGELETVAAELQITVTEDHNLLQLLRSIVQRYEDHYIE
EQGKQSNAIRDWDMYQKKETELLEENARMKKLNGEADTALQKANATLQDLNV
REQNLIKILISRVCKLASASRSLSYVASDIVWRAHVPCCFLMLWHKVVCG

Figure 2.1- *Anopheles stephensi* Sda500 LRIM1. Amino acid sequence of LRIM1 isolated and cloned from *Anopheles stephensi* Sda500. Characteristic feature of the leucine rich immune molecule family are shown. Signal peptide region-grey; leucine rich repeats-red; pattern of cysteine residues- blue and the coiled coil region- green.

Immune Response of *A. stephensi* Sda500 to *Plasmodium falciparum infection*

The carcass (all tissue remaining after removal of the midgut) and midgut of female *A. stephensi* were assessed for IMD pathway immune response at 24-26; 48-50; and 72-74 hours post blood feed infection. Using qRT-PCR, transcript levels of IMD effector genes *LRIM1*, *APLIC* and *TEP1* and also IMD pathway negative regulator *Caspar* were assessed in mosquitoes provided a *Plasmodium falciparum* infected blood meal, or a non-infected blood meal. Naïve mosquitoes maintained on 10% sucrose were used as controls. (Here, changes referred to as "modest" are significant but lower than 2 fold)

IMD Pathway Immune Response in Carcass

Between 24 to 26 hours post blood feed the transcript levels of *LRIM1*, *APLIC* and *TEP1* were specifically up-regulated in mosquitoes provided infected blood and non-infected blood compared to control mosquitoes maintained on sucrose. Average *LRIM1* expression in infected blood and non-infected blood-fed mosquitoes were respectively 5 and 2-fold greater than controls. *APLIC and TEP1* had average increases greater than 3-fold in *Plasmodium* infected mosquitoes compared to control mosquitoes, while there were modest increases in *APL1C* and *TEP1* in non-infected blood fed mosquitoes. Average *Caspar* transcript levels were lower in both infected and non-infected blood fed mosquitoes compared to control naïve mosquito (Figure 2.2).

In mosquitoes assessed 48 to 50 hours post blood feed, transcript levels of *LRIM1*, *APL1C* and *TEP1* decreased and were now lower in infected and non-infected

blood fed females compared to controls. However *Caspar* transcript levels in both infected and non-infected blood fed females were on average more than 4-fold higher than in comparable naïve sucrose maintained females (Figure 2.3).

Assessment of mosquitoes 72 to 74 hours post blood feed showed that transcript levels of *Caspar* decreased in both infected and non-infected blood fed mosquitoes but remained over 2 folds higher than controls. *LRIM1* transcript levels in both blood fed groups remained lower than in controls. *APL1C* and *TEP1* transcript levels were also lower in infected blood fed females compared to controls, however in females fed non-infected blood both *APL1C* and *TEP1* had modestly higher transcript levels (Figure 2.4).

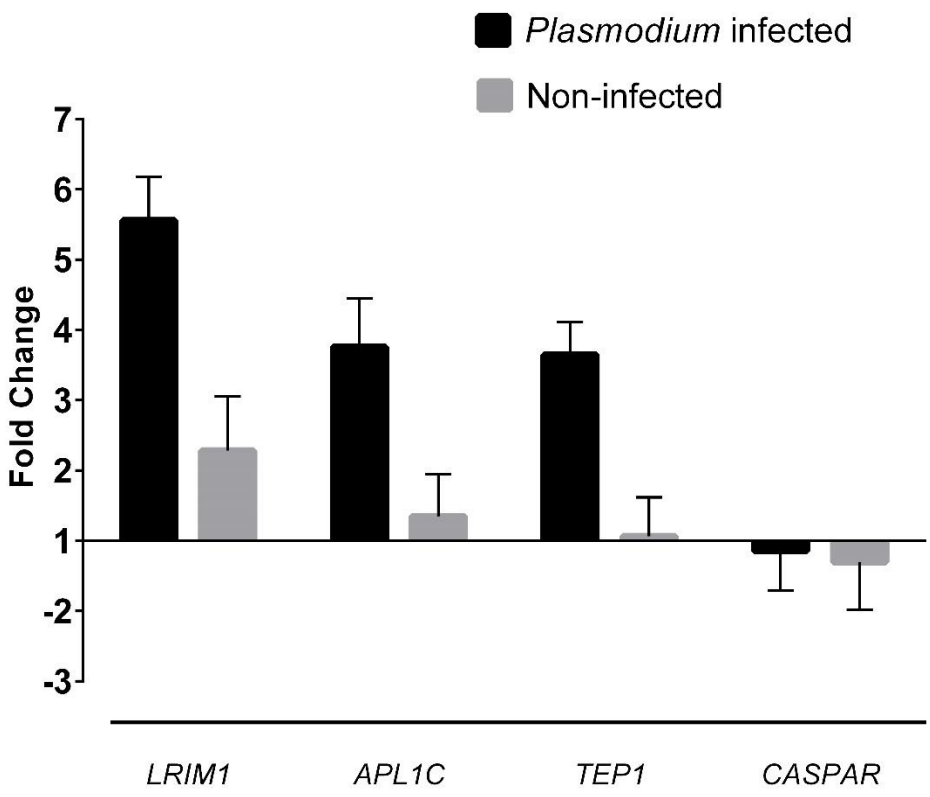

Figure 2.2 Transcript levels of *LRIM1*, *APL1C*, *TEP1* and *Caspar* in the carcass of *A. stephensi* females 24 -26 hours post *Plasmodium falciparum* infection. The carcass of 10 individual females were pooled and RNA extracted. Gene expression was measured as described in Materials and Methods. Transcript levels are reported as a fold expression compared to naïve non-blood fed females. Error bars indicate standard error of the mean of three independent replicates.

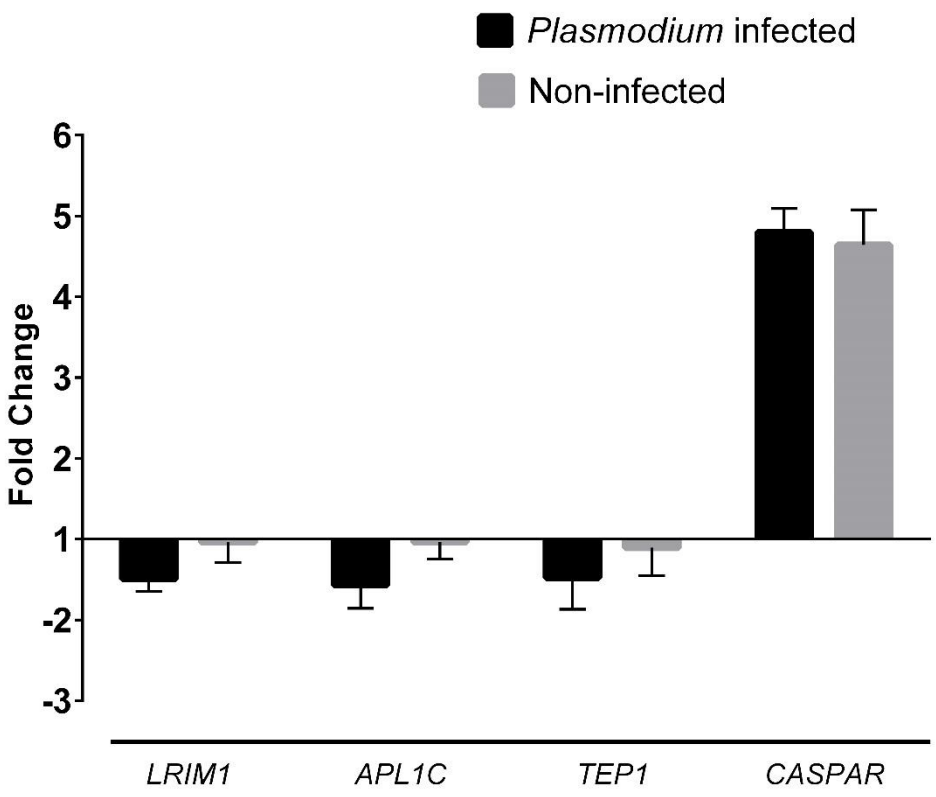

Figure 2.3- Transcript levels of *LRIM1*, *APL1C*, *TEP1* and *Caspar* in the carcass of *A. stephensi* females 48-50 hours post *Plasmodium falciparum* infection. The carcass of 10 individual females were pooled and RNA extracted. Gene expression was measured as described in Materials and Methods. Transcript levels are reported as a fold expression compared to naïve non-blood fed females. Error bars indicate standard error of the mean of three independent replicates.

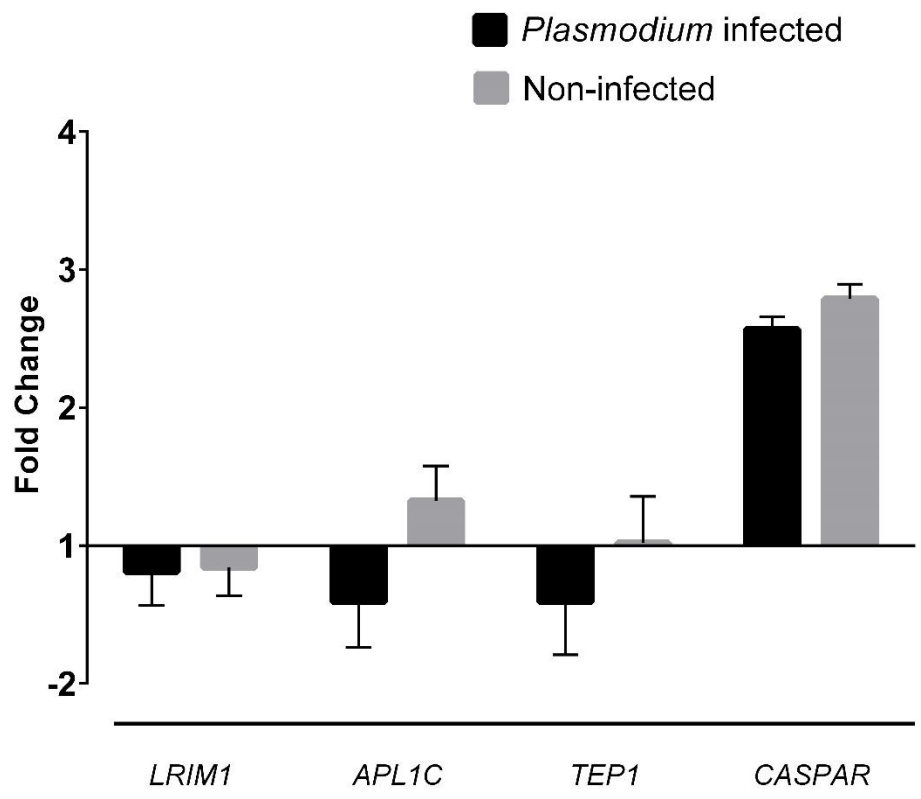

Figure 2.4- Transcript levels of *LRIM1*, *APL1C*, *TEP1* and *Caspar* in the carcass of *A. stephensi* females 72-74 hours post *Plasmodium falciparum* infection. The carcass of 10 individual females were pooled and RNA extracted. Gene expression was measured as described in Materials and Methods. Transcript levels are reported as a fold expression compared to naïve non-blood fed females. Error bars indicate standard error of the mean of three independent replicates.

IMD Pathway Immune Response in Midgut

Similar to transcript levels observed in the carcass, midgut transcript levels of *LRIM1*, *APL1C* and *TEP1* were higher in infected and non-infected blood-fed females compared to controls. However the fold increase observed in the midgut was lower than the upregulation observed in carcass 24 -26 hours post blood feed (Figure 2.6). Both blood fed groups had elevated *Caspar* transcript levels when compared to the controls, with the transcript abundance in infected blood fed females trending lower.

Between 48 to 50 hours the expression pattern in the midgut paralleled the expression observed in the carcass with increased *Caspar* and lower *LRIM1*, and *APL1C* transcripts compared to controls. *TEP1* transcript levels were marginally but not significantly higher in both blood fed groups compared to controls. *Caspar* transcript levels in infected and non-infected blood females were more than 3 and 2-fold higher respectively (Figure 2.7).

Between 72 to 74 hours post blood feed *Caspar* transcript levels fell in both blood fed groups but was still more than 2-fold higher than observed in controls. *TEP1* transcript levels in both blood fed groups were modestly higher than the controls, while transcript levels of *LRIM1* and *APL1C* in both blood fed groups were lower than the controls (Figure 2.8).

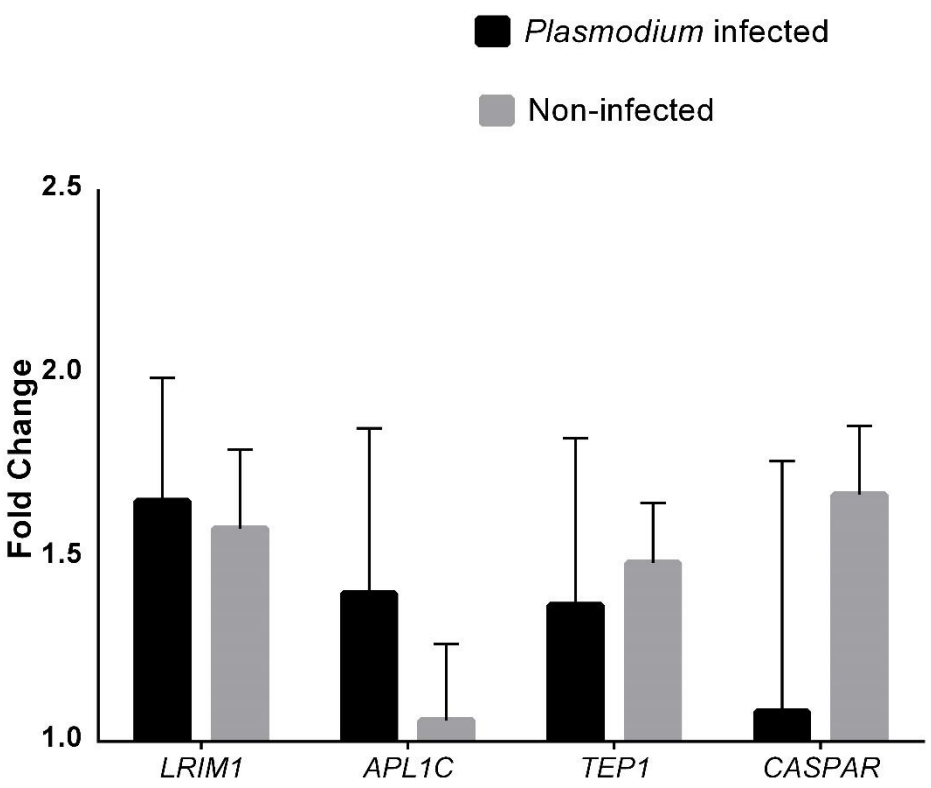

Figure 2.5- Transcript levels of *LRIM1*, *APL1C*, *TEP1* and *Caspar* in the midgut of *A. stephensi* females 24-26 hours post *Plasmodium falciparum* infection. The midgut of 10 individual females were pooled and RNA extracted. Gene expression was measured as described in Materials and Methods. Transcript levels are reported as a fold expression compared to naïve non-blood fed females. Error bars indicate standard error of the mean of three independent replicates.

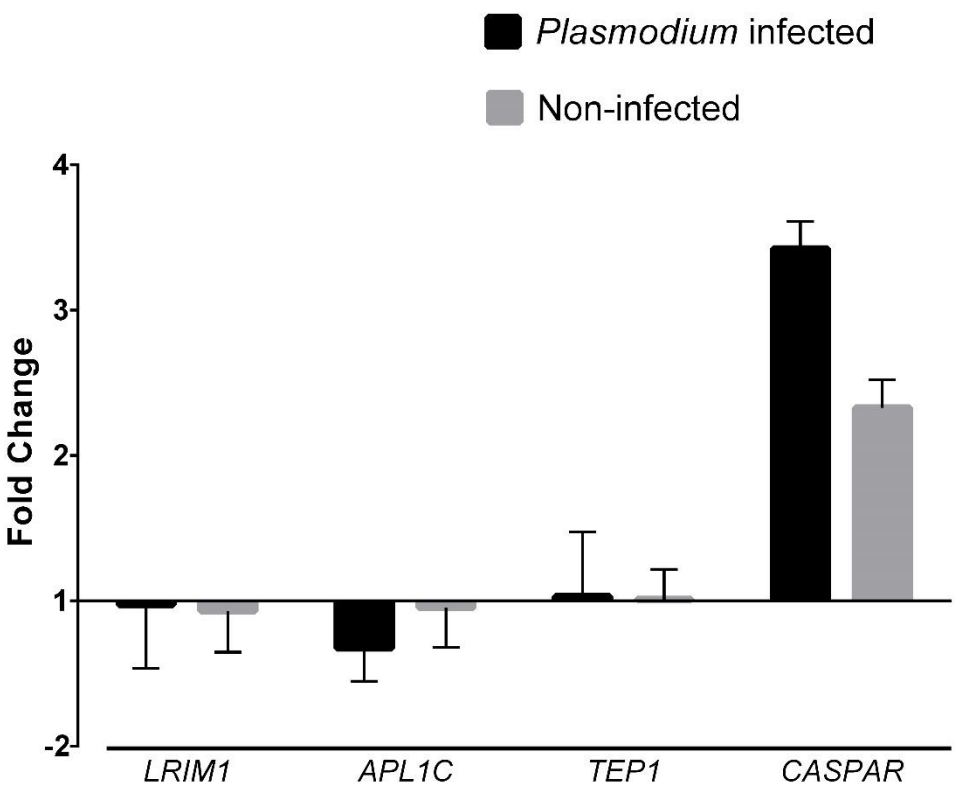

Figure 2.6- Transcript levels of *LRIM1*, *APL1C*, *TEP1* and *Caspar* in the midgut of *A. stephensi* females 48-50 hours post *Plasmodium falciparum* infection. The midgut of 10 individual females were pooled and RNA extracted. Gene expression was measured as described in Materials and Methods. Transcript levels are reported as a fold expression compared to naïve non-blood fed females. Error bars indicate standard error of the mean of three independent replicates.

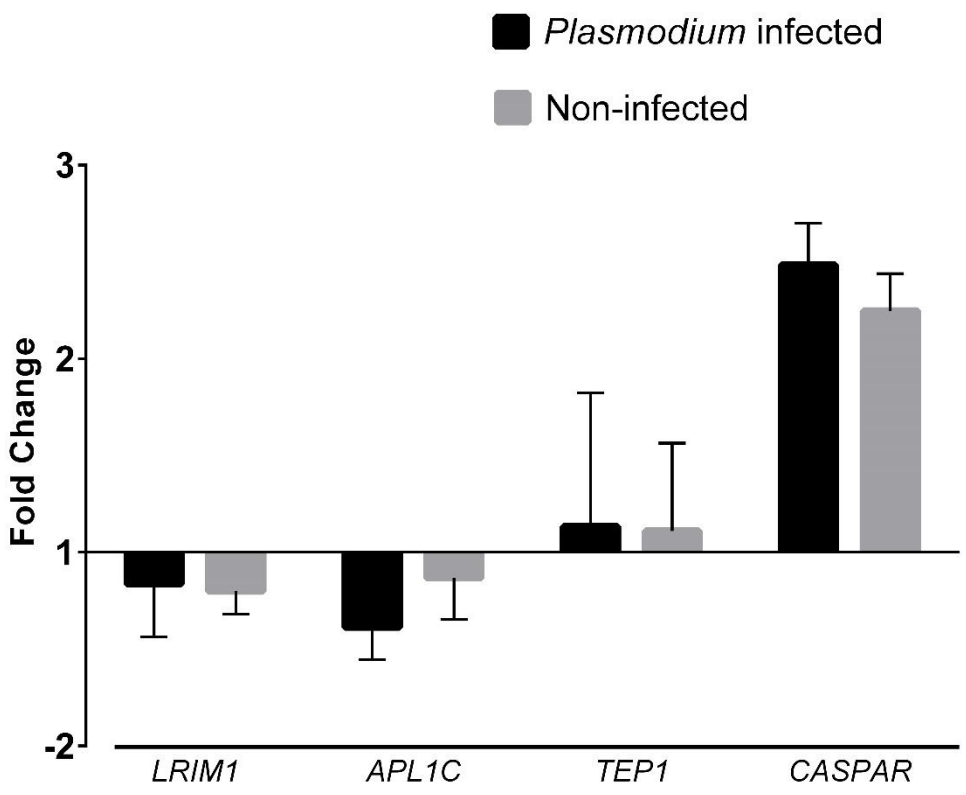

Figure 2.7- Transcript levels of *LRIM1*, *APL1C*, *TEP1* and *Caspar* in the midgut of *A. stephensi* females 72-74 hours post *Plasmodium falciparum* infection. The midgut of 10 individual females were pooled and RNA extracted. Gene expression was measured as described in Materials and Methods. Transcript levels are reported as a fold expression compared to naïve non-blood fed females. Error bars indicate standard error of the mean of three independent replicates.

Immune Response 14 days post infection in salivary glands

The salivary glands of infected females were assessed for IMD pathway response fourteen days post *Plasmodium* infection. This time point in the parasite life cycle, corresponds to salivary gland invasion by sporozoites. Both *APL1C* and *TEP1* showed greater than 2-fold increase in average transcript levels when compared to mosquitoes that fed on non-infected blood while *LRIM1* showed a 1.8-fold increase when compared to controls. There was also a modest but significant 1.3-fold increase in *Caspar* transcript levels when compared to non-infected blood fed females.

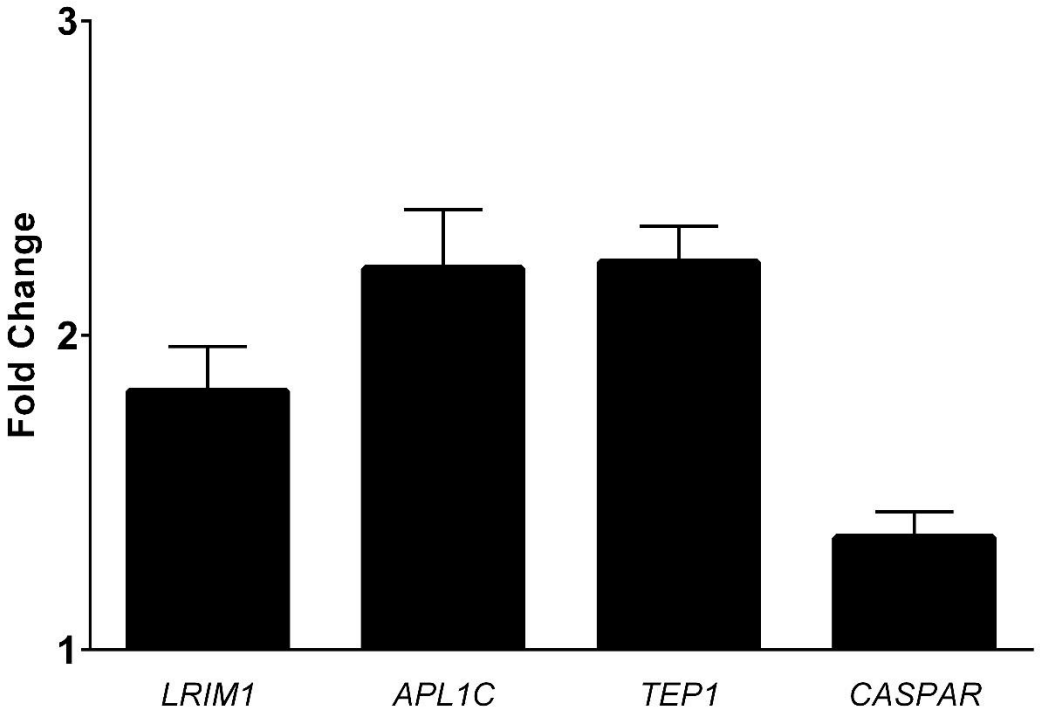

Figure 2.8- Transcript levels of *LRIM1*, *APL1C*, *TEP1* and *Caspar* in the salivary glands of *A. stephensi* females 14 days post *Plasmodium falciparum* infection. The salivary glands of 30 individual females were pooled and RNA extracted. Gene expression was measured as described in Materials and Methods. Transcript levels are reported as a fold expression compared to non- infected blood fed females. Error bars indicate standard error of the mean of three independent replicates.

Response of *Anopheles stephensi* Sda500 IMD pathway to *Escherichia coli* infection

To assess the role of the IMD pathway in response to infection by gram negative bacteria, four days old females were treated with *E. coli* via injections or through feeding. Transcript levels of *LRIM1*, *APL1C*, *TEP1 and* IMD pathway transcription factor Rel2 were assessed in the whole body of *E.coli* or PBS treated mosquitoes 24 hours post infection (Figure 2.9). All the genes assessed showed no upregulation in response to *E. coli* infection. Similar results were observed when *LRIM1* transcript levels were assessed 24 hours after mosquitoes were provided an artificial feeding buffer (AFB) that contained 100 CFU/mL of *E. coli* (Figure 2.10).

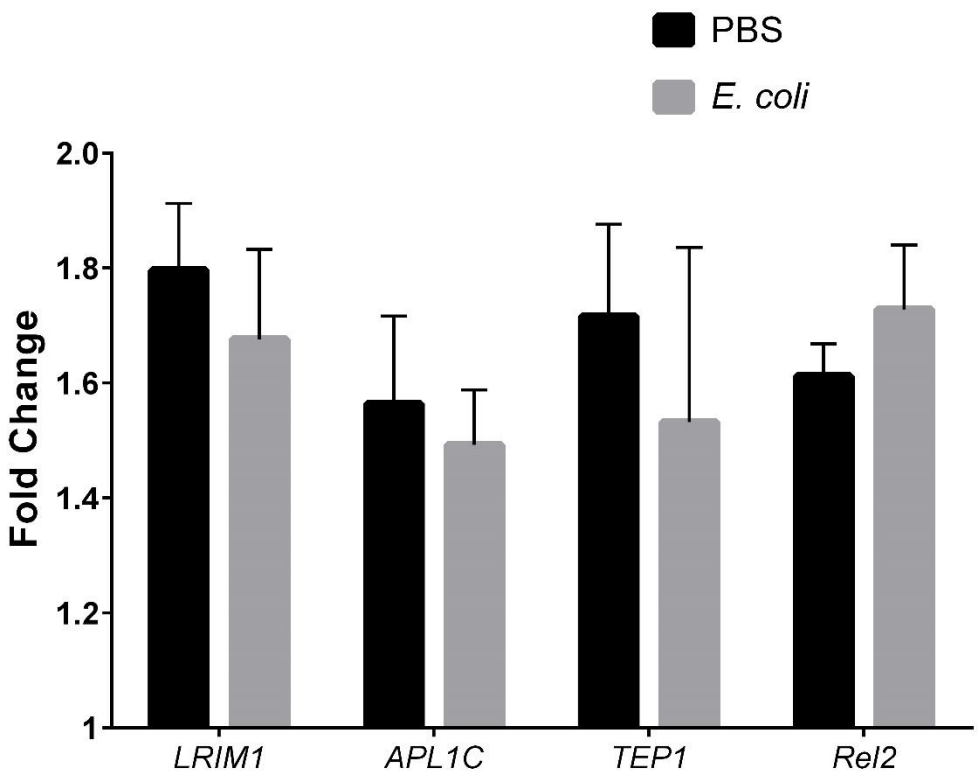

Figure 2.9- Transcript level of IMD pathway effector molecules and IMD pathway transcription factor Rel2 in the whole body of *A. stephensi* females 24 hours post *E. coli* infection. The carcass of 10 individual females were pooled and RNA extracted. Gene expression was measured as described in Materials and Methods. Transcript levels are reported as a fold expression compared to naïve non-infected females. Error bars indicate standard error of the mean of three independent replicates.

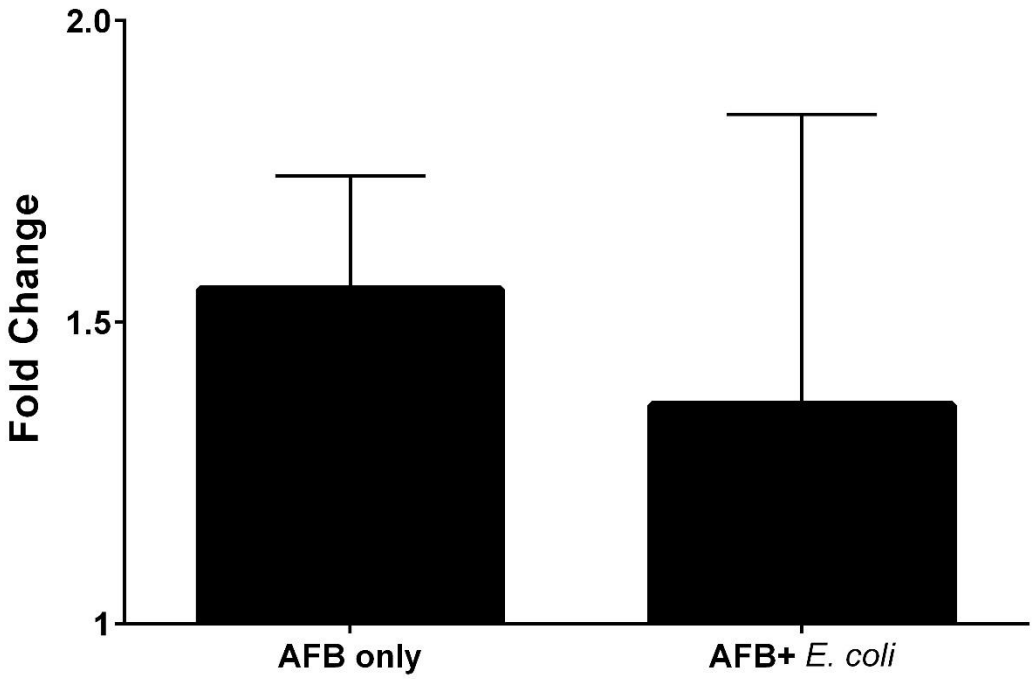

Figure 2.10- *LRIM1* transcript level in response to infection by gram-negative *E. coli* (100 CFU/ml) in sterilized artificial feeding buffer 24 hours post infection. The whole body of 10 individual females were pooled and RNA extracted. Gene expression was measured as described in Materials and Methods. Transcript levels are reported as a fold expression compared to naïve non-injected females. Error bars indicate standard error of the mean of three independent replicates.

2.4 Discussion

Anopheles stephensi LRIM1 is a member of the long LRIM sub-family

Analysis of the LRIM1 homolog isolated from *A. stephensi* identified it as member of the LRIM family. Like LRIM1 previously described in *A. gambiae, A. stephensi A. stephensi* Sda500 LRIM1 exhibited the conserved double coiled coil C-terminal domain (Waterhouse et al. 2010). These coiled coil domains are thought to facilitate the protein/protein interactions of LRIM1 and APL1 which form a heterodimer complex within the complement-like immune response (Povelones and Waterhouse 2009). Mosquito LRIMs are characterized by a variable number of 6 to 14 leucine-rich repeats, which distinguishes the short and long subfamily of LRIMs (Waterhouse et al. 2010). The short LRIM subfamily contains 6 to 7 leucine-rich repeats while the long LRIM subfamily contains 10 or more leucine-rich repeats (Waterhouse et al. 2010). The previously identified *A. gambiae* LRIM1 is characterized as a long LRIM with 10 LRRs. The LRIM1 gene isolated from *A. stephensi* had 9 LRRs predicted using *LRRfinder* and therefore also a long LRIM

An N-terminal signal peptide was predicted in LRIM1 isolated from *A. gambiae* and *A. stephensi*. This would suggest that LRIM1 is secreted from cells. However previous studies by (Povelones and Waterhouse 2009; Povelones et al. 2011) suggest that the *Anopheles gambiae* LRIM1 monomer is only secreted into the hemolymph, after the formation of the LRIM1/APL1 complex. In both *As*LRIM1 and *Ag*LRIM1 between the C-terminal coiled coil domain and the leucine-rich repeats is a conserved double cysteine motif. This motif has been implicated in the formation of the disulfide bond between LRIM1 and APL1 (Waterhouse et al. 2010; Povelones et al. 2011).

Plasmodium falciparum* infection regulates LRIM1 expression in female *Anopheles stephensi

It has been previously reported that *LRIM1* in *A. gambiae* functions as a strong suppressor to *Plasmodium berghei* development, (Warr et al. 2006; Habtewold et al. 2008; Gutierrez et al. 2009). Post blood meal or *P. berghei* infection the expression of *LRIM1* in *A. gambiae* significantly increases (Marinotti *et al.* 2006) with highest expression levels observed 24 hours after infection when ookinetes are traveling across the basal lamina of the mosquito midgut (Osta, Christophides, and Kafatos 2004). Later studies by Mendes et al. (2011) demonstrated that the midgut immune response, specifically the IMD pathway response, during *A. gambiae* infection by *P. falciparum* was infection intensity dependent with 972 genes regulated during low infection intensity (<15 oocysts in midgut) compared to 557 during high infection intensity (>15 oocyst in the midgut). This observation was later supported by (Garver et al. 2012) who reported on the novel intensity dependent role of *LRIM1* during *P. falciparum* infections in *A. gambiae.*

Our studies demonstrated that *A. stephensi* Sda500 that were provided a *P. falciparum* infected blood meal had significant increases in IMD effector molecules expression 24 -26 hours post infection compared to controls. However, the relatively small increase in transcript abundance in the midgut may support previous observations by Mendes et al. (2011) and Garver et al. (2012) of infection intensity dependent IMD pathway signaling in the midgut. Our observation of maximum *LRIM1* expression 24 hours post *Plasmodium* infection followed by downregulation 48 hours post infection

also paralleled previous studies by Osta et al. (2004) and Marinotti et al. (2005) studying *A. gambiae* response to *P. berghei* infection. The relationship shown here between *A. stephensi* IMD pathway and *Caspar* expression corresponded to previous observations (Garver et al. 2012) in their study of the relationship between the negative regulator *Caspar* and the IMD pathway response to *Plasmodium*. These observations along with the IMD pathway response to *P. falciparum* infection indicates that the IMD signaling pathway in *A. stephensi* Sda500 is induced in response to parasites.

Role of the *A. stephensi* salivary glands in *Plasmodium* defense

The novel observation of a statistically significant increase in expression of IMD effector genes in the salivary glands fourteen days post *P. falciparum* infection could provide significant insight into the mosquito's defense against the parasite. It is the prevailing thought that the humoral response against the parasite is concentrated in the midgut, but this new observation may suggest other tissues invaded by the parasite also mount an immune response. Unpublished studies by O'Brochta and colleagues where they observed that silencing *LRIM1* had no effect on *P. falciparum* oocyst intensity but increase sporozoite intensity 2.5 fold compared to control mosquitoes could support a post midgut immune response by IMD pathway immune effectors to *Plasmodium*. Future studies to elucidate the role of specific tissues in parasite defense should be performed and these answers could provide better targets for immune modification.

IMD pathway in *Anopheles stephensi* Sda500 was not regulated by *E. coli* infection

Previous studies have demonstrated the role of the IMD pathway (Dimopoulos et al. 1997; Dimopoulos et al in 2002) and specifically the role of TEP1 (Waterhouse et al. 2010; Yassine et al. 2014) in defense against *E. coli* in *A. gambiae*. In our attempt to upregulate the IMD pathway by injection of *E. coli* directly into the body cavity of the mosquito or introduction through feeding, there was no significant difference observed in the expression of genes involved in the mosquito complement like immune system. Further analysis of the IMD pathway transcription regulator *Rel2* also showed no significant difference in its level of expression following injection or feeding on *E. coli* compared to the control. Further studies using a wide range of bacteria should be performed to determine the role of the IMD pathway in bacterial pathogen defense in *A. stephensi*.

Feeding mechanism can increase *LRIM1* expression in *A. stephensi*

Studies by Marinotti et al. (2005) and results presented here demonstrated that female *Anopheles* mosquitoes provided with a non-infected blood meal had elevated *LRIM1* expression compared to non-fed controls. Our studies also demonstrated that the upregulation of *LRIM1* could be induced by feeding on a solution that did not contain blood. Mosquitoes that were provided a sterilized artificial feeding solution (Galun 1967) demonstrated modest increase in *LRIM1* transcripts compared to sucrose fed control. One hypothesis is that this observed response could be an evolutionary

conserved mechanism to protect the mosquito from possible harmful pathogens ingested during a blood meal similar to the formation the peritrophic membrane in *Anopheles* mosquitoes after a blood meal (Terra 2001).

The results presented here demonstrate that *A. stephensi* Sda500 can mount an IMD pathway immune response to *Plasmodium falciparum* infection. Taken together these results show that *LRIM1* is a suitable candidate for modification of the innate immune system in *Anopheles stephensi* Sda500 to increase *Plasmodium falciparum* sporozoite intensity in the salivary glands.

Chapter 3: Transgenic *Anopheles stephensi* Sda500 bioreactors for increased *Plasmodium falciparum* salivary gland infection intensity

3.1 Introduction

Production volume and cost of a live attenuated vaccine for malaria is expected to be directly correlated with infection intensity of *Plasmodium falciparum* sporozoites in the salivary glands (Sanaria Inc.) Numerous studies (Pike et al., 2014; Garver et al., 2012; Meister et al., 2005; Osta et al., 2004) have shown that the IMD pathway plays a major role in reducing *Plasmodium* infection intensity in *Anopheles* mosquitoes. In studies aimed at increasing infection intensity in the salivary glands of *A. stephensi* Sda500 and ultimately improving vaccine production, O'Brochta et al. (unpublished) demonstrated that silencing expression of the IMD pathway effector gene *LRIM1* increased the infection intensity of sporozoites 2.5 fold. In those studies, *LRIM1* gene expression in *A. stephensi* was reduced by RNAi using *A. gambiae* LRIM1 dsRNA. However given the high sequence variation observed among the LRR and coiled coil domains of LRIM1 among *Anopheles* species (Waterhouse et al. 2010), it was hypothesized that more effective silencing could be achieved using dsRNA identical to *A. stephensi LRIM1* and therefore increase sporozoite infection intensity.

Although those studies demonstrated that sporozoite intensity in the salivary glands could be increased by reducing *LRIM1* expression with dsRNA, introducing additional steps into the vaccine manufacturing protocol while maintaining strict

aseptic conditions would have the unwanted effect of increasing cost. It was therefore proposed that stable transgenic *A. stephensi* with a heritable *LRIM1* gene silencing transgene expressing LRIM1 dsRNA could be used as bioreactors for sporozoite production. *A. stephensi* is amenable to genetic manipulation and numerous examples of transgenic *A. stephensi* being created using *piggyBac* transposon-based vectors have been reported. (Brown et al. 2003; Catteruccia et al. 2000; Ito et al. 2002; Lycett 2004; Nolan et al. 2002; Yoshida & Watanabe 2006; Kim et al. 2004; O'Brochta et al. 2012). Furthermore, stable and heritable gene silencing using *in vivo*-expressed dsRNA has been demonstrated in *An. stephensi* (Brown et al. 2003). A *piggyBac* transformation vector containing the *LRIM1* target sequence cloned in an inverted repeat orientation, separated by a functional intron can be injected into preblastoderm embryos and screened for transgenics. Transcription of this cassette containing an inverted repeat fragment of *LRIM1* would result in DICER mediated post-transcriptional silencing.

Here I propose to use genetic technologies that have rarely if ever been used in *A. stephensi* to create a line of *A. stephensi* Sda500 with a partially dysfunctional immune system. I will combine *in vivo* expressed shRNA gene silencing with the Gal4/UAS binary transcription regulatory system, so that gene silencing can be regulated spatially and temporally (Elliott and Brand 2008). This approach will enable us to direct silencing of *LRIM1* to specific tissues such as the midgut, fat body and salivary glands that have been indicated in *LRIM1* expression throughout the vector stage of the parasite life cycle, thereby eliminating the temporal and spatial limitations reported with dsRNA injections. Unlike, previous studies (Osta et al. 2004; Jaramillo-

Gutierrez et al. 2009; Garver et al. 2012) where dsRNA was used to assess the role of *LRIM1* in the anti-*Plasmodium* response over a relatively small window of time, our approach will help to parse out the role of *LRIM1* during the entire vector parasite interaction.

This chapter focuses on the creation and characterization of transgenic *A. stephensi* lines that express stable hairpin RNA from transgenes integrated into the genome targeting *LRIM1* and the analysis of these lines for the increased susceptibility to *Plasmodium.*

3.2 Materials and Methods

Materials and Methods can be found on page 102

3.3 Results

Transient silencing of *A. stephensi LRIM1* with dsRNA

Silencing of *LRIM1* expression in the whole body of *A. stephensi* Sda500 females was assessed 4 days post dsRNA injection by quantitative reverse transcription polymerase chain reaction (qRTPCR) (Figure 3.1). Compared to control mosquitoes injected with *dsEGFP*, mosquitoes injected with *dsAgLRIM1* and *dsAsLRIM1* had average transcript abundance of 78.8% ± 7.1% and 53.5% ± 12.1% respectively.

Transient silencing of *A. stephensi LRIM1* with *dsAsLRIM1* reduces lifespan.

Adult female *A. stephensi* Sda500 injected with dsAsLRIM1 RNA showed a reduction in their life-span compared to dsEGFP and dsAgLRIM1, injected controls

(figure 3.2). On average 100 percent of dsAsLRIM1 injected females were dead 10 days post injection, compared to only 66 and 68 percent fatality in *dsEGFP* and *dsAgLRIM1* injected females respectively. In all injected groups there was approximately 40 percent fatality 24 hours post injection.

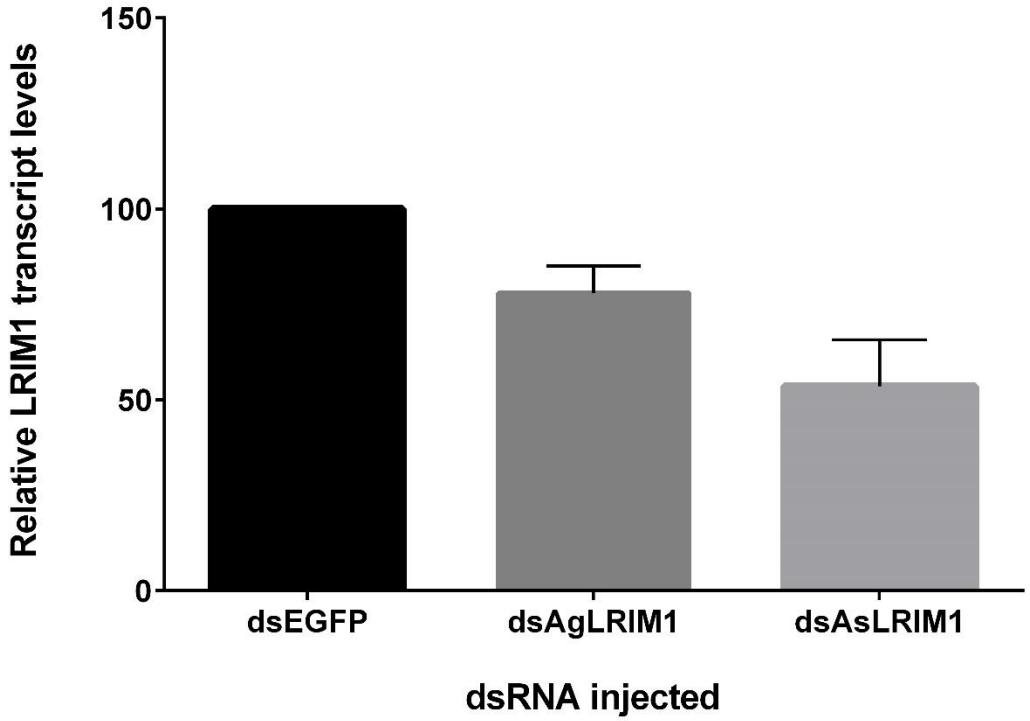

Figure 3.1- Transcript levels of *LRIM1* in the whole body of *A. stephensi* Sda500 females four days post dsRNA injection to silence *LRIM1* expression. The whole body of five females from each injection were pooled and RNA extracted. Gene expression was measured as described in Materials and Methods. Average transcript abundance is shown relative to control dsEGFP-injected mosquitoes. Transcript levels of ribosomal S7 gene were used as a calibrator. Bars indicate standard error of the mean of three independent experiments.

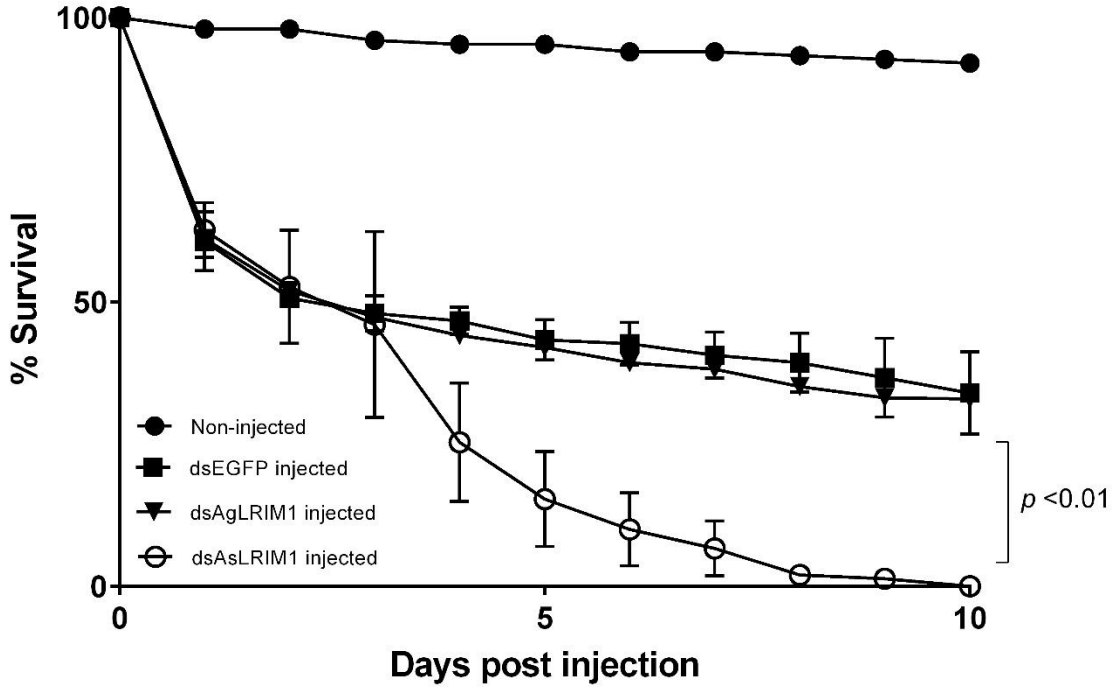

Figure 3.2- Survival of *A. stephensi* females after injection of dsRNA to silence *LRIM1* expression. *A. stephensi* Sda500 females injected with dsAsLRIM1 had 100 percent fatality 10 days post injection compared to 66 percent and 68 percent fatality of dsEGFP and dsAgLRIM1 injected controls respectively. 50 female mosquitoes were used for each treatment. Bars indicate standard error of the mean of three independent experiments.

Characterization of LRIM1-silencer lines

Transgene insertion site

Three *LRIM1* silencer lines; LRIM1-silencer F2, LRIM1-silencer M2 and LRIM1-silencer M7 (Figure 3.3), were created as described in the Material and Methods. Here we refer to lines LRIM1-silencer F2, LRIM1-silencer M2 and LRIM1-silencer M7 as F2, M2 and M7 respectively. Cytogenetic location of the transgene insertion site was determined using Splinkerette PCR and chromosomal location data of *A. stephensi* scaffolds provided by Igor Sharakov of Virginia Polytechnic Institute and State University. Integration site for F2 was determined to be in the intergenic region of scaffold KB664543 on Chromosome 3R. For M2 the transgene was found in the intergenic region of scaffold KB664524 located on Chromosome 2R while the M7 transgene was located in the intergenic region of scaffold KB664832 located on Chromosome 3L. For summary of results see Table 1.

Table 3.1- Cytogenetic location of the *LRIM1* silencing transgene in the *A. stephensi* genome.

	Insertion site	
Silencer line	**Scaffold**	**Chromosome**
LRIM1-silencer F2	KB664543	3R
LRIM1-silencer M2	KB664524	2R
LRIM1-silencer M7	KB664832	3L

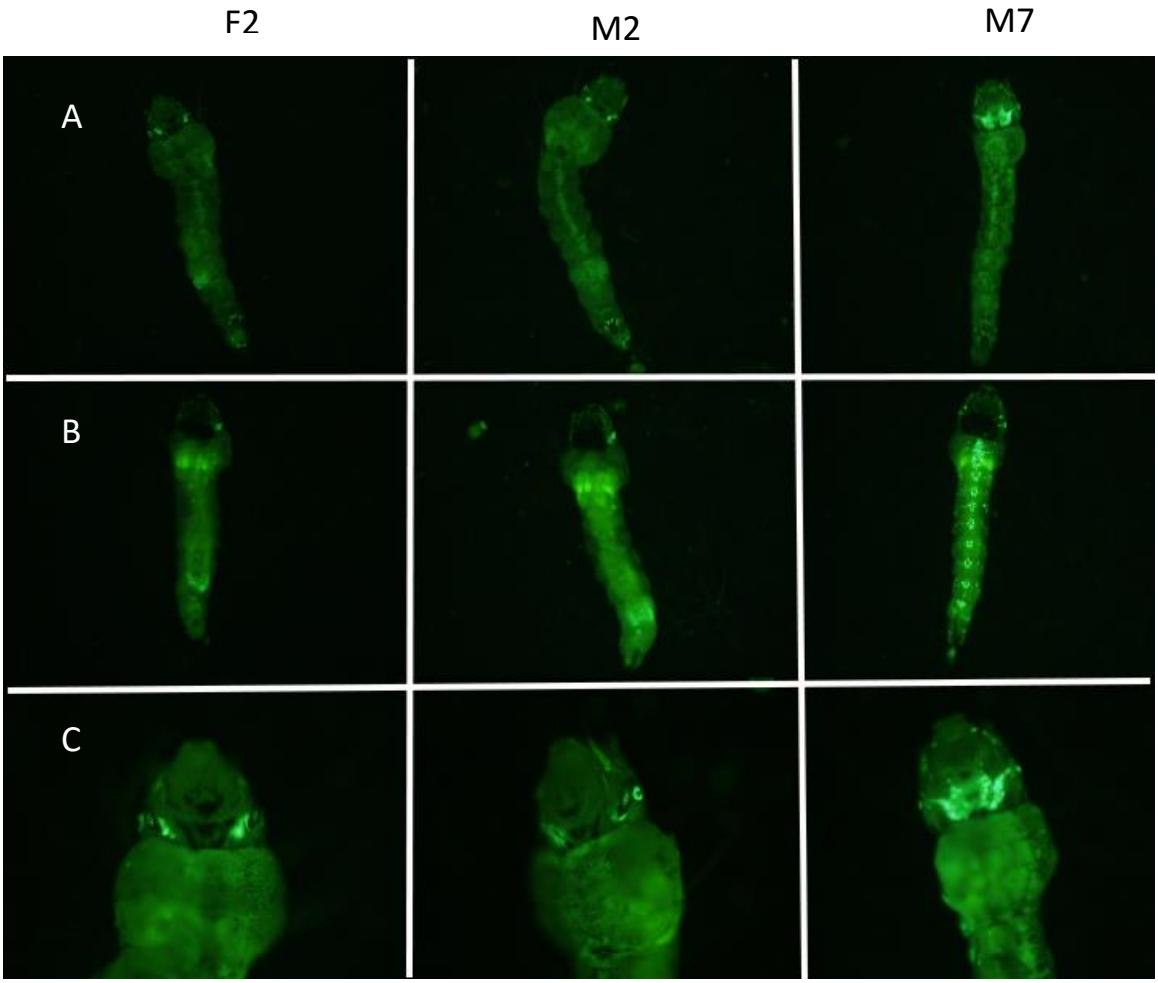

Figure 3.3- Silencer lines LRIM1-silencer F2, LRIM1-silencer M2 and LRIM1-silencer M7. (A) Dorsal view of whole third-instar larva showing nlsEGFP marker gene expression. (B) Ventral view of whole third-instar larva showing nlsEGFP marker gene expression. (C) Magnification of head showing nuclear localized expression.

in vivo* dsRNA silencing LRIM1 in transgenic *Anopheles stephensi

The progeny of the UAS:LRIM1-silencer lines were crossed with the MB24 Gal4 driver line (O'Brochta et al 2012) which expresses Gal4 in the midgut, fat body and salivary gland (see appendix). Progeny containing a copy of UAS::LRIM1-silencer and Gal4 were used to test for tissue specific silencing of *LRIM1* expression using qRTPCR. The abundance of *LRIM1* transcript in each genotype was compared to transcript abundance in the wildtype. Progeny that contained a single transgene element showed no statistically significant difference in *LRIM1* transcript abundance in tissues examined compared to wildtype. Progeny of the three silencer lines (F2, M2 and M7) that contained both the Gal4 and UAS::LRIM1-silencer elements showed reduction of *LRIM1* transcript abundance in the midgut, salivary gland and carcass (midgut and salivary glands removed) compared to wild type. In the midgut the average transcript abundance was reduced to 72% ± 6.0%, 65% ± 9.6% and 52% ± 6.2% (Figure 3.4 – 3.6) for lines F2, M2 and M7 respectively. Meanwhile the average carcass transcript levels in F2, M2 and M7 were reduced to 64% ± 13.2 %, 65% ± 7.4% and 63% ± 10.8% respectively (Figure 3.7 – 3.9)

Comparison among the 3 lines showed there was no statistical difference in *LRIM1* expression in the carcass (Figure 3.13), however analysis of the midgut and salivary gland showed that the transcript reduction in M7 was statistically significant compared to the other lines (Figures 3.14 & 3.15). For both the M2 and M7 lines transcript reduction was greater in the salivary glands with average transcript abundance of 56% ± 8.3% and 38% ± 4.1% respectively. Average transcript abundance in the salivary glands of the F2 line was 78.2 % ± 10.2% (Figures 3.10 – 3.12)

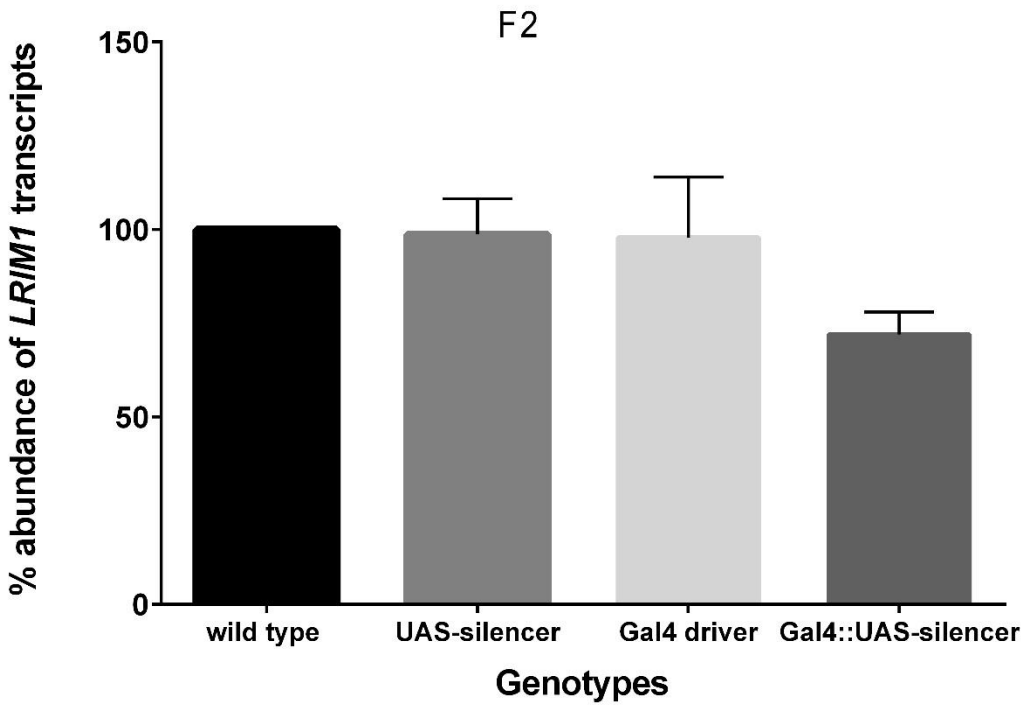

Figure 3.4- Transcript abundance of *LRIM1* in the midgut of GAL4::LRIM1-silencer F2 females 24 -26 hours post blood meal compared to controls. For each genotype the midgut of 10 individual females were pooled and RNA extracted. Gene expression was measured as described in Materials and Methods. Average transcript abundance is shown relative to wild type mosquitoes. Transcript levels of ribosomal *S7* gene were used as a calibrator. Bars indicate standard error of the mean of three independent experiments.

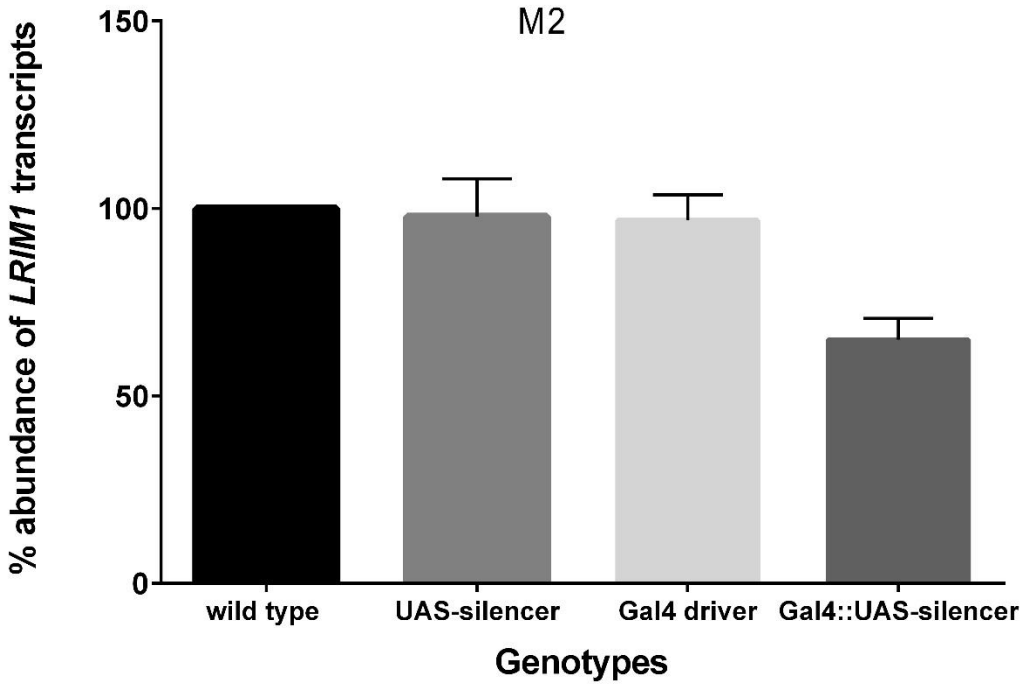

Figure 3.5- Transcript abundance of *LRIM1* in the midgut of GAL4::LRIM1-silencer M2, 24 -26 hours post blood meal compared to controls. For each genotype the carcass of 10 individual females were pooled and RNA extracted. Gene expression was measured as described in Materials and Methods. Average transcript abundance is shown relative to wild type. Transcript levels of ribosomal *S7* gene were used as a calibrator. Bars indicate standard error of the mean of three independent experiments.

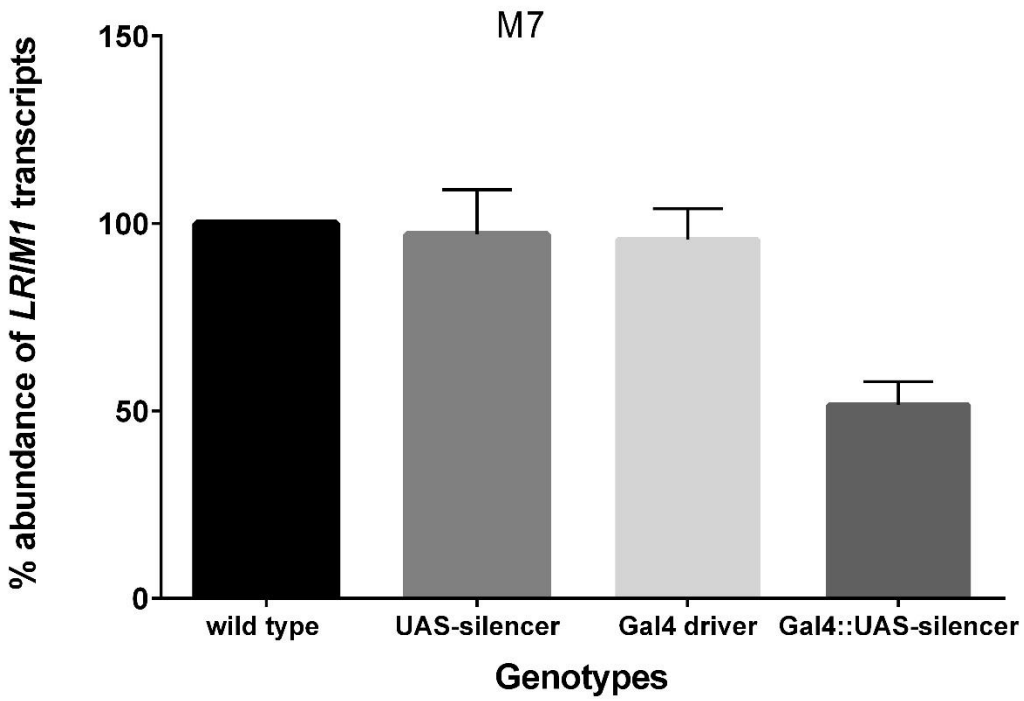

Figure 3.6- Transcript abundance of *LRIM1* in the midgut of GAL4::LRIM1-silencer M7 females 24 -26 hours post blood meal compared to controls. For each genotype the midgut of 10 individual females were pooled and RNA extracted. Gene expression was measured as described in Materials and Methods. Average transcript abundance is shown relative to wild type. Transcript levels of ribosomal *S7* gene were used as a calibrator. Bars indicate standard error of the mean of three independent experiments.

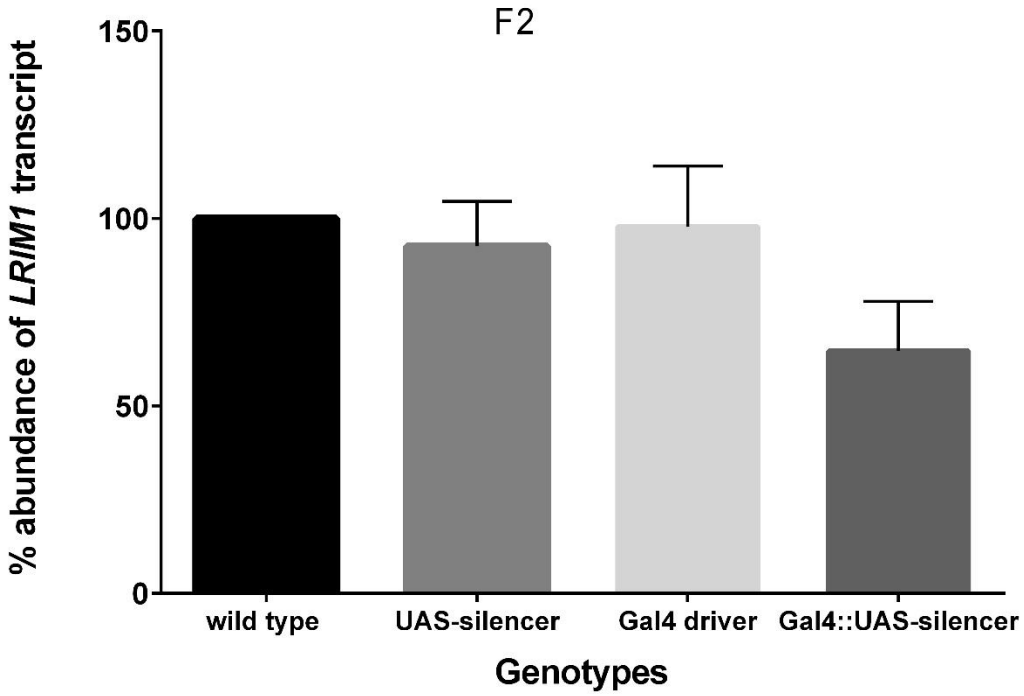

Figure 3.7- Transcript abundance of *LRIM1* in the carcass of GAL4::LRIM1-silencer F2, 24 -26 hours post blood meal compared to controls. For each genotype the carcass of 10 individual females were pooled and RNA extracted. Gene expression was measured as described in Materials and Methods. Average transcript abundance is shown relative to wild type. Transcript levels of ribosomal *S7* gene were used as a calibrator. Bars indicate standard error of the mean of three independent experiments.

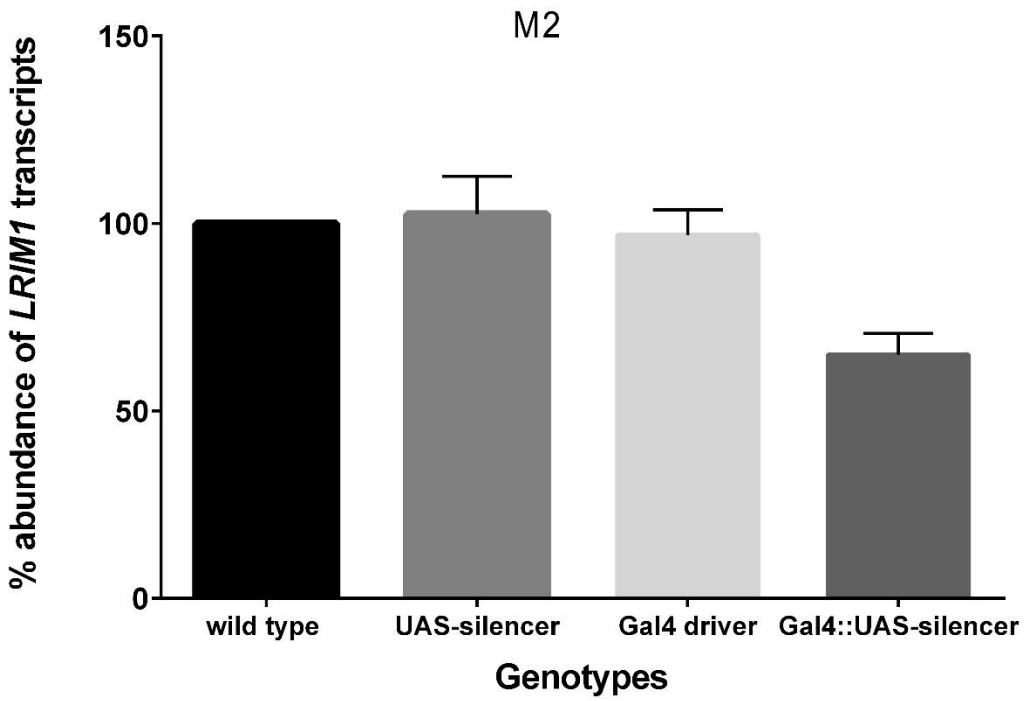

Figure 3.8- Transcript abundance of *LRIM1* in the carcass of GAL4::LRIM1-silencer M2, 24 -26 hours post blood meal compared to controls. For each genotype the carcass of 10 individual females were pooled and RNA extracted. Gene expression was measured as described in Materials and Methods. Average transcript abundance is shown relative to wild type. Transcript levels of ribosomal S7 gene were used as a calibrator. Bars indicate standard error of the mean of three independent experiments.

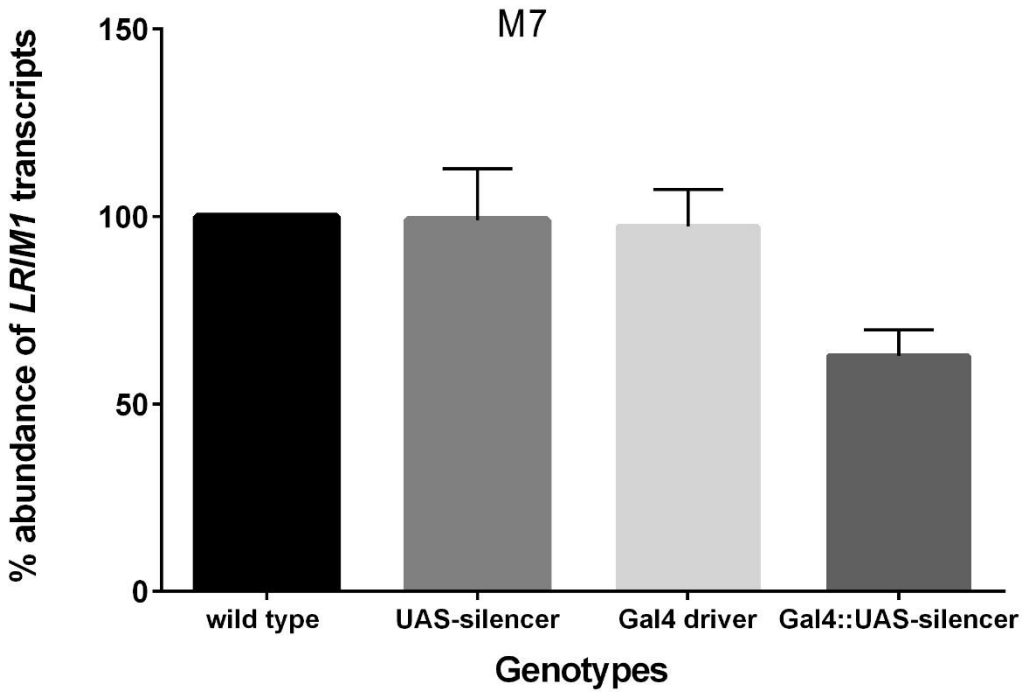

Figure 3.9- Transcript abundance of *LRIM1* in the carcass of GAL4::LRIM1-silencer M7, 24 -26 hours post blood meal compared to controls. For each genotype the carcass of 10 individual females were pooled and RNA extracted. Gene expression was measured as described in Materials and Methods. Average transcript abundance is shown relative to wild type. Transcript levels of ribosomal S7 gene were used as a calibrator. Bars indicate standard error of the mean of three independent experiments.

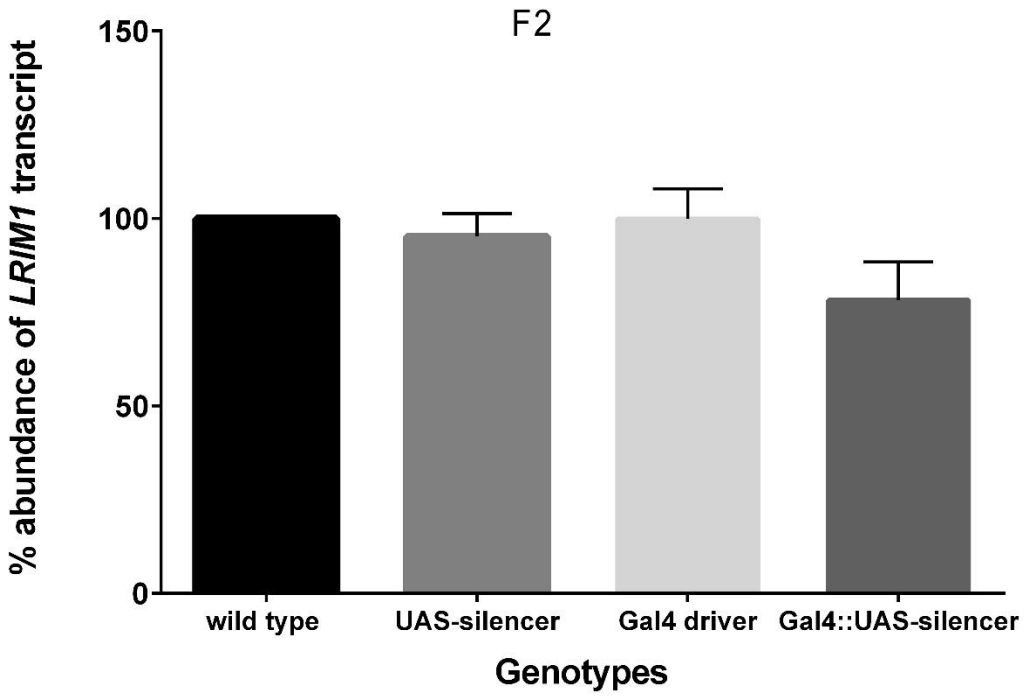

Figure 3.10- Transcript abundance of *LRIM1* in the salivary glands of GAL4::LRIM1-silencer F2, 14-15 days post blood meal compared to controls. For each genotype the carcass of 10 individual females were pooled and RNA extracted. Gene expression was measured as described in Materials and Methods. Average transcript abundance is shown relative to wild type. Transcript levels of ribosomal *S7* gene were used as a calibrator. Bars indicate standard error of the mean of three independent experiments.

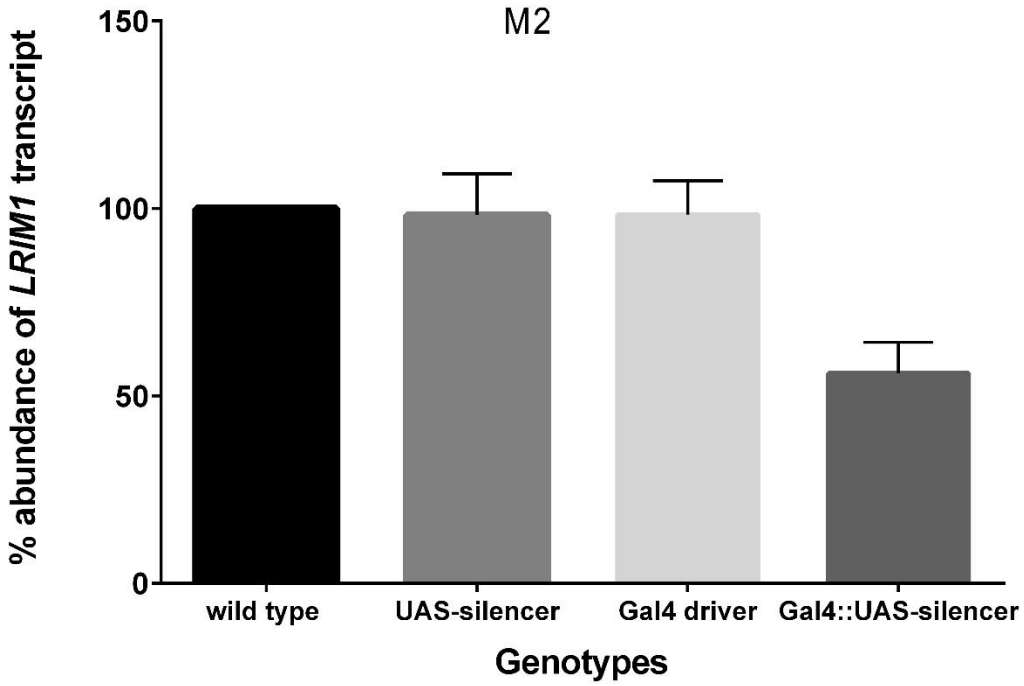

Figure 3.11- Transcript abundance of *LRIM1* in the salivary glands of GAL4::LRIM1-silencer M2, 14 -15 days post blood meal compared to controls. For each genotype the carcass of 10 individual females were pooled and RNA extracted. Gene expression was measured as described in Materials and Methods. Average transcript abundance is shown relative to wild type. Transcript levels of ribosomal *S7* gene were used as a calibrator. Bars indicate standard error of the mean of three independent experiments.

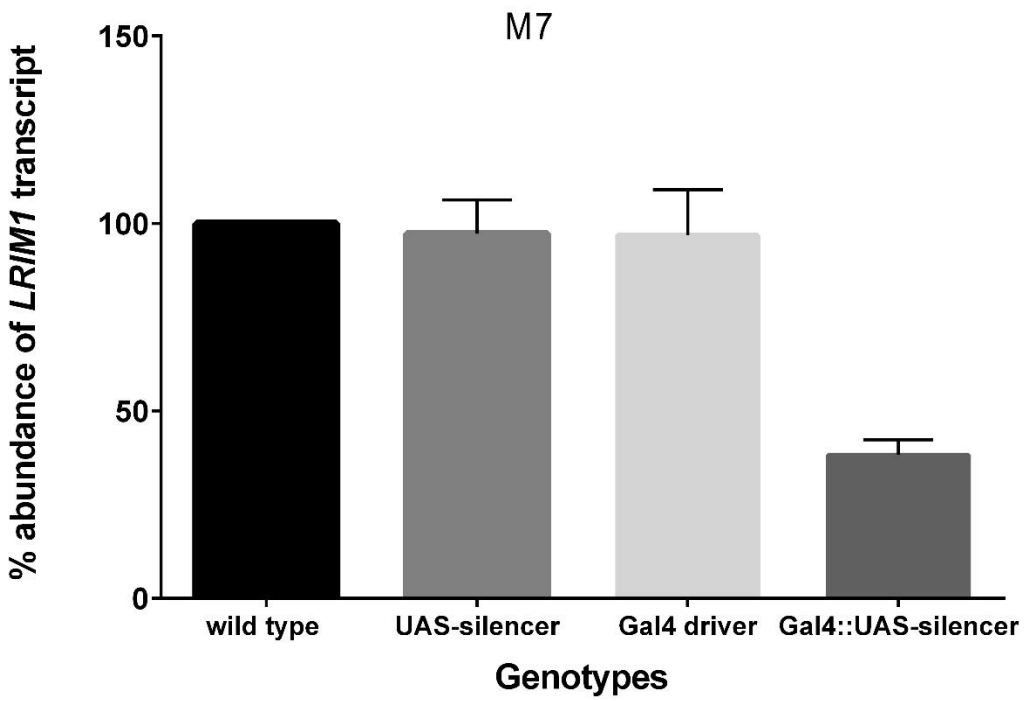

Figure 3.12- Transcript abundance of *LRIM1* in the salivary glands of GAL4::LRIM1-silencer M7, 14-15 days post blood meal compared to controls For each genotype the carcass of 10 individual females were pooled and RNA extracted. Gene expression was measured as described in Materials and Methods. Average transcript abundance is shown relative to wild type. Transcript levels of ribosomal *S7* gene were used as a calibrator. Bars indicate standard error of the mean of three independent experiments.

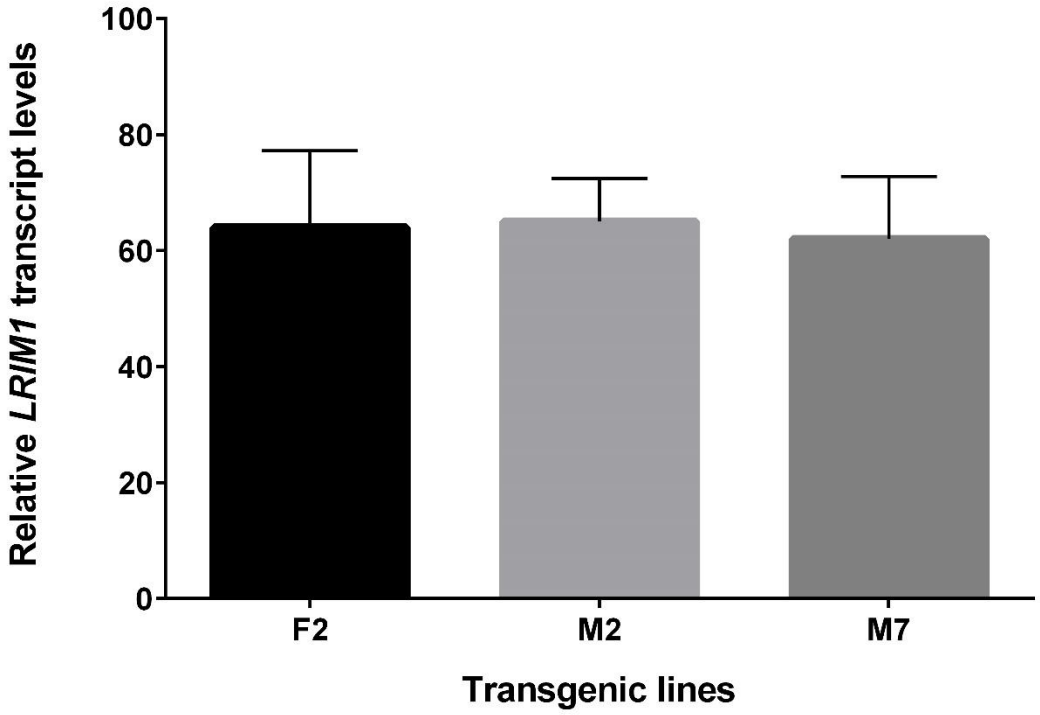

Figure 3.13- Comparison of *LRIM1* transcript abundance in the carcass of GAL4::LRIM1-silencer lines 24 -26 hours post blood meal. For each line the carcass of 10 individual females were pooled and RNA extracted. Gene expression was measured as described in Materials and Methods. Average transcript abundance is shown relative to wild type. Transcript levels of ribosomal *S7* gene were used as a calibrator. Bars indicate standard error of the mean of three independent experiments.

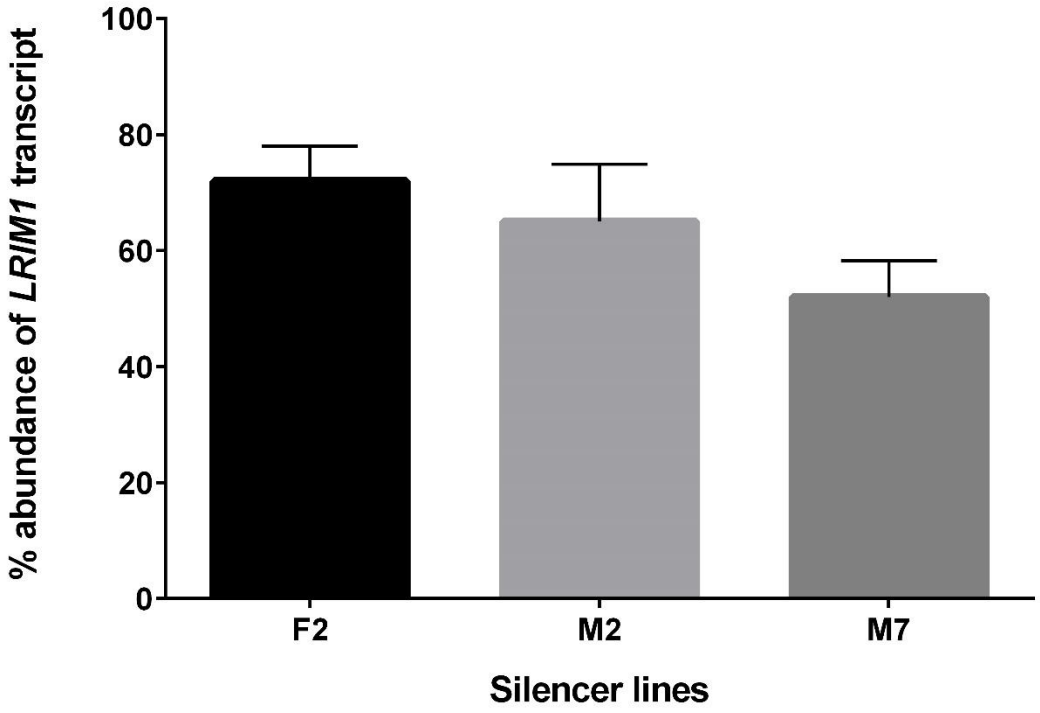

Figure 3.14- Comparison of LRIM1 transcript abundance in the midgut of GAL4::LRIM1-silencer lines 24 -26 hours post blood meal. For each line the carcass of 10 individual females were pooled and RNA extracted. Gene expression was measured as described in Materials and Methods. Average transcript abundance is shown relative to wild type. Transcript levels of ribosomal *S7* gene were used as a calibrator. Bars indicate standard error of the mean of three independent experiments.

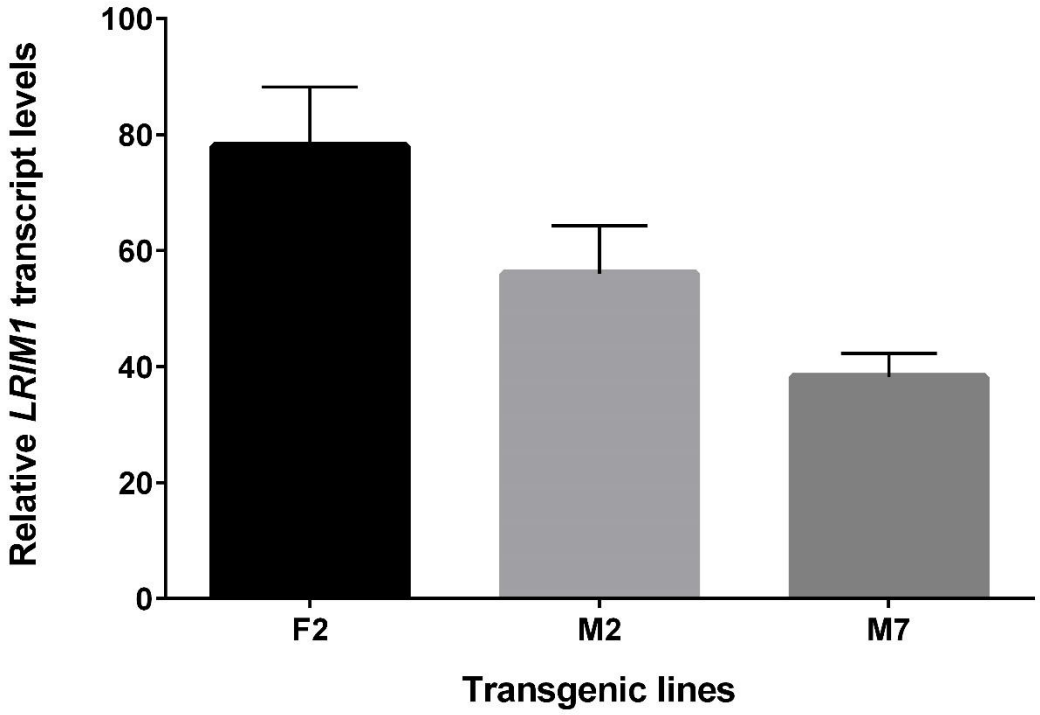

Figure 3.15- Comparison of LRIM1 transcript abundance in the salivary glands of GAL4::LRIM1-silencer lines 14-15days post blood meal. For each line the carcass of 10 individual females were pooled and RNA extracted. Gene expression was measured as described in Materials and Methods. Average transcript abundance is shown relative to wild type. Transcript levels of ribosomal *S7* gene were used as a calibrator. Bars indicate standard error of the mean of three independent experiments.

in vivo dsRNA silencing of *LRIM1* in *A. stephensi* Sda500 does not reduce lifespan

In our previous experiments it was shown that dsAsRNA injected into adult *A. stephensi* Sda500 females reduced their lifespan. To determine if *in vivo* shRNA silencing with a smaller and more specific target site would have a similar phenotype as injecting dsRNA, the life span of the progeny generated from crossing LRIM1-silencer/- lines with the MB24 Gal4/- driver line was assessed. No statistical difference was observed in the life span of the progeny when any of the three silencer lines were crossed with Gal4 driver line (Figure 3.16 – 3.18).

in vivo dsRNA silencing of *A. stephensi* LRIM1 in females showed no difference in midgut bacterial load.

To study the response of the gut microbiota to *LRIM1* silencing the bacterial load in the midgut of progeny from the cross of LRIM1silencer M7 with MLB24-Gal4 driver were determined (Figure 3.19) The M7 line was used in this experiment because earlier experiments demonstrated greater reduction in midgut expression of *LRIM1* compared to the F2 and M2 lines. No statistical difference was observed in bacterial load of the genotypes examined. The average Colony Forming Unit (CFU) in the female midgut range from 1.8×10^6 CFU/ml to 2.3×10^6 CFU/ml.

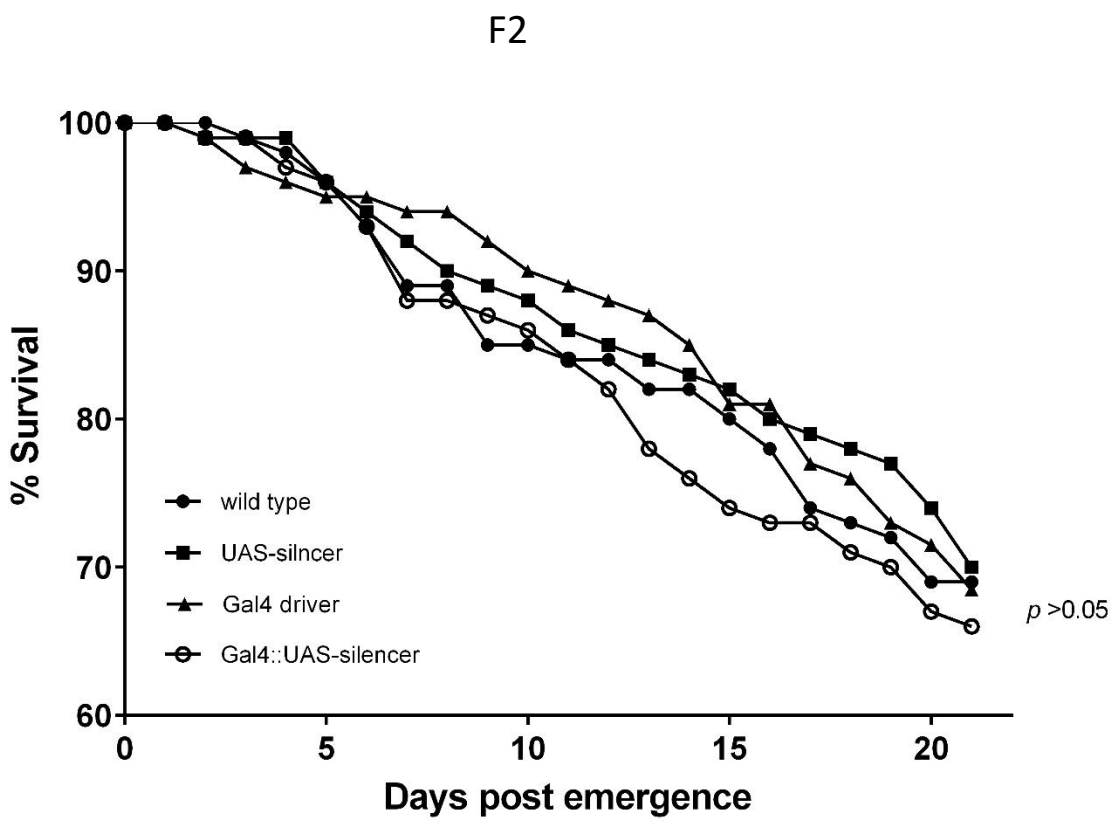

Figure 3.16- Survival comparison of the progeny from a cross of LRIM1-silencer F2 with the MLB24 Gal4 driver line. Fifty female pupae from each genotype were pooled in a cage and observed for 21 days post emergence. The cage was examined daily and dead individuals were removed and the genotype determined. No statistical difference was observed among the genotypes examined.

M2

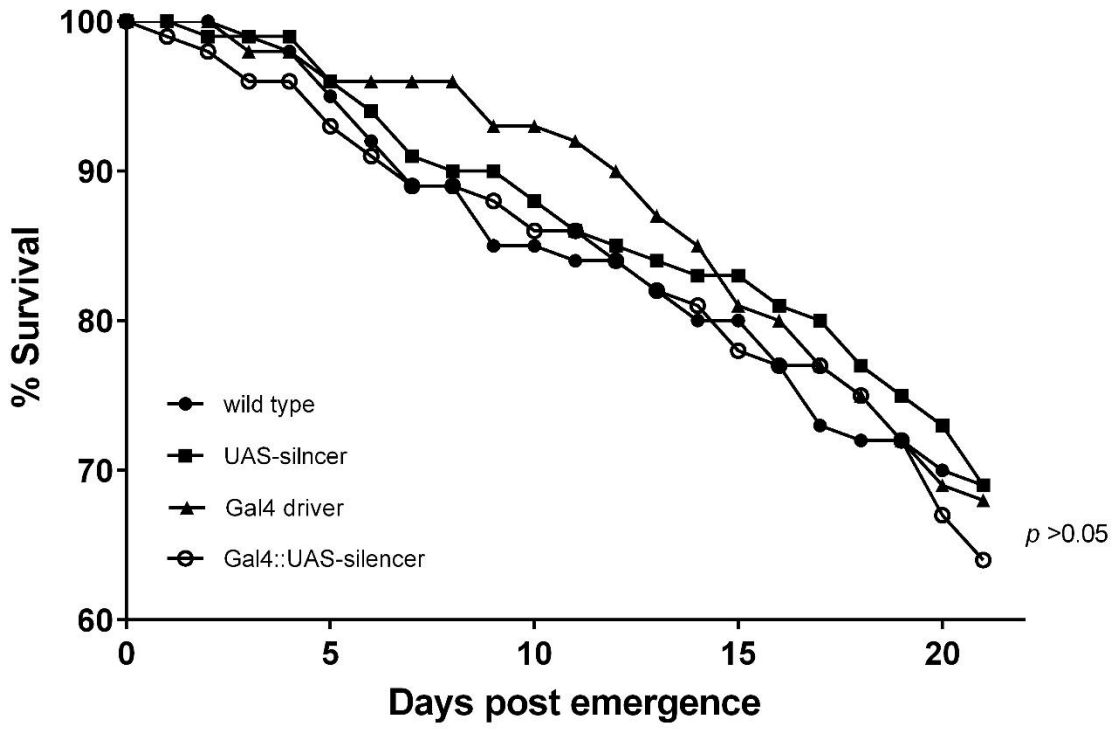

Figure 3.17- Survival comparison of the progeny from a cross of LRIM1-silencer M2 with the MLB24 Gal4 driver line. Fifty female pupae from each genotype were pooled in a cage and observed for 21 days post emergence. The cage was examined daily and dead individuals were removed and the genotype determined. No statistical difference was observed among the genotypes examined.

M7

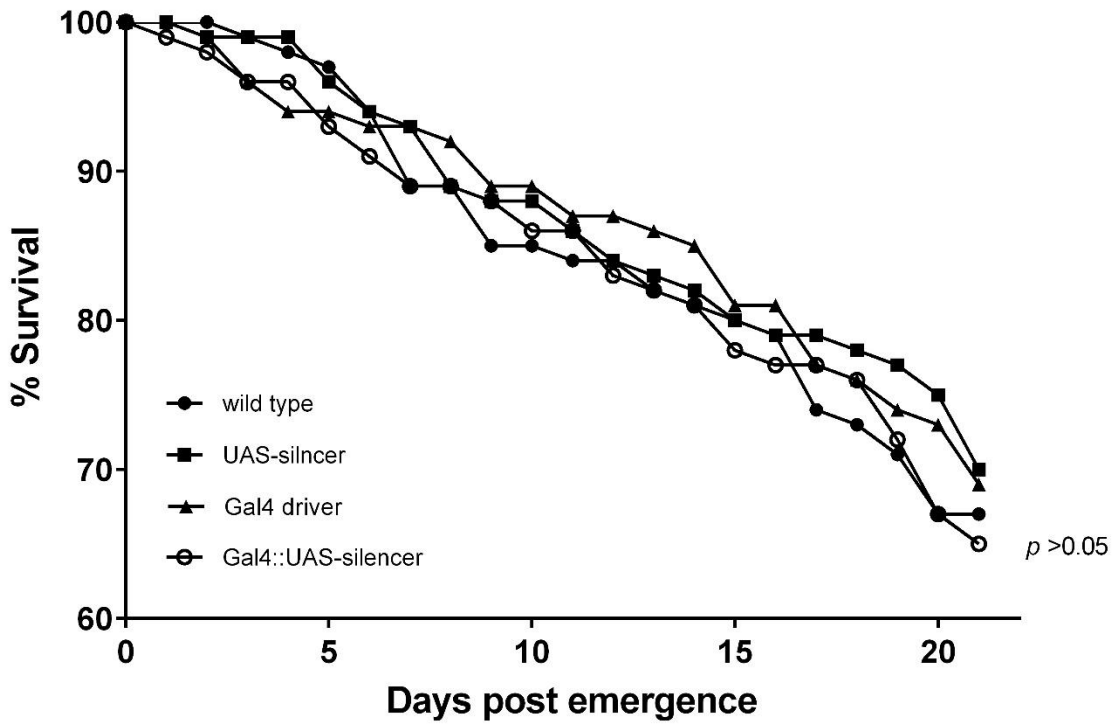

Figure 3.18- Survival comparison of the progeny from a cross of LRIM1-silencer M7 with the MLB24 Gal4 driver line. Fifty female pupae from each genotype were pooled in a cage and observed for 21 days post emergence. The cage was examined daily and dead individuals were removed and the genotype determined. No statistical difference was observed among the genotypes examined.

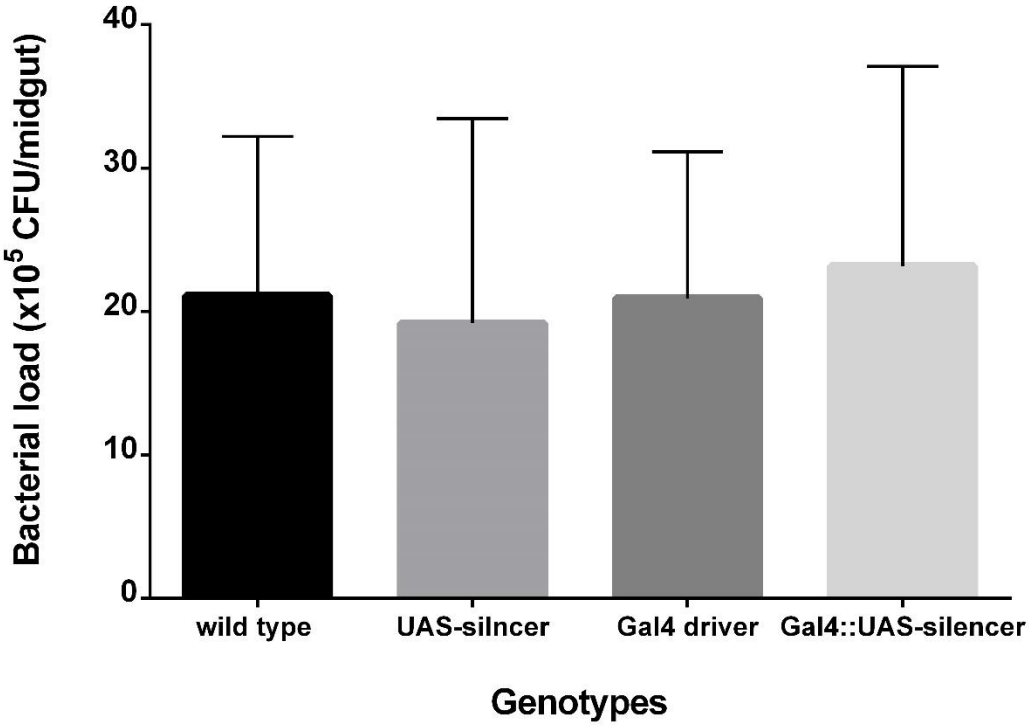

Figure 3.19- Midgut bacterial load among the progeny from a cross of LRIM1-silencer M7 with MLB24 Gal4 driver. Serial dilutions of midgut homogenate of 10 individual females of each genotype were plated on LB agar. CFU was calculated after 48 hour incubation at 27^{o}C. Error bars indicate the standard error of the mean of three independent experiments.

Plasmodium falciparum infections

Plasmodium falciparum Infection experiments were performed using the LRIM1-silencer M7 line. Heterozygous LRIM1-silencer M7 females were crossed with heterozygous MBL24/Gal4 driver males. The progeny were fed with *Plasmodium falciparum* infected blood and each genotype was assessed for prevalence, oocyst and sporozoite infection, in three replicate experiments (See table 2 for summary of results). Seven days post blood feed the mosquitoes were assessed for oocyst infection.

MBL24Gal4/UAS::LRIM1-silencer mosquitoes expressing the hairpin silencing construct had a geomean number of oocyst of 51.3 ± 77.5, 117.8 ± 65 and 37.5 ± 97.3 for the three respective experiments. Corresponding geomean number of oocyts in wildtype individuals were 4.6 – 13 fold lower with counts of 7.1 ± 63.5, 9.0 ± 66.6 and 8.0 ± 37.3. Transgenic mosquitoes with only the GAL4 element or UAS LRIM1 silencer element had mean oocyst counts of 49.5 ± 68.2, 26.7 ± 66.3, 30.8 ± 49.7 and 28 ± 90.5, 23.8 ± 54.2 and 24.5 ± 52.5 respectively. (Figure 3.20) shows the pooled data from the three independent experiments.

Fourteen days PBF the salivary glands of infected mosquitoes were assessed for sporozoite infection (Figure 3.21). Mosquitoes expressing the *LRIM1* silencer construct consistently had 2.5-10 fold higher number of sporozoites in infected salivary glands compared to infected wild type salivary gland. Transgenic control, insects with only the MBL24 Gal4 transgene or the UAS::LRIM1 transgene consistenly had lower sporozoite counts than Gal4::LRIM1-silencer but consistently higher than the wildtype control.

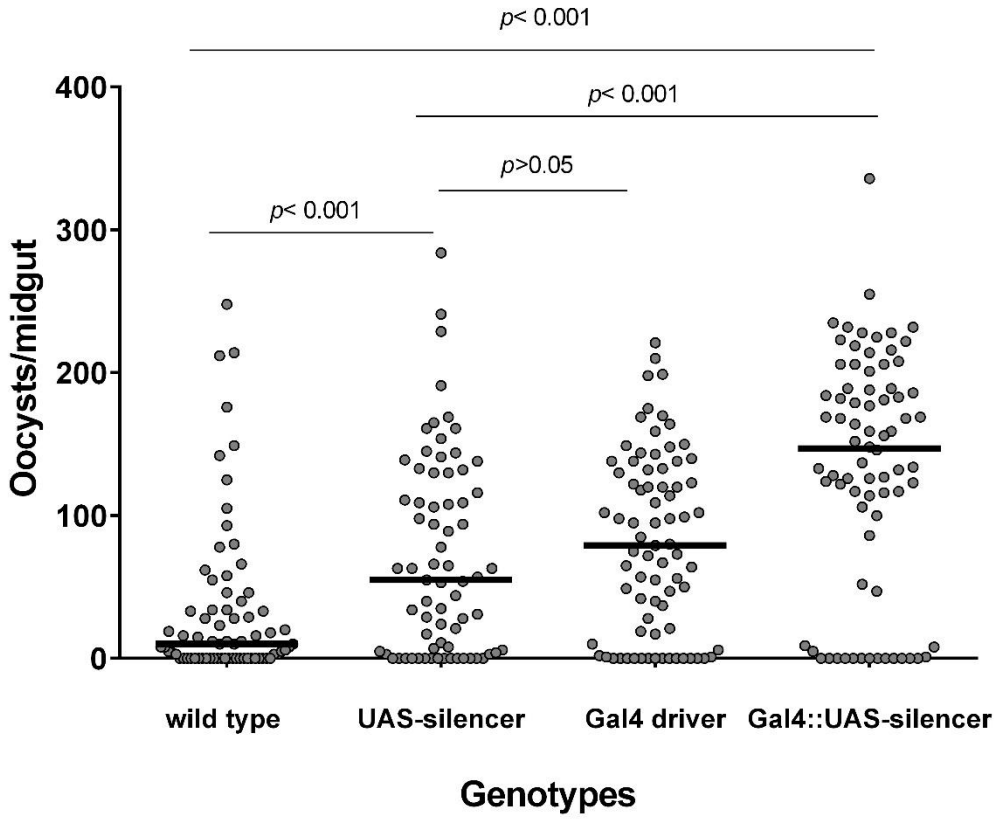

Figure 3.20- *Plasmodium falciparum* infection intensity in *A. stephensi* Sda500 seven days post infection. Circles represent the number of oocysts on a single midgut; horizontal black bars represent the median oocysts in each genotype. Three independent biological replicates were pooled, and significance was determined by a Kruskal-Wallis test followed by Dunn's post-test in the case of multiple comparisons.

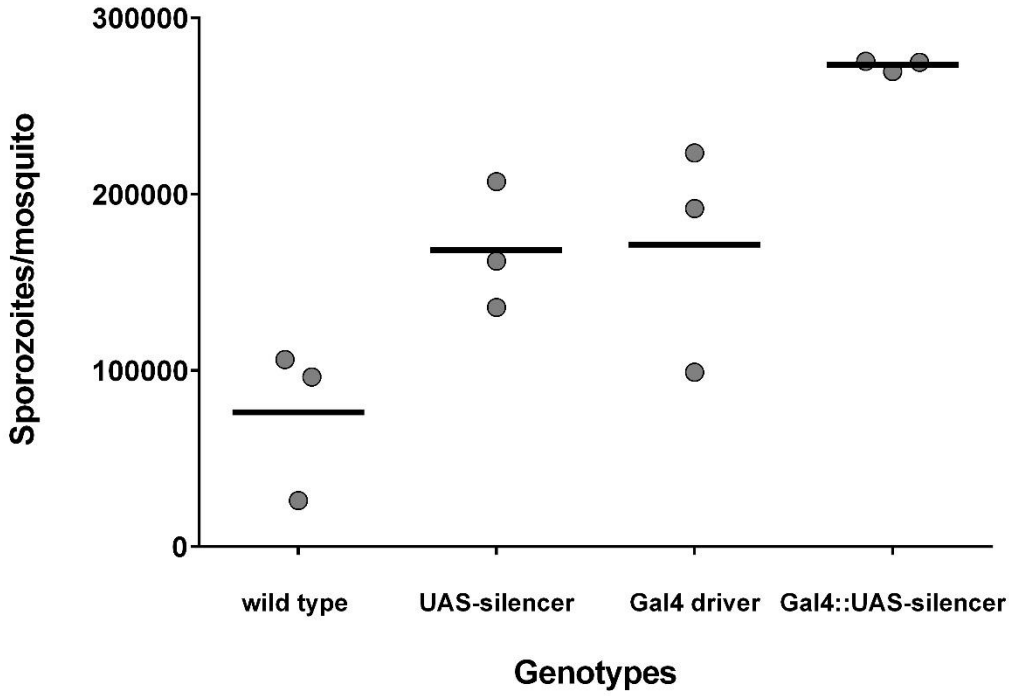

Figure 3.21- *Plasmodium falciparum* infection intensity in *A. stephensi* Sda500 fourteen days post infection. Circles represent the average number of sporozoites from a single mosquito; horizontal black bars represent the mean sporozoites in each genotype. Salivary glands of 21-25 mosquitoes were dissected and pooled and sporozoites intensity assessed.

Table 3.2- Summary statistics from *Plasmodium falciparum* infection assay in figure 3.20.

	P. falciparum infection	GAL4::LRIM1silencer	GAL4 driver	LRIM1silencer	wildtype
Feed A	**Gametocytemia**	0.5	0.5	0.5	0.5
	Prevalence (%) N= 21-25	79.2	88	77.2	64
	Mean oocyst/mosquito (Geomean)	51.3	49.5	28	7.1
	sporozoites/mosquito	274,890	191,889	207,117	26,270
	Prevalence (%, head squash; N= 10)	100	30	56	44
Feed B	**Gametocytemia**	0.5	0.5	0.5	0.5
	Prevalence (%) N= 21-25	96	70.8	78.3	65
	Mean oocyst/mosquito (Geomean)	117.8	26.7	23.8	9
	sporozoites/mosquito	275,438	223,483	162,060	96,365
	Prevalence (%, head squash; N= 10)	100	90	80	60
Feed C	**Gametocytemia**	0.5	0.5	0.5	0.5
	Prevalence (%) N= 21-25	70.8	84	82.6	62.5
	Mean oocyst/mosquito (Geomean)	37.5	30.8	24.5	8
	sporozoites/mosquito	269,733	98,980	135,800	106,210
	Prevalence (%, head squash; N= 10)	100	70	80	40

Plasmodium bergheii infections

Plasmodium berghei infection experiments were performed using the LRIM1-silencer M7 line. LRIM1-silencer M7 females were crossed with heterozygous MBL24/Gal4 driver males. The progeny was provided *Plasmodium berghei* infected mice and each genotype was assessed for prevalence, oocyst and sporozoite infection, in two separate experiments (See table 3 for summary of results). Seven days post blood feed the mosquitoes were assessed for oocyst infection.

Gal4::LRIM1-silencer mosquitoes expressing the hairpin silencing construct had mean oocyst counts of 60.5 and 17.9 for the two respective experiments (Figure 3.22-23). Corresponding counts for wildtype individuals were 41.1 and 12.3. Transgenic mosquitoes with only the GaL4 transgene or UAS::LRIM1 silencer transgene had mean oocyst counts of 44.2, and 13.5 and 36.7 and 12.9 respectively. At lower *Plasmodium berghei* infection intensity indicated by lower oocyts in the midgut, transgenic mosquitoes with the MBL24 Gal4 transgene and UAS::LRIM1-silencer transgene in their genome had statistically higher *Plasmodium* infection based on Kruskal-Wallis analysis.

Fourteen days PBF mosquitoes were assessed for sporozoite infection (Figure 3.24-25). In two independent experiments mosquitoes expressing *LRIM1* silencer construct consistently had increased sporozoite infection compared to wildtype with mean sporozoite counts 1.5 to 2 fold higher. Both transgenic controls (Gal4/+ and LRIM1silencer/+) consistently had lower sporozoite counts than Gal4::LRIM1-silencer but not significantly different to wildtype control based on Kruskal-Wallis analysis

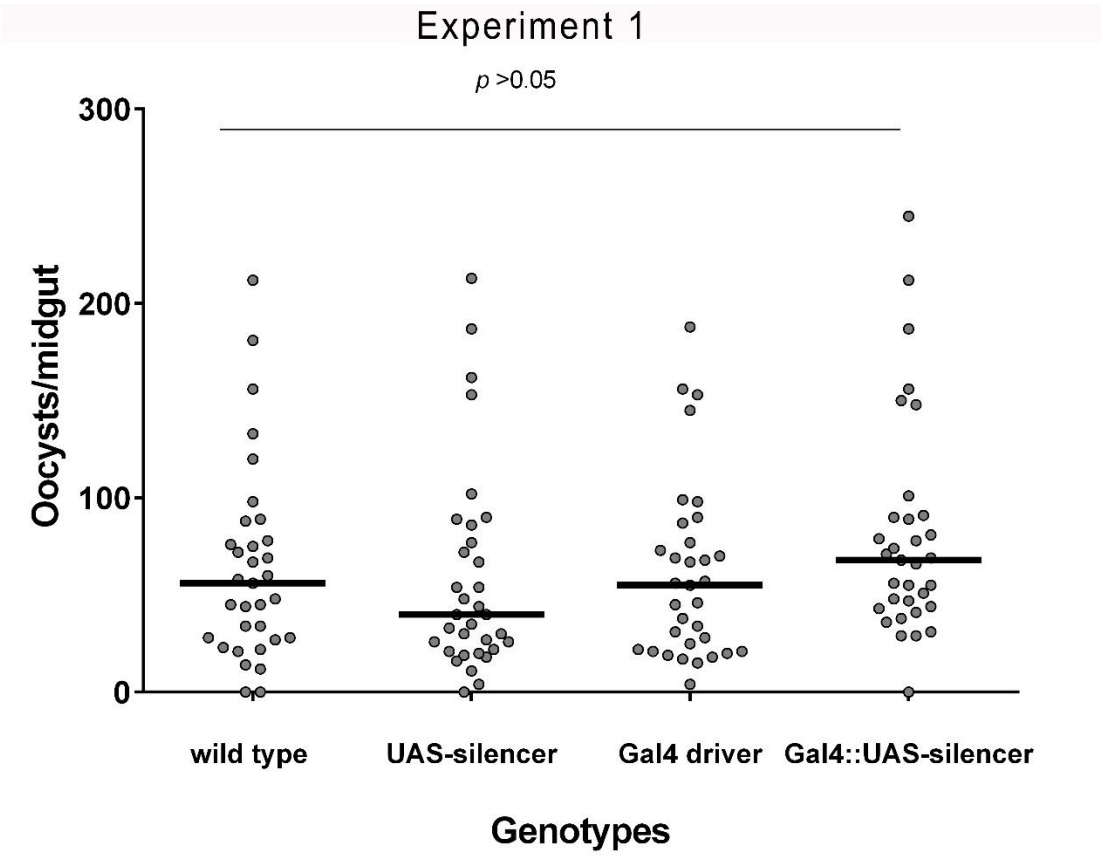

Figure 3.22- *Plasmodium berghei* infection intensity in *A. stephensi* Sda500 seven days post infection. Circles represent the number of oocysts from a single midgut; horizontal black bars represent the median oocysts in each genotype. Data represent a single experiment. Significance was determined by a Kruskal-Wallis test followed by Dunn's post-test in the case of multiple comparisons.

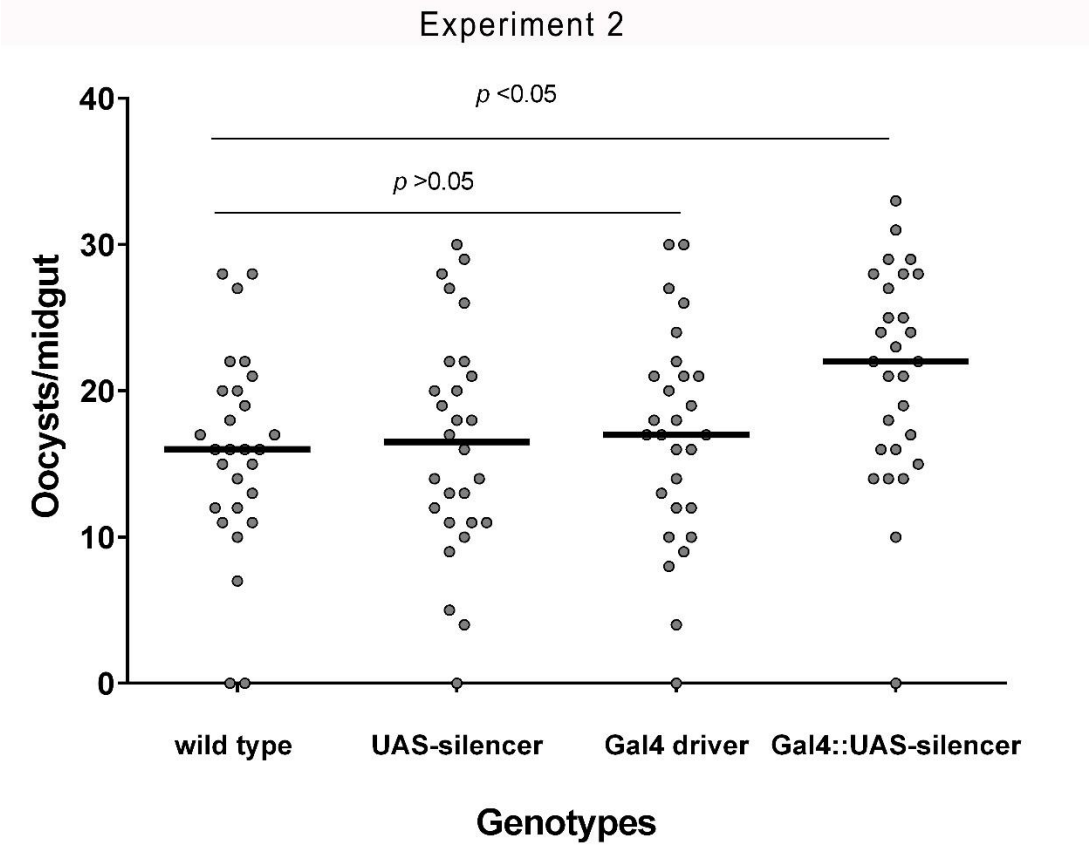

Figure 3.23- *Plasmodium berghei* infection intensity in *A. stephensi* Sda500 seven days post infection. Circles represent the number of oocysts from a single midgut; horizontal black bars represent the median oocysts in each genotype. Data represent a single experiment. Significance was determined by a Kruskal-Wallis test followed by Dunn's post-test in the case of multiple comparisons.

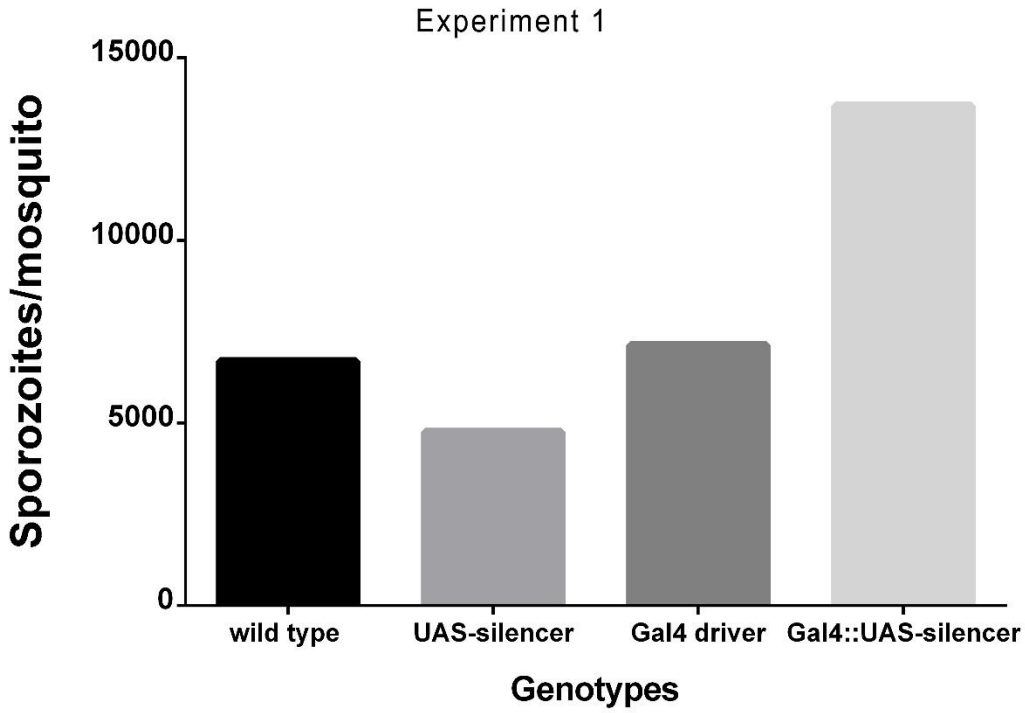

Figure 3.24- *Plasmodium berghei* infection intensity in *A. stephensi* Sda500 fourteen days post infection. Bars represent the average number of sporozoites from a single mosquito. Salivary glands of 25-30 mosquitoes were dissected and pooled and the sporozoite intensity assessed.

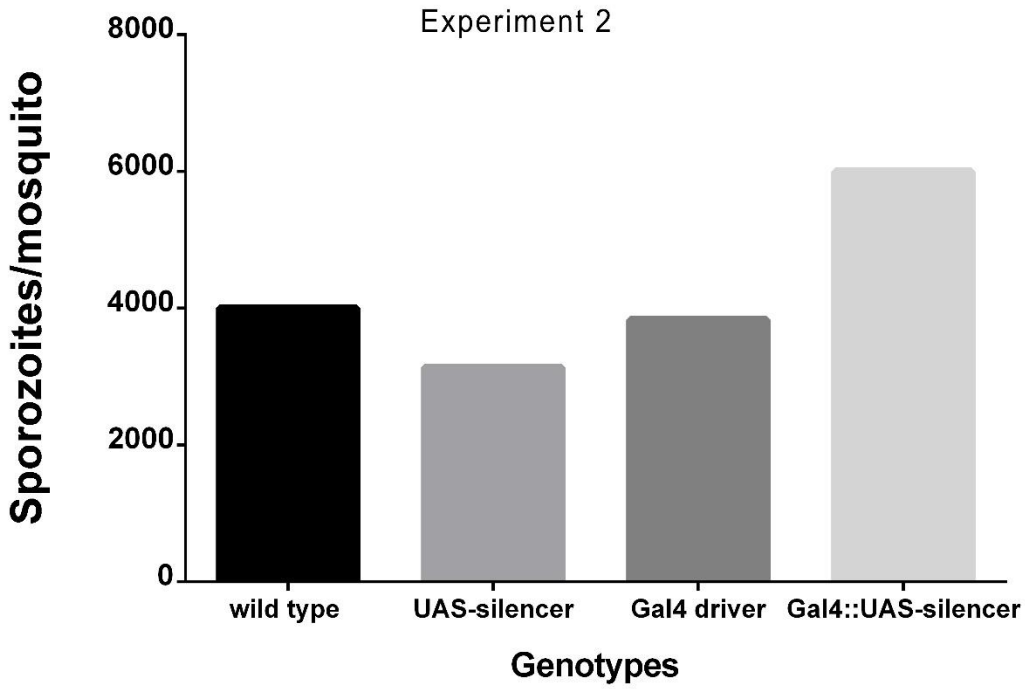

Figure 3.25- *Plasmodium berghei* infection intensity in *A. stephensi* Sda500 fourteen days post infection. Bars represent the average number of sporozoites from a single mosquito. Salivary glands of 25-30 mosquitoes were dissected and pooled and the sporozoite intensity assessed.

Table 3.3- Summary statistics from *Plasmodium berghei* infection assay in figure 3.22-3.23.

	P. berghei infection	wild type	LRIM1silencer	GAL4 driver	GAL4:: LRIM1silencer
Exp.1	**Gametocytemia**	20-24%	20-24%	20-24%	20-24%
	Prevalence (%) N= 33	93.9	100	100	96.9
	Mean oocyst/mosquito (Geomean)	41.09	36.73	44.22	60.51
	sporozoites/mosquito	6,695	4,759	7,133	13,688
Exp.2	**Gametocytemia**	20-24%	20-24%	20-24%	20-24%
	Prevalence (%) N= 28	92.8	96.4	96.4	96.4
	Mean oocyst/mosquito (Geomean)	12.27	12.95	13.55	17.90
	sporozoites/mosquito	4,000	3,133	3,833	6,000

3.4 Discussion

Tissue specific silencing using Gal4/UAS to control *in vivo* dsRNA expression

Reverse genetics approaches and its adaptation to mosquito biology has proven to be a crucial tool for dissecting aspects of mosquito biology and the vector parasite interaction (Blandin et al. 2002; Catteruccia & Levashina 2009). Transient gene silencing by direct injection of dsRNA and stable expression of hairpin RNAs from transgenes integrated into the genome are two approaches of RNAi silencing that have been established in mosquitoes (Catteruccia & Levashina 2009). However, experimental evidence suggests that the efficiency of direct injection of RNAi is limited in space and time (Kennerdell and Carthew 1998; Misquitta and Paterson 1999; Brown et al. 2003). Constitutive *in vivo* expression of hairpin RNAs has its own limitations, one being the analysis of genes with high fitness costs. In this study we demonstrated the adaptation of the bi-partite Gal4/UAS system for control of tissue specific *in vivo* expression of hairpin RNAs in *A. stephensi*. Using this approach we showed we were able to silence *LRIM1* expression in the midgut, fat body and salivary glands of *A. stephensi* throughout the entire vector parasite interaction, thereby eliminating the temporal and spatial limitations reported with the use of dsRNA injections. Unlike, previous studies (Osta, Christophides, & Kafatos, 2004; Jaramillo-Gutierrez et al., 2009; Garver et al., 2012) where dsRNA was used to assess the role of LRIM1 in the anti-*Plasmodium* response over a relatively small window of time, here we were able to study the role of LRIM1 during the entire vector parasite interaction.

Although silencing efficiency using dsRNA to target *LRIM1* has been reported to be upward of 80% (Osta, Christophides, & Kafatos, 2004; Jaramillo-Gutierrez et al., 2009) in this study we observed an average silencing efficiency of only 40% among the different tissues analyzed using three separate *LRIM1* silencing lines. In an attempt to repeat studies by (Osta, Christophides, & Kafatos, 2004; Jaramillo-Gutierrez et al., 2009) female mosquitoes injected with dsRNA against *A. stephensi LRIM1* and *A. gambiae LRIM1* had average silencing efficiencies of 46.5% and 21.2% respectively. It was also observed that *A. stephensi* injected with dsRNA against *A. stephensi* Sda500 *LRIM1* had reduced life span. This phenotype was not observed in mosquitoes expressing *in vivo* shRNA targeting *LRIM1*. Possible hypotheses for this observations are off target effects of the 500bp dsRNA or an increase in pathogenic microbiota in the mosquito in response to *LRIM1* silencing.

LRIM1 silencing did not regulate bacterial load in gut of *A. stephensi* Sda500

Previous studies have demonstrated the role of the IMD pathway (Dimopoulos et al. 1997; Dimopoulos et al in 2002) and specifically the role of TEP1 (Waterhouse et al. 2010; Yassine et al. 2014) in the mosquito defense against bacteria. In our studies silencing *LRIM1* did not change the bacterial load in the midgut. This observation coupled with earlier experiments looking at *LRIM1* expression in response to *E. coli* infection could suggest that LRIM1 in *A. stephsnsi* does not play a role in the immune response to bacterial pathogens. However further analysis of the *A. stephensi* microbiome is needed.

Sporozoite infection intensity is increased in transgenic *A. stephensi*

LRIM1 was originally identified as a strong antagonist of *Plasmodium* infection in a rodent malaria model but was subsequently shown to have little observable effect on the number *P. falciparum* oocyst developing on the basal surface of the midgut (Osta, Christophides, and Kafatos 2004; Cohuet et al. 2006). Later work revealed that LRIM1 does in fact contribute to the mosquito's anti-*P. falciparum* response, but only at medium levels of oocyst intensities with little observable effect at low intensities (Garver et al. 2012). In our study, transgenic *A. stephensi* expressing a transgene whose transcript formed a short hairpin RNA that lead to the silencing of *LRIM1* showed a statistically significant increase in oocysts intensity compared to wildtype. Further analysis also showed that sporozoite infection intensity was also higher in these mosquitoes compared to wildtype. Our data shows that transgenic mosquitoes with reduced *LRIM1* expression had more oocysts on the basal surface of the midgut seven days post infection with *Plasmodium falciparum*. Similar results were observed with lower infection levels of *Plasmodium berghei* suggesting an infection intensity dependent function of *LRIM1*. In both *P. berghei* and *P. falciparum* infections mosquitoes with reduced *LRIM1* expression consistently had higher sporozoite intensities in the salivary glands fourteen days post infection when compared to infected controls. Our data shows that transgenic mosquitoes with reduced *LRIM1* expression are excellent candidates for being incorporated into the sporozoite and vaccine production process at Sanaria Inc.

However, while results here are consistent with earlier findings that reduced LRIM1 expression results in increased infection intensity some uncertainty remains with regards to the mechanism of increased intensity. Infection data also indicated that transgenic mosquitoes that contained only the Gal4 transgene or LRIM1 silencer transgene had statistically significant increases in both oocyst and sporozoite intensity compared to wild type. Therefore, increases observed in mosquitoes with both transgenes in their genome could be interpreted as an additive effect of the transgenes and not *LRIM1* silencing. If increase in sporozoite intensity is in response to *LRIM1* silencing we believe the difference observed in our data and previous studies is due to the approach used for silencing that allowed targeting of *LRIM1* in organs directly involved in the parasite development cycle in the mosquito.

Overproduction of Gal4 in our MBL24 driver line (Kramer and Staveley 2003; Lynd and Lycett 2012; Balciuniene et al. 2013) or transgene position (Clark et al. 1994; Feng et al. 2001) could affect mosquito fitness and compromise the anti-*Plasmodium* response. On the other hand, leaky expression of the hairpin RNA could reduce LRIM1 transcripts enhancing *Plasmodium* susceptibility.

Further analysis on the effects transgene integration might exert on the immune response is needed before we can attribute increased salivary gland sporozoite intensity to LRIM1 silencing. However, average increase in sporozoite intensity (>5 fold) compared to wildtype Sda500 can significantly impact Sanaria's manufacturing platform, increasing manufacturing efficiency and ultimately reducing vaccine cost.

Chapter 4: Effort to develop a *LRIM1* promoter regulated Gal4 driver line

4.1 Introduction

The current model of LRIM1 function proposes that *LRIM1* is expressed in the fat body, midgut and hemocytes (Yassine and Osta 2010). However, microarray experiments of *A. gambiae* have shown evidence of *LRIM1* expression in the head, salivary glands, ovaries and malpighian tubules of adult females (Pinto et al. 2009; Baker et al. 2011). Previous microarray methods used to determine the spatial and temporal pattern of *LRIM1* expression were limited in their resolution and were dependent on the quality of tissue collection (Groen 2001). Here, we aim to determine the spatial and temporal pattern of *LRIM1* expression by creating transgenic *A. stephensi* Sda500 that will make use of the bi-partite GaL4::UAS system to control a fluorescent marker gene. Use of an *A. stephensi* Gal4 line with Gal4 ORF under regulatory control of the *LRIM1* promoter, can allow for the spatial, and temporal pattern of *LRIM1* expression to be assessed visually during pathogenic, non-pathogenic, and other developmental conditions, when crossed with a responder line, containing a fluorescence gene such as TdTomato (Shaner et al. 2004) under regulatory control of UAS.

Furthermore a transgenic *LRIM1* regulated Gal4 line when crossed with an *in vivo* shRNA silencer line like the LRIM1-silencer created here, would target all tissues where *LRIM1* is expressed. This could significantly reduce the level of *LRIM1* transcript reduction currently observed and further increase *Plasmodium* infection intensity.

4.2 Materials and Methods

For Materials and Methods see page 111.

4.3 Results

Cloning LRIM1 promoter

Based on an assembled draft genome of *A. stephensi* sequence (created and made available by Dr. Zhijian Tu at Virginia Polytechnic Institute and State University, Blacksburg, VA 24061) a 3.2 kilobase fragment upstream of the predicted *LRIM1* ORF was amplified using *A. stephensi* genomic DNA as template and primers LRIM1fw 835 (5'- GCG AGG ATG ACC CAC TAG AG-3') and LRIMrv (5'-ATA GGA TCC TAG GCG CGC CCC TCC TGA -3')

Characterization of LRIM1pGal4 lines

Transgene insertion site

Three LRIM1pGal4 lines; LRIMpGal4 M2, LRIMpGal4 M4, and LRIMpGal4 (Figure 4.1), were created as described in the Material and Methods. (Here we refers to lines LRIMpGal4 M2, LRIMpGal4 M4, and LRIMpGal4 as GM2, GM4 and GM8 respectively). Cytogenetic location of the transgene insertion site was determined using Splinkerette PCR and chromosomal location data of *A. stephensi* scaffolds provided by Igor Sharakov of Virginia Polytechnic Institute and State University. Integration site for GM2 was determined to be in the intergenic region of scaffold KB665354 on chromosome 2L. For GM4 the transgene was found in the intergenic region of scaffold

KB665343 located on chromosome 3R while the GM8 transgene was located in the intergenic region of KB664529. (scaffold location of M8 was undertermined) For summary of results see Table 4.

Table 4.1- Cytogenetic location of LRIMpGal4 transgene integration sites in the *A. stephensi* genome.

	Insertion site	
Silencer line	**Scaffold**	**Chromosome**
LRIMpGal4 M2	KB665354	2L
LRIMpGal4 M4	KB665343	3R
LRIMpGal4 M8	KB664529	unknown

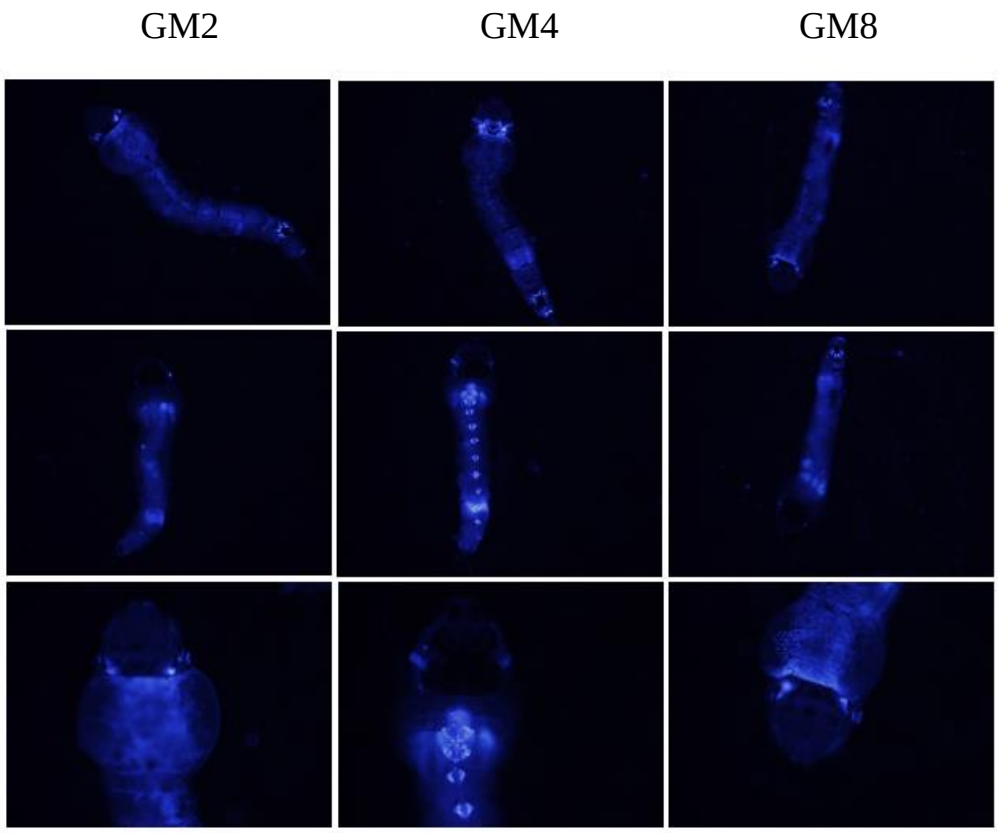

Figure 4.1- Transgenic lines LRIMpGal4 M2, LRIMpGal4 M4, and LRIMpGal4. (A) Dorsal view of whole third-instar larva showing ECFP expression. (B) Ventral view of whole third-instar larva showing ECFP marker gene expression. (C) Magnification of head showing nuclear localized expression.

Assessment of functional promoter

Crossing of the LRIM1pGal4 line with a UAS::TdTomato responder line (O'Brochta et al. 2012) generated no visible fluorescence response in tissues observed. (Figure 4.2)

P. bergheii infected *A. stephensi* Sda500 containing the LRIMpGal4 transgene and the UAS::TdTomato transgene where analyzed using qRT-PCR 24 and 72 hours post infection to assess native *LRIM1* promoter function and transgenic LRIM1 promoter function. Gal4 expression was used as a proxy for transgenic promoter function. 24 hours post infection expression of *LRIM1* increased on average 4 fold and expression of the transgenic Gal4 increase an average of 3-fold. The expression of LRIM1 and the transgenic Gal4 were significantly reduced 72 hours post infection (Figure 4.3)

Midgut

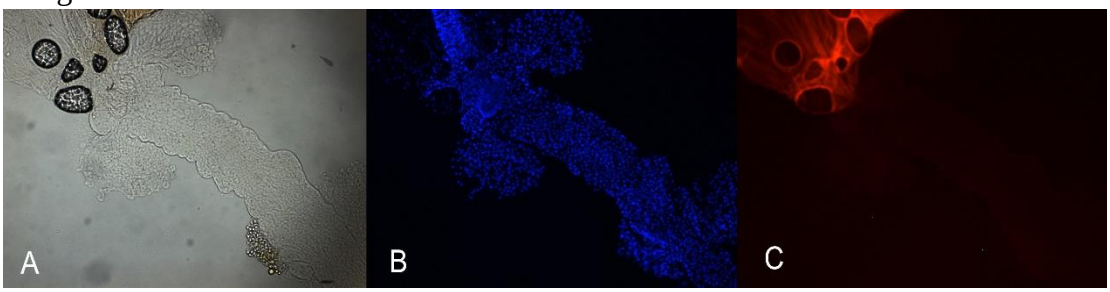

Ovaries

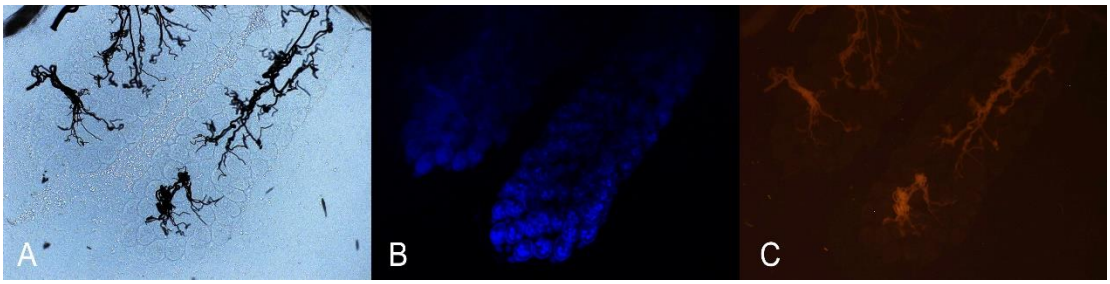

Fat bodies (adipocytes)

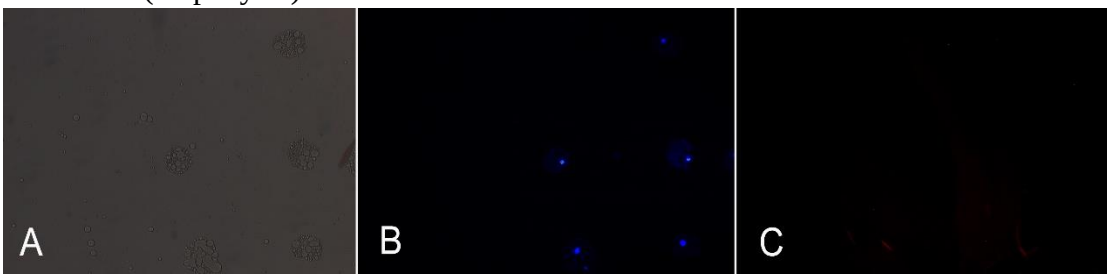

Pupae

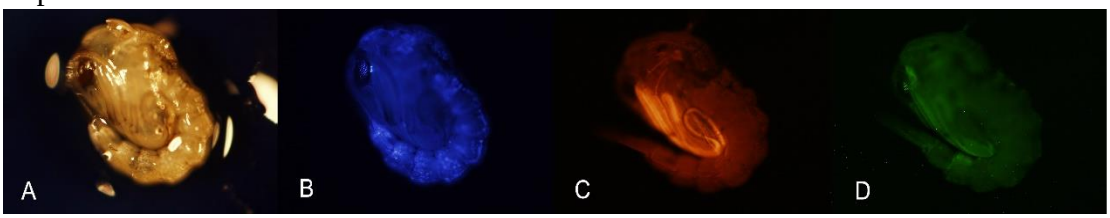

Figure 4.2- *A. stephensi* Sda500 with the LRIMpGal4 transgene and UAS::TdTomato transgene in the genome. A - Brightfield image; B- DAPI stain showing cell nuclei; C- ET-DsRed filter for TdTomato visualization; D- GFP filter (negative control).

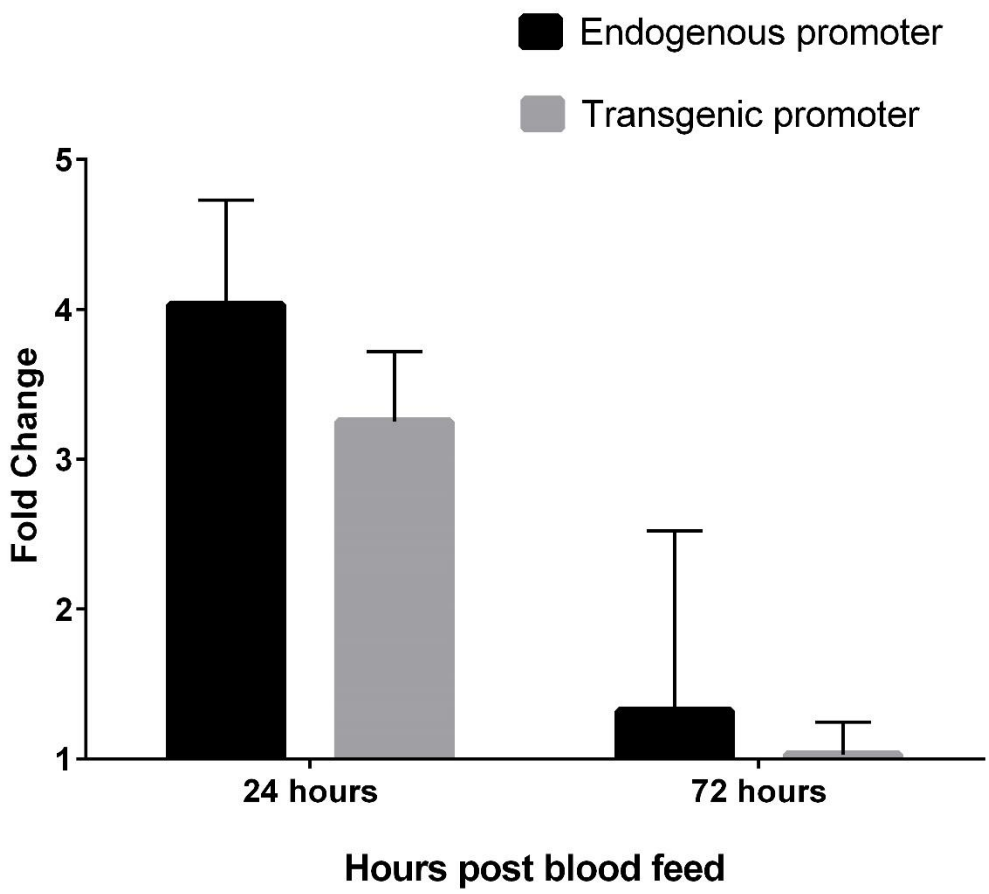

Figure 4.3- Expression profile of *LRIM1* post *P. berghei* infection showing maximum expression 24 hours post infection. Expression is significantly lower 72 hours post infection. The activity of the transgenic *LRIM1* promoter parallels the endogenous *LRIM1* promoter and shown by the Gal4 expression. Gene expression was measured as described in Materials and Methods. Average transcript abundance is shown relative to non-infected transgenic mosquitoes. Transcript levels of ribosomal *S7* gene were used as a calibrator. Bars indicate standard error of the mean of three independent experiments.

4.4 **Discussion**

O'Brochta et al. (2012) showed that the expression of TdTomato in transgenic *A. stephensi* with a gene encoding TdTomato under the control of UAS could be regulated using Gal4 driver lines. In my experiments, an *LRIM1* regulated Gal4 driver line when crossed with a UAS::TdTomato transgenic line did not generate any visible TdTomato reponse. However, qRT-PCR data indicated that we were successful in cloning a 3.2 kilobases fragment upstream of the ORF of *LRIM1* that contains the promoter. One hypothesis for no visual TdTomato response being observed is that the threshold of TdTomato translated protein needed for it to be visualized under fluorescence microscopy is not being achieved. Another hypothesis purports a possible conformational change in the Gal4 protein thereby reducing efficient binding to the UAS sequence. Lynd and Lycett (2012) have also reported on minimum activity of the native Gal4 used in my experiments in mosquito species. Future experiments using variants of the Gal4 trans-activator, and assessing threshold activity required for visual TdTomato response in *A. stephensi* Sda500 are required.

Chapter 5: Conclusion and Discussion

In the preceding work, I sought to increase the *Plasmodium* sporozoite intensity in the salivary glands in order to enhance vaccine production. Using molecular tools rarely, if ever used in *A. stephensi* Sda500 the overarching goal of the project was successfully achieved.

In chapter 2 *Plasmodium* infections assays and qRT-PCR were used to characterize the response of the IMD pathway effector gene *LRIM1* in response to parasite infection. These findings lead to the validation of *LRIM1* as a suitable target for immune modification. However many questions remain. What is the role of the salivary gland in response to *Plasmodium* infection? Are there other pathways for IMD signaling and what is the transcription factor? Aside from these remaining questions, future directions should include a rigorous biochemical characterization of leucine rich repeat proteins. There are also other regulated gene transcripts in the non-pathogenic gene response transcriptome awaiting characterization. These studies could provide additional targets genes for function studies and translational applications utilizing transgenic mosquitoes.

In Chapter 3, it was confirmed that sporozoite intensity in the salivary glands can be increased by using transgenic mosquitoes with modified immune systems. While our result are consistent with earlier studies that showed that reducing *LRIM1* expression increased infection intensity some uncertainty remains. These questions must be answered to understand the role of *LRIM* in *Plasmodium* defense. In the future the use of Gal4 driver lines that regulate expression in a single tissue will allow the role

of different tissues in the response to pathogens to be determined. Also an active *A. stephensi* line with the Gal4 ORF under the regulatory control of the LRIM1 promoter can provide important answers about the biology of LRIM1.

Chapter 6: Materials and Methods

Mosquito strain

Anopheles stephensi Sda 500 is a laboratory strain of *A. stephensi*, which was first isolated in Pakistan and selected in the laboratory for susceptibility to *Plasmodium falciparum* infection (Feldman *et al.* 1990)

Mosquito rearing

Anopheles stephensi Sda500 mosquitoes were grown in a Conviron environmental chamber at 28^{o}C, with 80% relative humidity under a 12-hour light/dark cycle. Larvae were fed pulverized fish food (TetraMin Tropical Flakes) *ad libitum* while adults were provided 10% sucrose continuously. Seven day old adult females were provided a blood meal of bovine whole blood in acid citrate dextrose (Lampire Biological Laboratories, Pipersville, PA) at 37^{o}C through a parafilm membrane on a Mosquito Feeder (Chemglass Life Sciences, Vineland, N.J.) for reproduction. Eggs were collected in 50 mL of deionized water in a 250 mL Biostor multipurpose container (Fisher Scientific), lined with Whatman filter paper (Cat No. 1001 090).

Artificial feeding buffer

Artificial feeding buffer composed of 150 mM NaCl; 10 mM $NaHCO_3$; 1mM Adenosine -5-triphosphate (ATP) (Galun 1967) was substituted for blood in experiments were blood could not be used. The solution was fed through a parafilm membrane on a Mosquito Feeder (Chemglass Life Sciences, Vineland, N.J.) at 37^{o}C

Experimental infection of *A. stephensi* with *P. falciparum*

A. stephensi Sda 500 female mosquitoes were infected with *P. falciparum* NF54 by feeding mosquitoes *P. falciparum* gametocytes in transfusion-quality human erythrocytes and serum. Fresh transfusion quality human blood and serum were incubated at 37ºC. Using aseptic techniques, 1 mL of warm blood was aliquoted into an Eppendorf tube and centrifuged for 5 minutes at 2200 RPM. The clear serum was discarded and the pelleted erythrocytes were washed with an equal volume of new serum three times to obtain the whole blood for the gametocytes.

Sixteen day old gametocyte culture in RPMI media was removed from the CO_2 incubator and the gametocytemia percent was determined by making a smear on a glass slide with one drop of blood. The smear was stained with Giemsa stain (Sigma Aldrich 48900). The number of gametes in a field of parasite culture was determined, and the volume of whole blood needed for a final percent gametocytemia of 0.5 percent was calculated.

Without disturbing the parasite most of the RPMI media was removed from the gametocyte culture using a pipette (parasites appear black and media light red/pink). The remaining gametocyte culture was transferred to a 15 mL falcon tube (Thermo Fisher Scientific Inc. Rockville MD, USA) and centrifuged for five minutes at 2200 RPM. The supernatant was discarded without disturbing the pelleted gametocytes and erythrocytes. The gametocytes were then combined with the required volume of whole blood for a final gametocytemia of 0.5 percent. The gametocytes were re-suspended in the whole blood and incubated at 37ºC.

Three separate cohorts of approximately 400 female wild-type *A. stephensi* were fed *Plasmodium falciparum* infected blood. Females observed not feeding were removed from the cage. Twenty four hours post feeding, 20 mosquitoes with visual signs of blood in the midgut were removed from each cohort and anesthetized in cold phosphate buffered saline (PBS).The mosquitoes were dissected and the midguts and carcasses of the separate mosquito cohorts were immediately flash frozen in RNase free tubes on dry ice and pooled for subsequent RNA extraction and real-time PCR. This process was repeated 48 and 72 hours post infection. Seven days post infection, the midguts of 30 mosquitoes from each cohort were dissected and the oocyst intensity determined using *Giemsa* staining. Fourteen days after blood feeding the salivary glands of approximately 20 mosquitoes were dissected and immediately flash frozen on dry ice for subsequent RNA extraction. The salivary glands of approximately 30 mosquitoes were dissected and sporozoite intensity and prevalence determined

Salivary glands were dissected and kept on ice in 30 µL of RPMI media until the dissections were complete. After dissections, the sporozoites were released from the salivary glands by aspirating the media containing the salivary glands, five times with a 26 gauge, 2 inch point style 3 Hamilton syringe (Reno Nevada, USA). 10 µL of the media with sporozoites was transferred to a Bright-Line hemocytometer (Hausser Scientific, Horsham Pennsylvania, USA). The hemocytometer was then placed on a wet Kimwipe (Kimberly-Clark, Irving Texas, USA) in a petri dish and covered. Sporozoites were allowed to settle for 10 to 15 minutes. The number of sporozoites in two of the four quadrants were then counted. The total number of sporozoites was then calculated.

Genomic DNA extraction and quantification

The following method is a modification of the Ashburner's method for genomic DNA extraction (Ashburner 1989). Mosquito tissue was homogenized in 50 µL of homogenization buffer (10 mM Tris-HCL pH 7.5, 10 mM EDTA, 5% sucrose [w/v], 0.15 mM spermine, 0.15 mM spermidine) and kept on ice. 50 µL of lysis buffer (300 mM Tris-HCL pH 9.0, 100 mM EDTA, 0.625% SDS [w/v], 5% sucrose [w/v] was added to the homogenized mixture, properly mixed and incubated at 70^{o}C for 15 minutes. The mixture was then cooled to room temperature and 15µL of 8M potassium acetate was added and mixed thoroughly. The mixture was then placed on ice for 30 minutes after which it was centrifuged at 14,000 RPM for 10 minutes at RT. The supernatant was transferred to a fresh tube and 90 µL of phenol/chloroform/isoamylic alcohol was added and mixed. The mixture was centrifuged at 14,000 RPM at 4^{o}C. The supernatant was transferred to a new tube and two volumes of absolute ethanol was used to precipitate DN*A.* The mixture was centrifuged at 14,000 RPM for 5 minutes at RT. The supernatant was discarded and the pellet was washed in 70 % ethanol. After centrifuging for 10 minutes at 14,000 RPM the supernatant was discarded and the DNA pellet was vacuum dried and suspended in 1× TE buffer pH 7.4. The concentration of nucleic acids was determined spectrophotometrically using the NanoDrop ND-1000 spectrophotometer (NanoDrop, Wilmington, USA) by measuring light absorption at 260 nm. Nucleic acid purity was checked by determining the absorption at a wavelength of 230 and 280 nm, respectively.

Cloning of *Anopheles stephensi* Sda 500 *Leucine Rich Immune Molecule 1*

Leucine rich immune molecule 1 (LRIM1) was cloned from *A. stephensi* cDNA using Polymerase chain reaction (PCR). *LRIM1* was amplified using primers AsLRIM1fw (5' - CCC GCC GGT ATA GCT TAT CAG – 3') and AsLRIM1rv (5'-CAA ATA GTG CTC GTC TGC GC - 3'). To design primers, a known *A. gambiae* LRIM1 sequence (AGAP0006348) was aligned using ApE-A plasmid Editor to an assembled draft genome sequence of *A. stephensi* created and made available by Dr. Zhijian Tu at Virginia Polytechnic Institute and State University, Blacksburg, VA 24061, and now publicly available on VectorBase (Lawson et al. 2007). Conserved regions in *A. gambiae* LRIM1and *A. stephensi* LRIM1 reported by Jaramillo-Gutierrez et al. (2009) were identified. The Open reading frame (ORF) was identified using ORF Finder (Wheeler et al. 2003). Primers were designed upstream of the ORF and downstream of the stop codon. Phusion High-Fidelity polymerase (New England Biolabs (NEB) Ipswich, Mass.) was employed for PCR. *LRIM1* PCR product was purified by gel electrophoresis and gel extraction (QIAquick gel extraction kit). Purified PCR product was inserted into Zero Blunt TOPO PCR Cloning vector (Thermo Fisher Scientific Inc., Rockville, MD) according to the manufacturer's instructions and transformed into *E. coli* DH10B (Gibco-BRL). Colonies were screened for insertion. Positive colonies were digested with *EcoRI* and agarose gel electrophoresis was used to identify insertion of *LRIM1* PCR product. Sequence identity was then confirmed with DNA sequencing (Macrogen Inc, Rockville MD)

Total RNA extraction and quantification

To isolate total RNA from mosquito tissue, Ambion Trizol Reagent was used according to the manufacturer's instructions. To avoid RNase activity, RNase-free water and RNase-free reaction tubes were used during the procedure. Briefly, total RNA was extracted by homogenizing the tissue in 1 mL of Trizol. The homogenized sample was incubated for 5 minutes at room temperature (RT) to allow for complete dissociation of the nucleoprotein complex. 0.2 mL of chloroform:isoamyl (49:1) was then added to the homogenized sample. The mixture was shaken vigorously by hand for 15 seconds and incubated at RT for 3 minutes before centrifugation at 12,000 × g for 15 minutes at 4^{o}C. The aqueous phase containing RNA was transferred to a new tube. RNA was precipitated with 0.5 ml of 100% isopropanol. The mixture was left at RT for 10 minutes before centrifuging at 12,000 × g for 10 minutes at 4^{o}C. The RNA pellet was washed with 1 mL of 75% ethanol. After centrifuging at 7,500 × g for 5 minutes, the wash was discarded and the RNA pellet vacuum dried and suspended in RNase-free water. DNase I (RQ1 RNase free DNase – Promega, Cat. No. M610A) treatment was done at 37^{o}C for 20 minutes to eliminate any DNA contamination. After inactivating the DNase I, the volume of the reaction mix is made up to 50 µL. The concentration of nucleic acids was determined spectrophotometrically using the NanoDrop ND-1000 spectrophotometer (NanoDrop, Wilmington, USA) by measuring light absorption at 260 nm. Nucleic acid purity was checked by determining the absorption at a wavelength of 230 and 280 nm, respectively.

Reverse Transcription PCR (cDNA synthesis)

To generate a representative cDNA pool from RNA templates, 1-5 µg of total RNA were mixed with 1 µL of oligo(dT)20 primer (50 µM), 10 mM dNTP mix and RNase free water to a total volume of 10 µL. To facilitate hybrid formation of the oligo dT-primers with polyA-tails of mRNA, the mixture was heated to 65° C for 5 minutes and then quickly chilled on ice. A master mix containing 2 µL of 10X Reverse transcriptase (RT) buffer; 4 µL of 25 mM $MgCl_2$; 2 µL of 0.1 M DTT; 1 µL of RNase OUT (40 U/µL); 1 µL of Superscript III Reverse transcriptase (RT) (200 U/µL), was added to the mixture:

The content of the tube was gently mixed and incubated at 50° C for 50 minutes for first strand cDNA synthesis. The reaction was then inactivated by incubating the mixture at 85° C for 5 minutes and then chilled on ice. After brief centrifugation, 1 µL of RNase H was added to the mixture and incubated at 37°C for 20 minutes. The cDNA sample was then used for PCR reactions.

Real-time polymerase chain reaction

Template for the Real-time PCR from cDNA synthesis was diluted to 200 ng. All the samples to be compared were processed in parallel and 3 independent experiments were performed. PCR reaction was done with 96 well plates (MicroAmp; Applied Biosystems; Cat No. N801-0560) covered with optical adhesive covers (Applied Biosystems; Cat No. 4313663). The instrument used was an ABI PRISM 7000 Sequence Detection System (Applied Biosystems). Reaction conditions were as follows: one step of 95°C for 3 minutes, 40 cycles of 95°C for 30 s denaturation and

52°C for 30 s annealing and 72°C for 15 s extension. Flouresence readings were taken at 72°C after each cycle. A final extension of 72°C for 5 minutes was completed before deriving a melting curve. Reaction master mix was made with GoTaq colorless master mix (Promega, Fitchburg, WI). Primers and templates were added according the manufacturer's instructions. Gene expression was assessed with SYBR green (Life Technologies). The reference gene used for the experiments was the ribosomal *S7* gene.

Synthesis of dsRNA for *LRIM1* silencing

A cDNA fragment of 500 bp of *LRIM1* was amplified using the following primers, LRIM1 dsRNAfw (5'- TAA TAC GAC TCA CTA TAG GGA GAC GAC TGT ATC TGG CCA ACA ATA - 3') and LRIM1 dsRNArv (5'- TAA TAC GAC TCA CTA TAG GGA GAT CGG TGT CCG TGC ACG CCT CCT - 3') with T7 sites flanking the 5 prime ends and cDNA template from one week old *A. stephensi* females as template. The resulting PCR fragment was cloned into the pCR II-TOPO vector (Invitrogen, Carlsbad, CA) and transformed in *E. coli* DH10B (Gibco-BRL). Colonies were screened for insertion using restriction enzyme digestion with *EcoRI* and gel electrophoresis. High yield plasmid DNA was isolated using QUIAGEN Plasmid Maxi Kit. The T7 flank fragment used for dsRNA synthesized was removed from the plasmid by digestion with EcoRI. Double stranded RNA was generated and purified using the MEGAscript kit (Ambion, Austin, TX).

Silencing *Anopheles stephensi LRIM1* and bacterial infection

Four days old *Anopheles stephensi* females were anesthetized on ice for 5 minutes and transferred to a 4^{o}C injection plate. Approximately 100 nL of *LRIM1* dsRNA (3ng/nL) or EGFP dsRNA control was injected into the thorax of the mosquitoes using a Pneumatic PicoPump PV820 (World Precision Instrument Inc., Sarasota, FL.). After injection the mosquitoes were allowed to recover at RT for one hour before being transferred to an environmental chamber (28^{o}C, 80% humidity, and 12 hour light/dark cycle) (Conviron, Winnipeg, Manitoba) and provided 10% sucrose. *LRIM1* silencing was confirmed 4 days post dsRNA injection by real-time quantitative PCR. For bacterial infections the needle was dipped in a pellet of *E. coli* (DH10B) OD600 of 0.1 and injected into the thorax of the mosquito. For bacterial infections by feeding, artificial feeding buffer was inoculated with *E. coli* to a final CFU of 100 CFU/ml

Mosquito survival post dsRNA injection

Three cohorts of 50 four day old adult *Anopheles stephensi* females were obtained. *A. stephensi* females were anesthetized on ice for 5 minutes and transferred to a 4^{o}C injection plate. Approximately 100 nL of *LRIM1* dsRNA (3ng/nL) or EGFP dsRNA control was injected into the thorax of the mosquitoes using a Pneumatic PicoPump PV820 (World Precision Instrument Inc., Sarasota, FL.). After injection the mosquitoes were allowed to recover at room temperature (RT) for one hour before being transferred to an environmental chamber (28^{o}C, 80% humidity, and 12 hour light/dark cycle) (Conviron, Winnipeg, Manitoba) and provided 10% sucrose.

Mosquitoes were observed over the following days and the number of dead mosquitoes were recorded. A cohort of 50 un-injected adults *A. stephensi* females was simultaneously observed under the conditions mentioned above.

Survival comparison of transgenic mosquitoes.

LRIM1-silencer/- lines were crossed with the MB24 Gal4/- driver line. From the progeny of the cross, 100 female pupae of each genotype were screened for using the fluorescence marker gene. The pupae were pooled, and placed in a one gallon mosquito cage. After emergence, the mosquitoes were maintained on a 10 percent sucrose solution. The cage was examined each day for dead mosquitoes. The dead mosquitoes were screened and scored.

Isolation of midgut microbiota for microbial load assessment.

Individual *A. stephensi* Sda500 were surface-sterilized by washing three times with alternating 70% ethanol and sterile phosphate-buffered saline (PBS) washes. The midguts were then dissected in PBS using flame-sterilized forceps and homogenized in 200µl of PBS using a sterilized pestle. Each midgut homogenate was then serially diluted and inoculated on Luria-Bertani (LB) agar and incubated at 27^{o}C for 48 hours. After 48 hours the culture plates were removed from the incubator and individual colonies counted.

Vectors

LRIM1-Gal4

This is a *piggyBac* vector with 672 bases of 5' terminal and 675 bases of 3' terminal sequences of piggBac containing the Gal4 ORF under the regulatory control of the LRIM1 promoter in addition to a marker gene encoding enhanced cyan fluorescent protein (ECFP) under the regulatory control of the 3xP3 promoter (Berghammer et al. 1999). This vector was constructed using Gateway recombination cloning technology (Invitrogen, Grand Island, NY), in which 4 recombination modules were simultaneously recombined into a destination plasmid. The first module consisted of the *piggyBac* left terminal with gateway recombination site (Invitrogen, Grand Island, NY). The second module contained Gal4 ORF under control of the LRIM1 promoter, the third module consisted of the ECFP marker gene under the regulatory control of 3xP3 (Berghammer et al. 1999) and module four contained the *piggyBac* right terminal. Modules 1, 3 and 4 were present in-house. To make the second module a 3.0 kilobase fragment upstream of the LRIM1 ORF was amplified using primers LRIM1fw 835 (5'- GCG AGG ATG ACC CAC TAG AG-3') and LRIMrvAscBam (5'-ATA GGA TCC TAG GCG CGC CCC TCC TGA TAA GCT ATA CCG GC-3') with AscI and BamHI restriction sites and inserted into a PCR4-TOPO vector (Thermo Fisher Scientific Inc., Rockville, MD). A 3.0 kilobase fragment of Gal4hsp3 was amplified from plasmid PB-Gal4 (O'Brochta et al. 2012) using primers AscI-GAL4fw (5'-ATA GGC GCG CCA GCG CAG CTG AAC AAG CT-3') and GAL4Rv-BamHI (5'-ATA GGC GCG CCG TAA TAC GAC TCA CTA TAG GGC-3') and inserted into a PCR Blunt II TOPO vector (Thermo Fisher Scientific Inc., Rockville, MD). The

cloning vectors were digested with AscI and BamHI (New England Biolabs (NEB) Ipswich, Mass.) and ligated with T4 DNA ligase (New England Biolabs (NEB) Ipswich, Mass.). Ligated product was transformed into *E. coli* DH10B (Gibco-BRL).

Colonies were screened for insertion. Positive colonies were cultured and plasmid DNA extracted. The LRIM::Gal4 region was amplified from the plasmid using primers attB5-LRIMPromoter835 (5'- GGG GAC AAC TTT GTA TAC AAA AGT TGG GGC GAGGATGACCCACTAGAG-3') and attB4-SV40Rv (5'-GGGGACAACTTTGTATAGAAAAGTTGGGTGGGTTAAGATACATTGATGAG TTTGGAC-3'that contained with gateway attachment sites. All the modules were brought together during site specific recombination.

LRIM1-silencer

This is a *piggyBac* vector with 1.7 kilobases of 5' terminal and 675 bases of 3' terminal sequences of *piggBac* containing an inverted repeat of *LRIM1* Gal4 under the regulatory control of the UAS enhancer in addition to a marker gene encoding nuclear localized enhanced green fluorescent protein (nls EGFP) under the regulatory control of the 3xP3 promoter (Berghammer et al. 1999). This vector was constructed using Gateway recombination cloning technology (Invitrogen, Grand Island, NY), in which 4 recombination modules were simultaneously recombined into a destination plasmid. The first module consisted of the *piggyBac* left terminal and a nuclear localized EGFP (Addgene, Cambridge MA, USA) marker gene under the regulatory control of the 3xP3 promoter (Berghammer et al. 1999). The second module contained a 202 base pair region of *LRIM1* juxtaposed to a seventy base pair functional intron and under the

regulatory control of the UAS enhancer. The third module contained the inverted repeat of the 200 base pair *LRIM1* region of the second module juxtaposed to SV40. The fourth module contained the *piggyBac* right terminal. Recombination between modules two and three joined the *LRIM1* regions such that transcription resulted in generation of a short hairpin RNA.

To create module one a 300 base pair (bp) region of 3xP3 (Berghammer et al. 1999) was amplified using primers NotI-Fse 3xP3fw (5'-GCG GCCGCGGCCGGC CGTTCCCACAATGGTTAATTCG-3') and PacI-AscI 3xP3rv (5'-GGCGCGCCT TAATTAAGGTACCGTCGACTCTAGC from plasmid attL5-3xP3-EGFP-SV40-attL4. The resulting fragment with NotI/FseI and PacI/AscI restriction sites was inserted into a pCR4 Blunt-TOPO vector (Thermo Fisher Scientific Rockville MD, USA) to create plasmid 3xP3-pCR4. A 1.7 kilobase (kb) region of *piggyBac* left end from an in-house *piggyBac* vector was amplified using primers NotI-PBLeft fw (5'-GCGGCCGCTACATACCTCGCTCTGC-3') and FseI-PBLeftrv. The resulting amplified fragment with NotI and FseI restriction sites was inserted into a pCR4 Blunt-TOPO vector (Thermo Fisher Scientific Rockville MD, USA) to create plasmid piggBacL-pCR4. A 1.1 kb region of nuclear localized eGFP (nls eGFP) from an in-house plasmid pUAS-Stringer GFP was amplified using primers PacI-nlseGFPfw (5'-TTAATTAAGATCCACCGGTCGCCAC-3') and AscI-SV40rv (GGCG-CGCCTTAAGATACATTGATGAGTTTGGACAAACC-3'). The resulting PCR product with PacI and AscI restriction sites was inserted into a pCR4 Blunt-TOPO vector (Thermo Fisher Scientific Rockville MD, USA) to generate the nlseGFP-pCR4 plasmid. Restriction digest using NotI (NEB) and FseI (NEB) was performed on both

the *piggyBac*L-pCR4 and 3xP3-pCR4 plasmids. The 1.7 kb *piggyBac* left fragment that was generated, was collected and then ligated into a linearized 3xP3-pCR4 blunt plasmid using T4 DNA ligase (NEB) to generate a piggBacL-3xP3-pCR4 plasmid. Restriction digest using PacI (NEB) AscI (NEB) was performed on both the nlseGFP-pCR4 and *piggyBac*L-3xP3-pCR4 plasmids. The 1.1 kb nlseGFP fragment that was generated, was collected and then ligated into a linearized *piggyBac*L-3xP3 pCR4 plasmid using T4 DNA ligase (NEB). The 3.0 kb *piggyBac*L-3xP3-nlseGFP cassette was amplified using primers attB1-PBleftfw (5'-GGGGACAAGTTTGTACAA AAA AGC AGG CTG GTA CAT ACC TCG CTC TGC-3') and attB5r-SV40 RV (5'- GGG GAC AAC TTTTGT ATA CAA AGTTGT TTAAGATACATTGATGAG TTT GGAC-3') The amplified fragment with gateway tails was used for a BP reaction with a pDONOR to generate module 1.

Plasmid pSLfa1180 i-CARB-SV40 (Kim, Koo, Richman, Seeley, Vizioli, et al. 2004) was digested with SacI (NEB) and ApaI (NEB) to remove a 1.4 kb region that contained a NotI restriction enzyme site. The overhang ends of the 3.0 kb backbone were blunted using T4 DNA polymerase (NEB) and then re-circularized using T4 DNA ligase (NEB) to form plasmid pSLfa1180 delta. A 202 bp region of *A. stephensi LRIM1* was amplified using primers NheI-NotI-LRIM1fw (5'-GCAGCTAGCGCG GCCGC CGACTGTATC TGGCCAACAATAA-3') and Xba-LRIM1 RV (5'- CAG TCT AGA GCG GCC GCC TAC GTT CCG CTG GTT CTT-3') to introduce NheI, NotI and XbaI restriction sites. The amplified fragment was inserted into a pCR4 pCR4 Blunt-TOPO vector (Thermo Fisher Scientific Rockville MD, USA). Plasmid pSL1180 delta and NheI-NotI-LRIM1-XbaI pCR4 were digested with XbaI (NEB) and NheI (NEB). The

200 bp fragment from the digest of NheI-NotI-LRIM1-XbaI pCR4 was inserted into the linearized pSL1180 delta backbone using T4 DNA ligase to make plasmid pSL1180 delta-LRIM1.

A 255 bp region of tdTomato, was amplified and inserted into a pCR4 TOPO Blunt vector. To amplify tdTomato and introduce NheI and NotI restriction sites, primers NheI-tdTfw (5'-GCAGCTAGCGCGGCCGCCGACTGTATCTGGC CA ACAATAA-3') and NotI tdTrv (5'-ATAGCGGCCGCCTACTTGTAC-3') were used. The amplified fragment was inserted into a pCR4 Blunt-TOPO vector (Thermo Fisher Scientific Rockville MD, USA). The NheI-tdTomato-NotI pCR4 plasmid and plasmid pSL1180 delta-LRIM1 were both digested with NheI (NEB) and NotI (NEB). The 255 bp fragment of tdTomato released from the NheI-tdTomato-NotI pCR4 plasmid was inserted into a linearized pSL1180 delta-LRIM1 plasmid using T4 DNA ligase (NEB) to form plasmid pSL1180 delta-LRIM1-tdT.

To make module two a 767 bp region of plasmid pSL1180 delta-LRIM1-tdT was amplified using primers attB4-intron-SV40- attB5fw (5'-GGGACAATTTGTAT ACAAAAGTTGCCTAC CACATTTGTAGAGGTTTTACTTGC-3') and attB4_intron_SV40_attB5rv (5'-GGGACAACTTTGTATAGAAAAGTTGGGTGAG GTGAGCACCCAATCATCAG-3'). The amplified fragment with gateway tails was used for a BP reaction with a pDONOR (Gateway, Thermo Fisher Rockville MD, USA) to generate module two.

To generate module three a 457 bp region of plasmid pSL1180 delta-LRIM1-tdT was amplified using primers attB3r-LRIM-tdTomato-attB4rfw (5'- GGGGAC AACTTTATTATACAAAGTTGTCGACTCTGGCCAACA ATAAGAT CG-3')

and attB3r-LRIM_tdTomato-attB4rrv (5'-GGGGACAACTTTTCTATACAAAGTT GGGGGCACGCTGATCTACAAGGTG-3'). The amplified fragment with gateway tails was used for a BP reaction with a pDONOR (Gateway, Thermo Fisher Rockville MD, USA). To generate module 4 a 2210 bp region of an in-house plasmid ECFP-643 was amplified using primers attB3-UAS-PiggBacR-attB2fw (5'-GGGGA CAACTTTGTATAATAAAGTTGCCTATTCAGAGTTCTCTTCTTGTATTC-3') and attB3-UAS-PiggBacR-attB2rv (5'- GGGGACCACTTT GTACAAGAAAGCT GGGTAGGTGATGACGGTGAAAACCTC-3'). The amplified fragment with gateway tails was used for a BP reaction with a pDONOR (Gateway, Thermo Fisher Rockville MD, USA). The four modules where then recombined in a LR recombination reaction (Gateway, Thermo Fisher Rockville MD, USA).

Mosquito Transformation

Transgenic *A. stephensi* were created in the University of Maryland, College Park, Institute for Bioscience and Biotechnology Research's Insect Transformation Facility. Preblastoderm embryos of *A. stephensi* Sda 500 were injected with vector-containing plasmids and plasmids expressing *piggyBac* transposase (Handler and Harrell 1999). The concentration of vectors and transposase-expressing plasmids were each 50 ng/microliter in injection buffer (5mM KCl, 0.1mM NaPO4; pH 6.8). Insects that developed from injected embryos and survived to adulthood were pooled according to sex and mated to non-injected Sda 500 adults of the opposite sex. The progeny were screened as larvae for the expression of ECFP or nls-EGFP, and transgenic individuals

were used to establish lines. The *piggyBac* insertion sites were determined using splinkerette-PCR (Devon et al. 1995; Potter and Luo 2010) after lines were established.

Splinkerette-PCR

Genomic DNA was extracted from mosquito as described earlier and suspended in 25µL of deionized H_2O. 5µL of extracted DNA was digested with BstYI for 2 hours at 60^{o}C in a final reaction volume of 35 µL. Digestion was then heat inactivated at 80^{o}C for 20 mins. 50µL of SPLINK-BOT and SPLINK-GATC-TOP oligonucleotides were annealed in a NEB Buffer 2 solution of final volume 1000µL by heating at 95^{o}C for 3 minutes then cooled to room temperature. Annealed Spinkerette oligonucleotides are then ligated to digested genomic DNA using T4 DNA Ligase 400U/µL (New England Biolabs (NEB) Ipswich, Mass.) for 2 hours at room temperature. Round one of Splinkerette PCR was carried out using Phusion High-Fidelity polymerase (New England Biolabs (NEB) Ipswich, Mass.) with SPLNK#1 and 3'SPLNK-PB#1 or 5'SPLNK-PB#1 primers.

The PCR reaction was assembled as followed:

Component	Volume (µL)
5x HF Buffer	5.0µL
10mM dNTPs	0.5µL
10µM SPLNK#1 primer	0.5µL
10µM 5' or 3' SPLINK#1 primer	0.5µL
diH_20	8.25µL
DNA	10µL

Phusion Polymerase 0.25µL

PCR conditions

1 cycle

Denaturation 75 sec 98ºC

2 cycles

Denaturation 20 sec 98ºC

Anneal 15 sec 64ºC

30 cycles

Denaturation 20 sec 98ºC

Anneal 15 sec 58ºC or 64ºC

Elongation 2 min 72ºC

1 cycle

Elongation 7 min 72ºC

For the second round of amplification 1µL of the first PCR reaction was carried out using the secondary Splinkerette primers SPLNK#2 and 3'SPLNK-PB#2 or 5'SPLNK-PB#2 under the following conditions:

1 cycle

Denaturation 75 sec 98ºC

30 cycles

Denaturation 20 sec 98ºC

Anneal 15 sec 59ºC or 66ºC

Elongation 90 sec 72ºC

1 cycle

Elongation 7 min 72^{o}C

The PCR product obtained was purified by gel electrophoresis on a 1.25% agarose gel then extracted using Quiagen, QIAquick gel extraction kit and sequenced using 5'PB sequence primer or 3'PB-sequence primer at Macrogen Inc, Rockville MD.

Crossing Lines with Gal4 transgene with UAS-silencer lines

For all experiments that required analysis of mosquitoes with both the Gal4 transgene and UAS::LRIM1silencer transgene in their genome, Heterozygous individuals of the UAS::LRIM1silencer and MBL24 GAL4 line were mated to produce progeny with all four genotypes: wild type; MBL24-Gal4/+ ; UAS::LRIM1silener/+ and MBL24-Gal4/UAS::LRIM1silencer. MBL24-Gal4 /+ ; UAS::LRIM1silener/+ and wild type mosquitoes were used as controls.

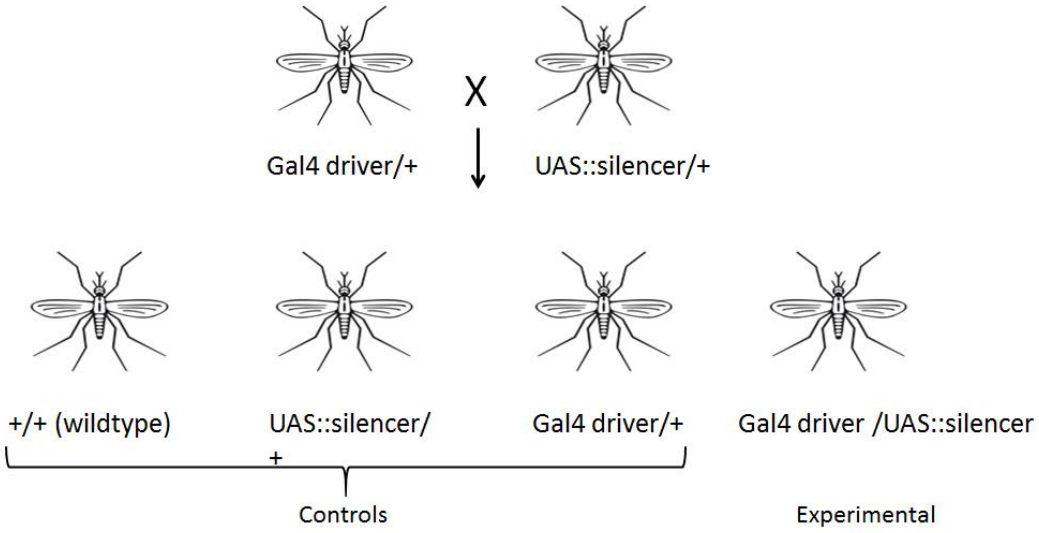

Figure 6.1: Schematic for crossing Gal4 driver line with UAS responder line.

Microscopy

To screen for transgenic mosquitoes by microscopic observation of larvae, pupae, and adults an Olympus MVX10 fluorescent dissecting microscope equipped with Chroma filters (Chroma Technology Corporation, Bellows Falls, VT) 49001 ET-CFP (excitation, 436/20; emission, 480/40; dichroic, 455), 49002 ET-GFP (excitation, 470/40; emission, 525/50; dichroic, 495), 49003 ET-EYFP (excitation, 500/20; emission, 535/30; dichroic, 515), 49005 ET-DsRed (excitation, 545/30; emission, 620/60; dichroic, 570) was used.

For tissue imaging a Zeiss Axiom Imager A1 fluorescent compound microscope equipped with Zeiss filter set 20 (excitation, 546/12; emission, 575–640; dichroic, 560) and filter set 38HE (excitation, 470/40; emission, 525/50; dichroic, 495) was used.

Appendices

Appendix 1. Primers used for quantitative real-time polymerase chain reaction

Name	**Sequence**
AsLRIM1-F	GAG GAA AAT GCT CGG ATG AA
AsLRIM1-R	CGA CGG CTG AAC CTT ACT GA
AsAPL1-F	CTA CAG AGC GAA ATA CAG CA
AsAPL1-R	CAG ATG TGC TAT CAC CTT GT
AsTEP1-F	TTG CTG TCG TTC GTG ATA
AsTEP1-R	AGC GTG ATG GTG TAG TCG
AsCaspar-F	TGA CAT CTT CAC CGA AAC GCC
AsCaspar-R	AAC TGG ATG CTG CCA ATC GTC T
AsRel2-F	GTT CCG CTT CCG CTA TCA GT
AsRel2-R	CGC AAC TCT ACC GTG GGG AA
tdTomato RT fw	GCG TGA TGA ACT TCG AGG
tdTomato RT rv	CCT TGT AGA TCA GCG TGC C
GAL1-fw	CCA AAG AAA AAC CGA AGT GC
GAL1-Rv	CCC TAG TCA GCG GAG ACC TT
AsS7r	TTC GTT GTG AAC CCA AAT AAA AAT C
AsS7f	TGC GGC TTC AGA TCC GAG TTC

Appendix 2. Primers used to construct LRIM1-silencer vector

Names	sequence
attB4_intron rv	5'-CCCCTGTTGAAACATATCTTTTCAACCCACTCCACTCGTGGGTTAGTAGTC -3'
attB5-SV40for	5’-GGGGACAACTTTGTATACAAAAGTTGCCATGGTGTAAACATCTCCAAAATGAACG -3'
attB3r_LRIM_tdTomato_attB4r fw	CCCCTGTTGAAAAGATATGTTTCAACCCCCGTGCGACTAGATGTTCCAC
attB3r_LRIM_tdTomato_attB4r rv	GGGGACAACTTTATTATACAAAGTTGTGCTGACATAGACCGGTTGTTATTCTAGC
attB3_UAS_PiggBacR_attB2 fw	GGGGACAACTTTGTATAATAAAGTTGCCTATTCAGAGTTCTCTTCTTGTATTC
attB3_UAS_PiggBacR_attB2 rv	CCCCTGGTGAAACATGTTCTTTCGACCCATTTAACCCTAGAAAGATAATCATATTGTGACG

Appendix 3. Primers used for Splinkerette PCR

Names	Sequence
5'SPNLK-PB-SEQ	CGA CTG AGA TGT CCT AAA TGC
5'SPLNK-PB#1	ACC GCA TTG ACA AGC ACG
5'SPLNK-PB#2	CTC CAA GCG GCG ACT GAG
3'SPLNK-PB-SEQ	ACG CAT GAT TAT CTT TAA C
3'SPLNK-PB#1	GTT TGT TGA ATT TAT TAT TAG TAT GTA AG
3'SPLNK-PB#2	CGA TAA AAC ACA TGC GTC
SPLNK#1	CGA AGA GTA ACC GTT GCT AGG AGA GAC C
SPLNK#2	GTG GCT GAA TGA GAC TGG TGT CGA C
SPLNK-GATC-TOP	GAT CCC ACT AGT GTC GAC ACC AGT CTC TAA TTT TTT TTT TCA AAA AAA
SPLNK-BOT	CGA AGA GTA ACC GTT GCT AGG AGA GAC CGT GGC TGA ATG AGA CTG GTG TCG ACA CTA GTG G
SPLNK-Blunt-TOP	CC ACT AGT GTC GAC ACC AGT CTC TAA TTT TTT TTT TCA AAA AAA

Appendix 4. Splinkerette sequence data from transgenic lines

Transgenic Line	**3' Splinkerette sequence data**
LRIM1 silencer F2	NA
LRIM1 silencer M2	NA
LRIM1 silencer M7	NA
LRIM1p Gal4M2	TTAAGTGAGATTTCATGATGACAGTATCTGTTGGCATTAGATTGTAATCGATTATTTCAGTTTTCACTCGTAGACTCTCTCCTAATCGAGATC
LRIM1p Gal4M4	TTAGGTCTTCGGAGGTCTCGAGCGAAATGGCAGATGAAGCCCCTCTAATTGTGTTTGTTAGTAAGACCAACTGGATTCCCCTC
LRIM1p Gal4M8	TTAAGGATGGATTAAGTCAGAGACAAACNGGGAGAAGCAACAAGCAAAAAAAAAAAAATGCTTCCCCAATT
	5' Splinkerette sequence data
LRIM1 silencer F2	TTAACGGTGAGTCGCAACTTCCTGTTGATGCAACCGGGGCGCGCAACATTATCATAGGGTTGCTCCCCTTCCCGAACCGATAGAA
LRIM1 silencer M2	TTAAGGAGCTCAATGAGCAGCAATTTAGGGAAACTTTGCAATCAAAGTGATGTTTTGTGGTTATCGAAACTACGCAATATGCAAGATA
LRIM1 silencer M7	TTAAATAGCTGCACACAGGCGCATGAGAGATGTGGGTTAAAGGATGGCTGTTCGGGCCAGCGCTATTTATTTGCTACATTTTCAA
LRIM1p Gal4M2	TTAACAACAAAAATGAAAATCGATCCGTATAAAGATC
LRIM1p Gal4M4	NA
LRIM1p Gal4M8	NA

Appendix 5. MBL24 Gal4 driver lines used to drive *LRIM1* silencer expression

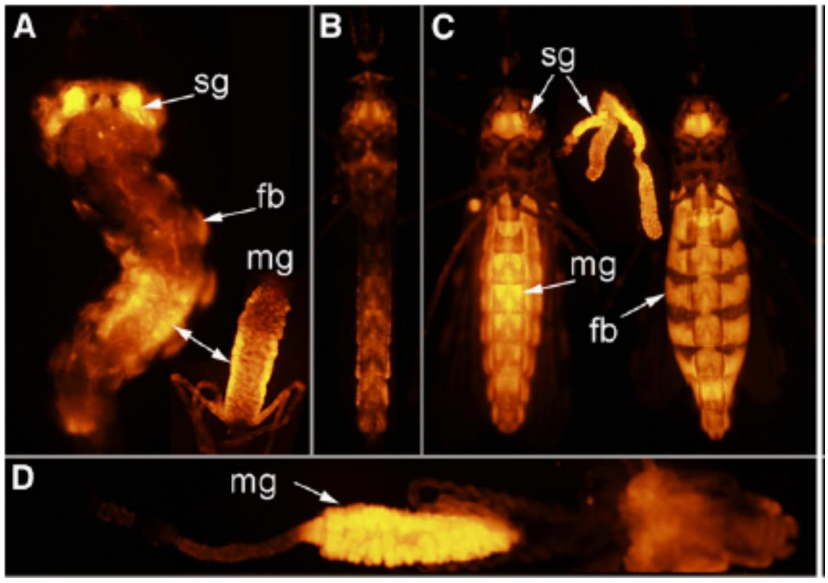

Appendix 6. LRIM1-silencer vector and LRIM1pGal4 vector

References

Agaisse H, Perrimon N. 2004. The roles of JAK/STAT signaling in *Drosophila* immune responses. Immunol. Rev. 198:72–82.

Aggarwal K, Silverman N. 2008. Positive and negative regulation of the *Drosophila* immune response. BMB Rep. 41:267–277.

Alavi Y, Arai M, Mendoza J, Tufet-Bayona M, Sinha R, Fowler K, Billker O, Franke-Fayard B, Janse CJ, Waters a., et al. 2003. The dynamics of interactions between *Plasmodium* and the mosquito: a study of the infectivity of *Plasmodium berghei* and *Plasmodium gallinaceum*, and their transmission by *Anopheles stephensi, Anopheles gambiae* and *Aedes aegypti*. Int. J. Parasitol. 33:933–943.

Aly ASI, Vaughan AM, Kappe SHI. 2009. Malaria Parasite Development in the Mosquito and Infection of the Mammalian Host. Annu. Rev. Microbiol. 63:195–221.

Arévalo-Herrera M, Solarte Y, Marin C, Santos M, Castellanos J, Beier JC, Valencia SH. 2011. Malaria transmission blocking immunity and sexual stage vaccines for interrupting malaria transmission in Latin America. Mem. Inst. Oswaldo Cruz 106:202–211.

Ashburner M. 1989. *Drosophila*: A Laboratory Handbook and Manual. Two volumes.

Balciuniene J, Nagelberg D, Walsh KT, Camerota D, Georlette D, Biemar F, Bellipanni G, Balciunas D. 2013. Efficient disruption of Zebrafish genes using a Gal4-containing gene trap. BMC Genomics 14:619.

Bannister L., Hopkins J., Fowler R., Krishna S, Mitchell G. 2000. A Brief Illustrated Guide to the Ultrastructure of *Plasmodium falciparum* Asexual Blood Stages. Parasitol. Today 16:427–433.

Barillas-Mury C, Charlesworth A, Gross I, Richman A, Hoffmann JA, Kafatos FC. 1996. Immune factor Gambif1, a new rel family member from the human malaria vector, *Anopheles gambiae*. EMBO J. 15:4691–4701.

Baxter RHG, Steinert S, Chelliah Y, Volohonsky G, Levashina E a, Deisenhofer J. 2010. A heterodimeric complex of the LRR proteins LRIM1 and APL1C regulates complement-like immunity in *Anopheles gambiae*. Proc. Natl. Acad. Sci. U. S. A. 107:16817–22.

Bej A, Sahoo BR, Swain B, Basu M, Jayasankar P, Samanta M. 2014. LRRsearch: An asynchronous server-based application for the prediction of leucine-rich repeat motifs and an integrative database of NOD-like receptors. Comput. Biol. Med. 53:164–170.

Belvin MP, Jin Y, Anderson K V. 1995. Cactus protein degradation mediates *Drosophila* dorsal-ventral signaling. Genes Dev. 9:783–793.

Berghammer AJ, Klingler M, A. Wimmer E. 1999. Genetic techniques: A universal marker for transgenic insects. Nature 402:370–371.

Blandin S, Moita LF, Köcher T, Wilm M, Kafatos FC, Levashina E a. 2002. Reverse genetics in the mosquito *Anopheles gambiae*: targeted disruption of the Defensin gene. EMBO Rep. 3:852–6.

Blandin S, Shiao S-H, Moita LF, Janse CJ, Waters AP, Kafatos FC, Levashina E a. 2004. Complement-like protein TEP1 is a determinant of vectorial capacity in the malaria vector *Anopheles gambiae*. Cell 116:661–70.

Brand AH, Perrimon N. 1993. Targeted gene expression as a means of altering cell fates and generating dominant phenotypes. Development 118:401–415.

Brand AH, Perrimon N. 1994. Raf acts downstream of the EGF receptor to determine dorsoventral polarity during *Drosophila* oogenesis. Genes Dev. 8:629–639.

Bray RS, Garnham PCC. 1982. The life-cycle of primate malaria parasites. Br. Med. Bull. 38 :117–122.

Brown AE, Bugeon L, Crisanti A, Catteruccia F. 2003. Stable and heritable gene silencing in the malaria vector *Anopheles stephensi*. Nucleic Acids Res. 31:e85.

Buchon N, Broderick NA, Poidevin M, Pradervand S, Lemaitre B. 2009. *Drosophila* intestinal response to bacterial infection: activation of host defense and stem cell proliferation. Cell Host Microbe 5:200–211.

Butler NS, Vaughan AM, Harty JT, Kappe SHI. 2012. Whole parasite vaccination approaches for prevention of malaria infection. Trends Immunol. 33:247–54.

Carter R, Chen DH. 1976. Malaria transmission blocked by immunisation with gametes of the malaria parasite. Nature 263:57–60.

Catteruccia F, Levashina EA. 2009. RNAi in the malaria vector, *Anopheles gambiae*. Methods Mol. Biol. 555:63–75.

Catteruccia F, Nolan T, Loukeris TG, Blass C, Savakis C, Kafatos FC, Crisanti a. 2000. Stable germline transformation of the malaria mosquito *Anopheles stephensi*. Nature 405:959–962.

Chia WN, Goh YS, Rénia L, Zarling S, Army WR. 2014. Novel approaches to identify protective malaria vaccine candidates. Front. Microbiol. 5:1–9.

Choe K-M, Lee H, Anderson K V. 2005. *Drosophila* peptidoglycan recognition protein LC (PGRP-LC) acts as a signal-transducing innate immune receptor. Proc. Natl. Acad. Sci. U. S. A. 102:1122–1126.

Choe K-M, Werner T, Stoven S, Hultmark D, Anderson K V. 2002. Requirement for a peptidoglycan recognition protein (PGRP) in Relish activation and antibacterial immune responses in *Drosophila*. Science 296:359–362.

Christophides GK. 2005. Transgenic mosquitoes and malaria transmission. Cell. Microbiol. 7:325–33.

Christophides GK, Zdobnov E, Barillas-Mury C, Birney E, Blandin S, Blass C, Brey PT, Collins FH, Danielli A, Dimopoulos G, Hetru C, Hoa NT, Hoffmann J a, et al. 2002. Immunity-related genes and gene families in *Anopheles gambiae*. Science 298:159–65.

Christophides GK, Zdobnov E, Barillas-Mury C, Birney E, Blandin S, Blass C, Brey PT, Collins FH, Danielli A, Dimopoulos G, Hetru C, Hoa NT, Hoffmann JA, et al. 2002. Immunity-related genes and gene families in *Anopheles gambiae*. Science 298:159–165.

Chuang I, Sedegah M, Cicatelli S, Spring M, Polhemus M, Tamminga C, Patterson N, Guerrero M, Bennett JW, Mcgrath S, et al. 2013. DNA Prime / *Adenovirus* Boost Malaria Vaccine Encoding *P . falciparum* CSP and AMA1 Induces Sterile Protection Associated with Cell-Mediated Immunity. 8.

Cirimotich C, Dong Y, Garver L. 2010. Mosquito immune defenses against *Plasmodium* infection. Dev. 34:387–395.

Cirimotich CM, Dong Y, Garver LS, Sim S, Dimopoulos G. 2010. Mosquito immune defenses against *Plasmodium* infection. Dev. Comp. Immunol. 34:387–95.

Clark AJ, Bissinger P, Bullock DW, Damak S, Wallace R, Whitelaw CB, Yull F. 1994. Chromosomal position effects and the modulation of transgene expression. Reprod. Fertil. Dev. 6:589–598.

Clyde DF, McCARTHY VC, Miller RM, Hornick RB. 1973. Specificity of protection of man immunized against sporozoite-induced *falciparum* malaria. Am. J. Med. Sci. 266:398–403.

Clyde DF, McCARTHY VC, Miller RM, Woodward WE. 1975. Immunization of man against *falciparum* and *vivax* malaria by use of attenuated sporozoites. Am. J. Trop. Med. Hyg. 24:397–401.

Clyde DF, Most H, McCARTHY VC, Vanderbe.JP. 1973. Immunization of man against sporozite-induced *falciparum* malaria. Am. J. Med. Sci. 266:169–177.

Cohuet A, Osta M a, Morlais I, Awono-Ambene PH, Michel K, Simard F, Christophides GK, Fontenille D, Kafatos FC. 2006. Anopheles and *Plasmodium*: from laboratory models to natural systems in the field. EMBO Rep. 7:1285–1289.

Coutinho-Abreu I V., Ramalho-Ortigao M. 2010. Transmission blocking vaccines to control insect-borne diseases - A review. Mem. Inst. Oswaldo Cruz 105:1–12.

Cox FE. 1991. Malaria vaccines--progress and problems. Trends Biotechnol. 9:389–94.

Cronin SJF, Nehme NT, Limmer S, Liegeois S, Pospisilik JA, Schramek D, Leibbrandt A, Simoes R de M, Gruber S, Puc U, et al. 2009. Genome-wide RNAi screen identifies genes involved in intestinal pathogenic bacterial infection. Science 325:340–343.

Delorenzi M, Speed T. 2002. An HMM model for coiled-coil domains and a comparison with PSSM-based predictions. Bioinformatics 18:617–625.

Devon RS, Porteous DJ, Brookes AJ. 1995. Splinkerettes—improved vectorettes for greater efficiency in PCR walking. Nucleic Acids Res. 23:1644–1645.

Dimopoulos G. 1997. Molecular immune responses of the mosquito *Anopheles gambiae* to bacteria and malaria parasites. Proc. Natl. Acad. Sci. 94:11508–11513.

Dimopoulos G, Richman A, Muller H-M, Kafatos FC. 1997. Molecular immune responses of the mosquito *Anopheles gambiae* to bacteria and malaria parasites. Proc. Natl. Acad. Sci. 94:11508–11513.

Dinglasan RR, Kalume DE, Kanzok SM, Ghosh AK, Muratova O, Pandey A, Jacobs-Lorena M. 2007. Disruption of *Plasmodium falciparum* development by antibodies against a conserved mosquito midgut antigen. Proc. Natl. Acad. Sci. U. S. A. 104:13461–13466.

Dong Y, Aguilar R, Xi Z, Warr E, Mongin E, Dimopoulos G. 2006. *Anopheles gambiae* immune responses to human and rodent *Plasmodium* parasite species. PLoS Pathog. 2:e52.

Doolan DL, Hoffman SL. 1997. Pre–erythrocytic–stage immune effector mechanisms in *Plasmodium* spp. infections. Philos. Trans. R. Soc. London B Biol. Sci. 352:1361–1367.

Dostert C, Jouanguy E, Irving P, Troxler L, Galiana-Arnoux D, Hetru C, Hoffmann JA, Imler J-L. 2005. The Jak-STAT signaling pathway is required but not sufficient for the antiviral response of drosophila. Nat. Immunol. 6:946–953.

Druilhe P, Spertini F, Soesoe D, Corradin G, Mejia P, Singh S, Audran R, Bouzidi A, Oeuvray C, Roussilhon C. 2005. A Malaria Vaccine That Elicits in Humans Antibodies Able to Kill *Plasmodiumfalciparum*. PLoS Med 2:e344.

Duffy JB. 2002. GAL4 system in *Drosophila*: a fly geneticist's Swiss army knife. Genesis 34:1–15.

Dushay MS, Asling B, Hultmark D. 1996. Origins of immunity: Relish, a compound Rel-like gene in the antibacterial defense of *Drosophila*. Proc. Natl. Acad. Sci. U. S. A. 93:10343–10347.

Elliott DA, Brand AH. 2008. The GAL4 system : a versatile system for the expression of genes. Methods Mol. Biol. 420:79–95.

Elliott R. 1972. The Influence of Vector Behavior on Malaria Transmission. Am. J. Trop. Med. Hyg. 21 :755–763.

Ellis RD, Mullen GED, Pierce M, Martin LB, Miura K, Fay MP, Long CA, Shaffer D, Saul A, Miller LH, et al. 2009. A Phase 1 study of the blood-stage malaria vaccine candidate AMA1-C1/Alhydrogel® with CPG 7909, using two different formulations and dosing intervals. Vaccine 27:4104–4109.

Ewer KJ, Hara GAO, Duncan CJA, Collins KA, Sheehy SH, Reyes-sandoval A, Goodman AL, Edwards NJ, Elias SC, Halstead FD, et al. 2013. Protective CD8(+) T-cell immunity to human malaria induced by chimpanzee adenovirus-MVA immunisation. Nat. Commun. 4:2836.

Feldmann AM, Billingsley PF, Savelkoul E. 1990. Bloodmeal digestion by strains of *Anopheles stephensi* liston (Diptera: Culicidae) of differing susceptibility to *Plasmodium falciparum*. Parasitology 101 Pt 2:193–200.

Feng YQ, Lorincz MC, Fiering S, Greally JM, Bouhassira EE. 2001. Position effects are influenced by the orientation of a transgene with respect to flanking chromatin. Mol. Cell. Biol. 21:298–309.

Filler SJ, MacArthur JR, Parise M, Wirtz R, Eliades MJ, Dasilva A, Steketee R. 2006. Locally acquired mosquito-transmitted malaria: a guide for investigations in the United States. MMWR. Recomm. Rep. 55:1–9.

Fischer JA, Giniger E, Maniatis T, Ptashne M. 1988. GAL4 activates transcription in *Drosophila*. Nature 332:853–856.

Foquet L, Hermsen CC, Gemert G Van, Braeckel E Van, Weening KE, Sauerwein R, Meuleman P, Leroux-roels G. 2014. Brief report Vaccine-induced monoclonal antibodies targeting circumsporozoite protein prevent *Plasmodium falciparum* infection. 124.

Fraiture M, Baxter RHG, Steinert S, Chelliah Y, Frolet C, Quispe-Tintaya W, Hoffmann J a, Blandin S a, Levashina E a. 2009. Two mosquito LRR proteins function as complement control factors in the TEP1-mediated killing of *Plasmodium*. Cell Host Microbe 5:273–84.

Frolet C, Thoma M, Blandin S, Hoffmann JA, Levashina EA. 2006. Boosting NF-kappaB-dependent basal immunity of *Anopheles gambiae* aborts development of *Plasmodium berghei*. Immunity 25:677–685.

Galun R. 1967. Feeding stimuli and artificial feeding. Bull. World Health Organ.:590–593.

Gardner MJ, Hall N, Fung E, White O, Berriman M, Hyman RW, Carlton JM, Pain A, Nelson KE, Bowman S, et al. 2002. Genome sequence of the human malaria parasite *Plasmodium falciparum*. Nature 419:498–511.

Garver LS, de Almeida Oliveira G, Barillas-Mury C. 2013. The JNK Pathway Is a Key Mediator of*Anopheles gambiae* Antiplasmodial Immunity. PLoS Pathog 9:e1003622.

Garver LS, Bahia AC, Das S, Souza-Neto J a, Shiao J, Dong Y, Dimopoulos G. 2012. Anopheles Imd pathway factors and effectors in infection intensity-dependent anti-*Plasmodium* action. PLoS Pathog. 8:e1002737.

Garver LS, Dong Y, Dimopoulos G. 2009. Caspar controls resistance to *Plasmodium falciparum* in diverse anopheline species. PLoS Pathog. 5:e1000335.

Georgel P, Naitza S, Kappler C, Ferrandon D, Zachary D, Swimmer C, Kopczynski C, Duyk G, Reichhart JM, Hoffmann JA. 2001. *Drosophila* immune deficiency (IMD) is a death domain protein that activates antibacterial defense and can promote apoptosis. Dev. Cell 1:503–514.

Goodman AL, Draper SJ. 2010. Blood-stage malaria vaccines — recent progress and future challenges. 104:189–211.

Groen a K. 2001. The pros and cons of gene expression analysis by microarrays. J. Hepatol. 35:295–6.

Gupta L, Molina-Cruz A, Kumar S, Rodrigues J, Dixit R, Zamora RE, Barillas-Mury C. 2009. The STAT pathway mediates late-phase immunity against *Plasmodium* in the mosquito *Anopheles gambiae*. Cell Host Microbe 5:498–507.

Habtewold T, Povelones M, Blagborough AM, Christophides GK. 2008. Transmission blocking immunity in the malaria non-vector mosquito *Anopheles quadriannulatus* species A. PLoS Pathog. 4:e1000070.

Han YS, Thompson J, Kafatos FC, Barillas-Mury C. 2000. Molecular interactions between *Anopheles stephensi* midgut cells and *Plasmodium berghei*: the time bomb theory of ookinete invasion of mosquitoes. EMBO J. 19:6030–40.

Han ZS, Ip YT. 1999. Interaction and specificity of Rel-related proteins in regulating *Drosophila* immunity gene expression. J. Biol. Chem. 274:21355–21361.

Hedengren M, Asling B, Dushay MS, Ando I, Ekengren S, Wihlborg M, Hultmark D. 1999. Relish, a central factor in the control of humoral but not cellular immunity in *Drosophila*. Mol. Cell 4:827–837.

Hill AVS. 2011. Vaccines against malaria. Philos. Trans. R. Soc. Lond. B. Biol. Sci. 366:2806–14.

Hill AVS, Reyes-sandoval A, Hara GO, Ewer K, Goodman A, Nicosia A, Folgori A, Colloca S, Cortese R, Gilbert SC, et al. 2010. Prime-boost vectored malaria vaccines : Progress and prospects Prime-boost vectored malaria vaccines Progress and prospects. 8600.

Hillyer J. 2010. Mosquito immunity. Invertebr. Immun.:218–238.

HOA NGOT, ZHENG L. 2007. Functional characterization of the NF-κB transcription factor gene Rel2 from *Anopheles gambiae*. Insect Sci. 14:175–184.

Hoffman SL, Billingsley PF, James E, Richman A, Loyevsky M, Li T, Chakravarty S, Gunasekera A, Chattopadhyay R, Li M, et al. 2010. Development of a metabolically active, non-replicating sporozoite vaccine to prevent *Plasmodium falciparum* malaria. Hum. Vaccin. 6:97–106.

Hoffman SL, Goh LML, Luke TC, Schneider I, Le TP, Doolan DL, Sacci J, de la Vega P, Dowler M, Paul C, et al. 2002. Protection of humans against malaria by immunization with radiation-attenuated *Plasmodium falciparum* sporozoites. J. Infect. Dis. 185:1155–64.

Huff CG, Coulston F. 1944. The Development of *Plasmodium* Gallinaceum from Sporozoite to Erythrocytic Trophozoite. J. Infect. Dis. 75 :231–249.

Ip YT, Reach M, Engstrom Y, Kadalayil L, Cai H, Gonzalez-Crespo S, Tatei K, Levine M. 1993. Dif, a dorsal-related gene that mediates an immune response in *Drosophila*. Cell 75:753–763.

Ito J, Ghosh A, Moreira LA, Wimmer EA, Jacobs-Lorena M. 2002. Transgenic anopheline mosquitoes impaired in transmission of a malaria parasite. Nature 417:452–455.

Jaramillo-Gutierrez G, Rodrigues J, Ndikuyeze G, Povelones M, Molina-Cruz A, Barillas-Mury C. 2009. Mosquito immune responses and compatibility between *Plasmodium* parasites and anopheline mosquitoes. BMC Microbiol. 9:154.

Jiang X, Peery A, Hall AB, Sharma A, Chen X-G, Waterhouse RM, Komissarov A, Riehle MM, Shouche Y, Sharakhova M V, et al. 2014. Genome analysis of a major urban malaria vector mosquito, *Anopheles stephensi*. Genome Biol. 15:459.

Kallio J, Leinonen A, Ulvila J, Valanne S, Ezekowitz RA, Ramet M. 2005. Functional analysis of immune response genes in *Drosophila* identifies JNK pathway as a regulator of antimicrobial peptide gene expression in S2 cells. Microbes Infect. 7:811–819.

Kaneko T, Silverman N. 2005. Bacterial recognition and signalling by the *Drosophila* IMD pathway. Cell. Microbiol. 7:461–469.

Kennerdell JR, Carthew RW. 1998. Use of dsRNA-mediated genetic interference to demonstrate that frizzled and frizzled 2 act in the wingless pathway. Cell 95:1017–1026.

Kim W, Koo H, Richman AM, Seeley D, Vizioli J, Klocko AD, O'brochta DA. 2004. Ectopic Expression of a Cecropin Transgene in the Human Malaria Vector Mosquito *Anopheles gambiae* (Diptera: Culicidae): Effects on Susceptibility to *Plasmodium*. J. Med. Entomol. 41:447–455.

Kiszewski A, Mellinger A, Spielman A, Malaney P, Sachs SE, Sachs J. 2004. A global index representing the stability of malaria transmission. Am. J. Trop. Med. Hyg. 70:486–498.

Kleino A, Valanne S, Ulvila J, Kallio J, Myllymaki H, Enwald H, Stoven S, Poidevin M, Ueda R, Hultmark D, et al. 2005. Inhibitor of apoptosis 2 and TAK1-binding protein are components of the *Drosophila* Imd pathway. EMBO J. 24:3423–3434.

Kramer JM, Staveley BE. 2003. GAL4 causes developmental defects and apoptosis when expressed in the developing eye of *Drosophila* melanogaster. Genet. Mol. Res. 2:43–47.

Leulier F, Parquet C, Pili-Floury S, Ryu J-H, Caroff M, Lee W-J, Mengin-Lecreulx D, Lemaitre B. 2003. The *Drosophila* immune system detects bacteria through specific peptidoglycan recognition. Nat. Immunol. 4:478–484.

Leulier F, Vidal S, Saigo K, Ueda R, Lemaitre B. 2002. Inducible expression of double-stranded RNA reveals a role for dFADD in the regulation of the antibacterial response in *Drosophila* adults. Curr. Biol. 12:996–1000.

Loimaranta V, Hytönen J, Pulliainen AT, Sharma A, Tenovuo J, Strömberg N, Finne J. 2009. Leucine-rich repeats of bacterial surface proteins serve as common pattern recognition motifs of human scavenger receptor gp340. J. Biol. Chem. 284:18614–23.

Luna C, Hoa NT, Lin H, Zhang L, Nguyen HLA, Kanzok SM, Zheng L. 2006. Expression of immune responsive genes in cell lines from two different Anopheline species. Insect Mol. Biol. 15:721–729.

Lycett GJ. 2004. Conditional Expression in the Malaria Mosquito *Anopheles stephensi* With Tet-On and Tet-Off Systems. Genetics 167:1781–1790.

Lycett GJ, McLaughlin LA, Ranson H, Hemingway J, Kafatos FC, Loukeris TG, Paine MJI. 2006. *Anopheles gambiae* P450 reductase is highly expressed in oenocytes and in vivo knockdown increases permethrin susceptibility. Insect Mol. Biol. 15:321–327.

Lynd A, Lycett GJ. 2012. Development of the Bi-Partite Gal4-UAS System in the African Malaria Mosquito, *Anopheles gambiae*. PLoS One 7:e31552.

Manfruelli P, Reichhart JM, Steward R, Hoffmann JA, Lemaitre B. 1999. A mosaic analysis in *Drosophila* fat body cells of the control of antimicrobial peptide genes by the Rel proteins Dorsal and DIF. EMBO J. 18:3380–3391.

Marinotti O, Nguyen QK, Calvo E, James a a, Ribeiro JMC. 2005. Microarray analysis of genes showing variable expression following a blood meal in *Anopheles gambiae*. Insect Mol. Biol. 14:365–73.

Marshall JM, Taylor CE. 2009. Malaria control with transgenic mosquitoes. PLoS Med. 6:e20.

McCarthy JS, Good MF. 2010. Whole parasite blood stage malaria vaccines: A convergence of evidence. Hum. Vaccin. 6:114–123.

Meister S, Agianian B, Turlure F, Relógio A, Morlais I, Kafatos FC, Christophides GK. 2009. *Anopheles gambiae* PGRPLC-mediated defense against bacteria modulates infections with malaria parasites. PLoS Pathog. 5:e1000542.

Meister S, Kanzok SM, Zheng X, Luna C, Li T, Hoa NT, Clayton JR, White KP, Kafatos FC, Christophides GK, et al. 2005. Immune signaling pathways regulating bacterial and malaria parasite infection of the mosquito *Anopheles gambiae*. Gene 102.

Meister S, Kanzok SM, Zheng X-L, Luna C, Li T-R, Hoa NT, Clayton JR, White KP, Kafatos FC, Christophides GK, et al. 2005. Immune signaling pathways regulating bacterial and malaria parasite infection of the mosquito *Anopheles gambiae*. Proc. Natl. Acad. Sci. U. S. A. 102:11420–11425.

Mendes AM, Awono-Ambene PH, Nsango SE, Cohuet A, Fontenille D, Kafatos FC, Christophides GK, Morlais I, Vlachou D. 2011. Infection intensity-dependent responses of *Anopheles gambiae* to the African malaria parasite *Plasmodium falciparum*. Infect. Immun. 79:4708–15.

Meng X, Khanuja BS, Ip YT. 1999. Toll receptor-mediated *Drosophila* immune response requires Dif, an NF-kappaB factor. Genes Dev. 13:792–797.

Misquitta L, Paterson BM. 1999. Targeted disruption of gene function in *Drosophila* by RNA interference (RNA-i): A role for nautilus in embryonic somatic muscle formation. Proc. Natl. Acad. Sci. U. S. A. 96:1451–1456.

Nolan T, Bower TM, Brown AE, Crisanti A, Catteruccia F. 2002. *piggyBac*-mediated Germline Transformation of the Malaria Mosquito *Anopheles stephensi* Using the Red Fluorescent Protein dsRED as a Selectable Marker. J. Biol. Chem. 277:8759–8762.

Nolan T, Bower TM, Brown AE, Crisanti A, Catteruccia F. 2002. *piggyBac*-mediated germline transformation of the malaria mosquito *Anopheles stephensi* using the red fluorescent protein dsRED as a selectable marker. J. Biol. Chem. 277:8759–62.

Nunes JK, Woods C, Carter T, Raphael T, Morin MJ, Diallo D, Leboulleux D, Jain S, Loucq C, Kaslow DC, et al. 2014. Development of a transmission-blocking malaria vaccine: Progress, challenges, and the path forward. Vaccine 32:5531–5539.

Nussenzweig RS, Vanderberg J, Most H, Orton C. 1967. Protective Immunity produced by the Injection of X-irradiated Sporozoites of *Plasmodium berghei*. Nature 216:160–162.

O'Brochta D a, Alford RT, Pilitt KL, Aluvihare CU, Harrell R a. 2011. *piggyBac* transposon remobilization and enhancer detection in Anopheles mosquitoes. Proc. Natl. Acad. Sci. U. S. A. 108:16339–44.

O'Brochta D a, Pilitt KL, Harrell R a, Aluvihare C, Alford RT. 2012. Gal4-based enhancer-trapping in the malaria mosquito *Anopheles stephensi*. G3 (Bethesda). 2:1305–15.

Organization WH. 2012. World malaria report 2010. 2010. … Geneva. Availabe http//www. who. int/malaria/ ….

Ornitz DM, Moreadith RW, Leder P. 1991. Binary system for regulating transgene expression in mice: targeting int-2 gene expression with yeast GAL4/UAS control elements. Proc. Natl. Acad. Sci. U. S. A. 88:698–702.

Osier FH, Mackinnon MJ, Crosnier C, Fegan G, Kamuyu G, Wanaguru M, Ogada E, McDade B, Rayner JC, Wright GJ, et al. 2014. New antigens for a multicomponent blood-stage malaria vaccine. Sci. Transl. Med. 6:247ra102–247ra102.

Osta M a, Christophides GK, Kafatos FC. 2004. Effects of mosquito genes on *Plasmodium* development. Science 303:2030–2.

Osta M a, Christophides GK, Vlachou D, Kafatos FC. 2004. Innate immunity in the malaria vector *Anopheles gambiae*: comparative and functional genomics. J. Exp. Biol. 207:2551–63.

Ott KJ. 1967. Malaria Parasites and Other *Haemosporidia*. P. C. C. Garnham. Blackwell, Oxford, England; Davis, Philadelphia, 1966. 1132 pp., Sci. 157 :1029.

Petersen TN, Brunak S, von Heijne G, Nielsen H. 2011. SignalP 4.0: discriminating signal peptides from transmembrane regions. Nat Meth 8:785–786.

Pike A, Vadlamani A, Sandiford SL, Gacita A, Dimopoulos G. 2014. Characterization of the Rel2-regulated transcriptome and proteome of *Anopheles stephensi* identifies new anti-*Plasmodium* factors. Insect Biochem. Mol. Biol. 52:82–93.

Potter CJ, Luo L. 2010. Splinkerette PCR for mapping transposable elements in *Drosophila*. PLoS One 5:e10168.

Povelones M, Upton LM, Sala K a, Christophides GK. 2011. Structure-function analysis of the *Anopheles gambiae* LRIM1/APL1C complex and its interaction with complement C3-like protein TEP1. PLoS Pathog. 7:e1002023.

Povelones M, Waterhouse R. 2009. Leucine-rich repeat protein complex activates mosquito complement in defense against *Plasmodium* parasites. Science (80-.). 324:258–261.

Rani A, Sharma A, Rajagopal R, Adak T, Bhatnagar RK. 2009. Bacterial diversity analysis of larvae and adult midgut microflora using culture-dependent and culture-independent methods in lab-reared and field-collected *Anopheles stephensi*-an Asian malarial vector. BMC Microbiol. 9:96.

Reyes-sandoval A, Berthoud T, Alder N, Siani L, Gilbert SC, Nicosia A, Colloca S, Cortese R, Hill AVS. 2010. Prime-Boost Immunization with Adenoviral and Modified Vaccinia Virus Ankara Vectors Enhances the Durability and Polyfunctionality of Protective Malaria CD8 *2* T-Cell Responses □ †. 78:145–153.

Rhoel R. Dinglasan and Marcelo Jacobs-Lorena. 2008. Flipping the paradigm on malaria transmission - blocking vaccines. Trends Parasitol. 24:364–370.

Richman AM, Dimopoulos G, Seeley D, Kafatos FC. 1997. *Plasmodium* activates the innate immune response of *Anopheles gambiae* mosquitoes. EMBO J. 16:6114–9.

Rosenmund A. 1991. Blood parasites - Mechanisms of coexistence. Schweiz. Med. Wochenschr. 121:1669–1674.

Rutschmann S, Jung AC, Zhou R, Silverman N, Hoffmann JA, Ferrandon D. 2000. Role of *Drosophila* IKK gamma in a toll-independent antibacterial immune response. Nat. Immunol. 1:342–347.

Seder RA, Chang L-J, Enama ME, Zephir KL, Sarwar UN, Gordon IJ, Holman LA, James ER, Billingsley PF, Gunasekera A, et al. 2013. Protection Against Malaria by Intravenous Immunization with a Nonreplicating Sporozoite Vaccine. Sci. 341 :1359–1365.

Shahabuddin M. 1998. *Plasmodium* ookinete development in the mosquito midgut: a case of reciprocal manipulation. Parasitology 116 Suppl:S83–93.

Shaner NC, Campbell RE, Steinbach PA, Giepmans BNG, Palmer AE, Tsien RY. 2004. Improved monomeric red, orange and yellow fluorescent proteins derived from Discosoma sp. red fluorescent protein. Nat. Biotechnol. 22:1567–1572.

Shin SW, Kokoza V, Lobkov I, Raikhel AS. 2003. Relish-mediated immune deficiency in the transgenic mosquito *Aedes aegypti*. Proc. Natl. Acad. Sci. U. S. A. 100:2616–21.

Shin SW, Kokoza VA, Raikhel AS. 2003. Transgenesis and reverse genetics of mosquito innate immunity. J. Exp. Biol. 206:3835–3843.

Silverman N, Zhou R, Stoven S, Pandey N, Hultmark D, Maniatis T. 2000. A *Drosophila* IkappaB kinase complex required for Relish cleavage and antibacterial immunity. Genes Dev. 14:2461–2471.

Sim S, Jupatanakul N, Dimopoulos G. 2014. Mosquito Immunity against Arboviruses. Viruses 6:4479–4504.

Sinka ME, Bangs MJ, Manguin S, Rubio-Palis Y, Chareonviriyaphap T, Coetzee M, Mbogo CM, Hemingway J, Patil AP, Temperley WH, et al. 2012. A global map of dominant malaria vectors. Parasit. Vectors 5:69.

Sluss HK, Han Z, Barrett T, Goberdhan DC, Wilson C, Davis RJ, Ip YT. 1996. A JNK signal transduction pathway that mediates morphogenesis and an immune response in *Drosophila*. Genes Dev. 10:2745–2758.

Soulard V, Bosson-Vanga H, Lorthiois A, Roucher C, Franetich J-F, Zanghi G, Bordessoulles M, Tefit M, Thellier M, Morosan S, et al. 2015. *Plasmodium falciparum* full life cycle and *Plasmodium* ovale liver stages in humanized mice. Nat. Commun. 6:7690.

Souza-Neto JA, Sim S, Dimopoulos G. 2009. An evolutionary conserved function of the JAK-STAT pathway in anti-dengue defense. Proc. Natl. Acad. Sci. U. S. A. 106:17841–17846.

Stoven S, Ando I, Kadalayil L, Engstrom Y, Hultmark D. 2000. Activation of the *Drosophila* NF-kappaB factor Relish by rapid endoproteolytic cleavage. EMBO Rep. 1:347–352.

Stoven S, Silverman N, Junell A, Hedengren-Olcott M, Erturk D, Engstrom Y, Maniatis T, Hultmark D. 2003. Caspase-mediated processing of the *Drosophila* NF-kappaB factor Relish. Proc. Natl. Acad. Sci. U. S. A. 100:5991–5996.

Suhrbier A. 1991. Immunity to the liver stage of malaria. Parasitol. TODAY 7:160–163.

World Health Organization. Summary E. 2006. Malaria Vaccine Technology Roadmap.

Takala SL, Coulibaly D, Thera MA, Batchelor AH, Cummings MP, Escalante AA, Ouattara A, Traoré K, Niangaly A, Djimdé AA, et al. 2009. Extreme Polymorphism in a Vaccine Antigen and Risk of Clinical Malaria: Implications for Vaccine Development. Sci. Transl. Med. 1:2ra5–2ra5.

Tanji T, Ip YT. 2005a. Regulators of the Toll and Imd pathways in the *Drosophila* innate immune response. Trends Immunol. 26:193–198.

Tanji T, Ip YT. 2005b. Regulators of the Toll and Imd pathways in the *Drosophila* innate immune response. Trends Immunol. 26:193–8.

Terra WR. 2001. The origin and functions of the insect peritrophic membrane and peritrophic gel. Arch. Insect Biochem. Physiol. 47:47–61.

Vanderberg JP, Frevert U. 2004. Intravital microscopy demonstrating antibody-mediated immobilisation of *Plasmodium berghei* sporozoites injected into skin by mosquitoes. Int. J. Parasitol. 34:991–996.

Vasselon T, Detmers PA. 2002. Toll receptors: a central element in innate immune responses. Infect. Immun. 70:1033–41.

Vaughan A, Wang R, Kappe SHI. 2010. Genetically engineered, attenuated whole-cell vaccine approaches for malaria. Hum. Vaccin. 6:107–113.

Vaughan AM, Aly ASI, Kappe SHI. 2008. Malaria parasite pre-erythrocytic stage infection: gliding and hiding. Cell Host Microbe 4:209–218.

Walker K. 2002. A review of control methods for African malaria vectors. Off. Heal. Infect. Dis. Nutr. Glob. Heal. U.S. Agency Int. Dev.:54.

Warr E, Lambrechts L, Koella JC, Bourgouin C, Dimopoulos G. 2006. *Anopheles gambiae* immune responses to Sephadex beads: involvement of anti-*Plasmodium* factors in regulating melanization. Insect Biochem. Mol. Biol. 36:769–78.

Waterhouse RM, Povelones M, Christophides GK. 2010. Sequence-structure-function relations of the mosquito leucine-rich repeat immune proteins. BMC Genomics 11:531.

Wheeler DL, Church DM, Federhen S, Lash AE, Madden TL, Pontius JU, Schuler GD, Schriml LM, Sequeira E, Tatusova TA, et al. 2003. Database resources of the National Center for Biotechnology. Nucleic Acids Res. 31:28–33.

White NJ. 2008. *Plasmodium* knowlesi: The Fifth Human Malaria Parasite. Clin. Infect. Dis. 46:172–173.

Wiser M. 2009. *Plasmodium* Life Cycle. Tulane Univ.:1–4.

World Health Organization. (2008). World Malaria Report 2008..

World Health Organization. (2010). World Malaria Report 2010.

World Health Organization. (2014). World Malaria Report 2014.

Wu LP, Anderson K V. 1998. Regulated nuclear import of Rel proteins in the *Drosophila* immune response. Nature 392:93–97.

Xi Z, Ramirez JL, Dimopoulos G. 2008. The Aedes aegypti toll pathway controls dengue virus infection. PLoS Pathog. 4:e1000098.

Yassine H, Kamareddine L, Chamat S, Christophides GK, Osta MA. 2014. A Serine Protease Homolog Negatively Regulates TEP1 Consumption in Systemic Infections of the Malaria Vector *Anopheles gambiae*. J. Innate Immun. 6:806–818.

Yassine H, Kamareddine L, Osta MA. 2012. The Mosquito Melanization Response Is Implicated in Defense against the Entomopathogenic Fungus Beauveria bassiana. PLoS Pathog 8:e1003029.

Yassine H, Osta M a. 2010. *Anopheles gambiae* innate immunity. Cell. Microbiol. 12:1–9.

Yassine H, Osta MA. 2010. *Anopheles gambiae* innate immunity. Cell. Microbiol. 12:1–9.

Yoshida S, Watanabe H. 2006. Robust salivary gland-specific transgene expression in *Anopheles stephensi* mosquito. Insect Mol. Biol. 15:403–410.

Zambon RA, Nandakumar M, Vakharia VN, Wu LP. 2005. The Toll pathway is important for an antiviral response in *Drosophila*. Proc. Natl. Acad. Sci. U. S. A. 102:7257–7262.